UNICA

UNIVERSITÀ
DEGLI STUDI
DI CAGLIARI

Ph.D. DEGREE IN
Civil Engineering and Architecture
Cycle XXXVIII

TITLE OF THE Ph.D. THESIS

Concrete with Fine and Coarse Recycled Concrete Aggregates (RCA): Mechanical Performance and Durability

Scientific Disciplinary Sector(s)

CEAR 07a - Tecnica delle Costruzioni

Ph.D. Student:	Alireza Alibeigibeni
Supervisor:	Prof. Flavio Stochino
Co-supervisor:	Prof. Mauro Sassu

Final exam. Academic Year 2024/2025
Thesis defence session: February 2026

Index:

List of figures:

List of tables:

1. Introduction

1.1. Background and Motivation

Concrete is the most used construction material; its production causes significant environmental impacts, including natural resource depletion and carbon emissions. In response to these challenges, the incorporation of recycled materials, such as Recycled Concrete Aggregates (RCAs) derived from Construction and Demolition Waste (CDW), has emerged as a sustainable solution to reduce the environmental impact of concrete production while enhancing its mechanical and durability properties [1].

The construction industry is one of the largest consumers of natural resources worldwide. Global production of virgin aggregates has increased significantly, from 21 billion tons in 2007 to 50 billion tons in 2017, marking a 138% rise. Projections indicate that this demand will continue to grow, reaching 60 billion tons by 2030 [2,3]. China is the largest consumer, using 40% of these aggregates, followed by India at 10% and other Asian countries, including Indonesia, Malaysia, and Thailand, with a combined total of 16%. Additional major consumers are Turkey (0.96%), Africa (8%), Europe and the European Free Trade Association (EFTA) (6%), the United States (4.8%), Central and South America (4%), the Middle East (5.6%), and Russia together with the Commonwealth of Independent States (CIS) (5%) [2–4], as illustrated in Figure 1 [5].

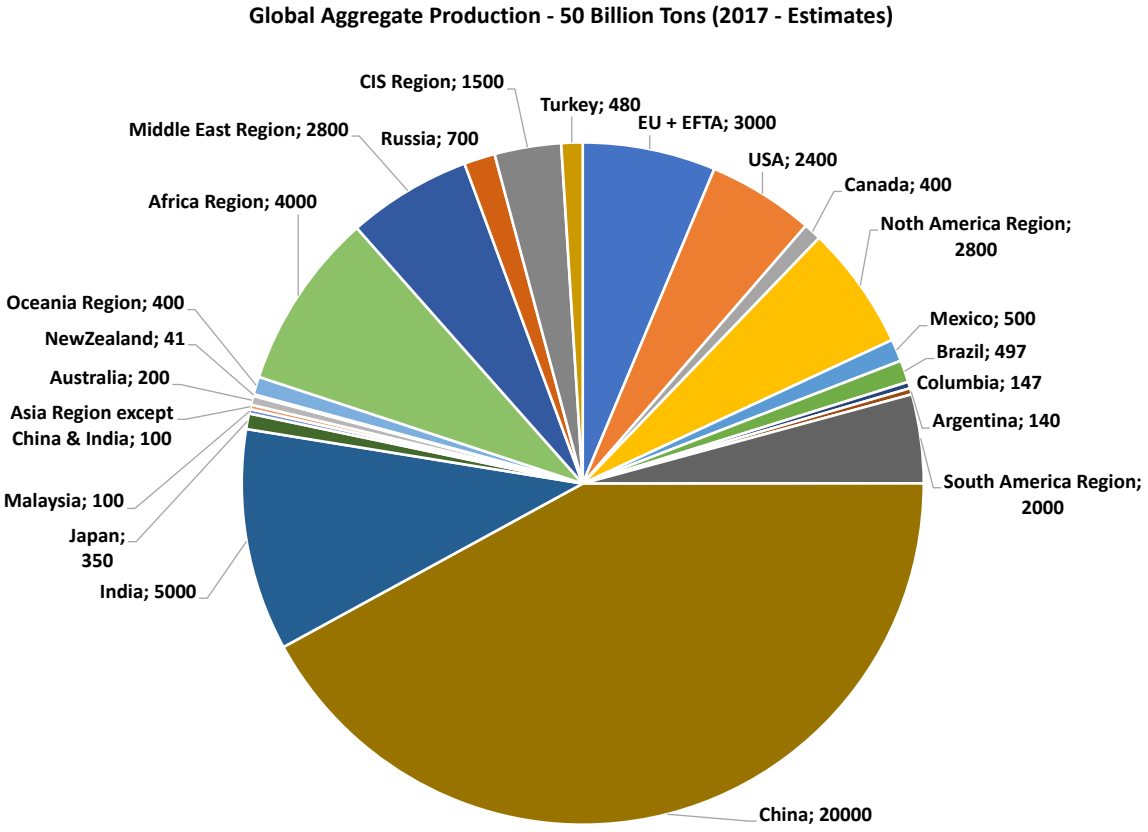

Figure 1. Worldwide production of virgin aggregates (million tons) [5].

RCAs derived from demolished concrete structures offer a sustainable alternative to conventional aggregates. The utilization of RCAs in concrete not only diverts construction waste from landfills, but also conserves natural resources and reduces energy consumption associated with aggregate extraction and processing [6]. Furthermore, incorporating RCAs

into concrete mixtures can contribute to mitigating the carbon footprint of the construction industry, aligning with global efforts towards sustainable development and environmental stewardship [7].

The water-intensive nature of concrete production, coupled with improper waste disposal from construction and demolition activities, poses risks to water resources and amplifies the global waste stream. Concrete's high thermal conductivity contributes to the urban heat island effect, altering local climates, while its reflective properties influence the albedo effect, potentially impacting regional climate patterns. Improper disposal of concrete-related chemicals can lead to groundwater contamination, posing risks to both human health and aquatic ecosystems. Construction and demolition processes, see [8], generate airborne concrete dust with adverse respiratory effects on humans and surrounding ecosystems. Furthermore, the long lifespan and inflexibility of concrete structures inhibit adaptive responses to changing environmental needs and conditions, emphasizing the need for sustainable alternatives and responsible construction practices.

Recycled Concrete Aggregate (RCA) emerges as a very promising solution to mitigate the depletion of natural resources induced by traditional concrete construction [9]. By utilizing RCA in concrete production, the demand for fresh aggregates extracted from quarries can be remarkably reduced, thereby preserving natural ecosystems and mitigating habitat disruption. This practice not only extends the lifespan of existing resources but also minimizes the environmental impact associated with extraction processes [10]. Recycling concrete not only diverts waste from landfills but also lessens the need for virgin materials, addressing the sustainability challenges posed by resource depletion. Consequently, the incorporation of RCA in concrete promotes a more circular and environmentally conscious approach to construction, contributing to the conservation of natural resources and fostering a more sustainable built environment.

The incorporation of RCAs in concrete raises questions regarding their impact on mechanical and durability properties. The heterogeneous nature of RCAs, varying in size, shape, and quality, presents challenges in predicting their influence on concrete performance [11]. Moreover, factors such as the content of adhered mortar, contaminants, and the presence of residual cementitious materials can influence the properties of RCAs and, consequently, the performance of recycled aggregate concrete [12].

The use of RCAs in structural elements is gaining attention for its environmental and mechanical benefits. Stochino et al. (2024) investigated steel–concrete composite slabs incorporating RCAs and found that, while compressive strength decreased with higher RCA content, structural integrity remained intact. Their study suggests that RCAs can enhance composite action with steel decking, supporting their feasibility for sustainable construction without compromising mechanical performance [13].

Understanding the effects of using RCAs on the mechanical and durability properties of concrete is crucial for optimizing concrete mix designs and ensuring the long-term performance of sustainable construction materials. Previous research has explored various aspects of recycled aggregate concrete, including its compressive strength, tensile strength, modulus of elasticity, durability against freeze–thaw cycles, chloride penetration resistance, and sulfate attack resistance [14,15].

Despite the growing body of research, as illustrated in Figure 2 [16], existing studies often focus on isolated properties of RCA concrete, such as compressive strength or durability against specific environmental factors. To generate this figure, a keyword search was conducted on the Scopus database using the term 'recycled concrete aggregate.' The search was limited to publications from 2000 to 2024 to analyze the trend in research output over time.

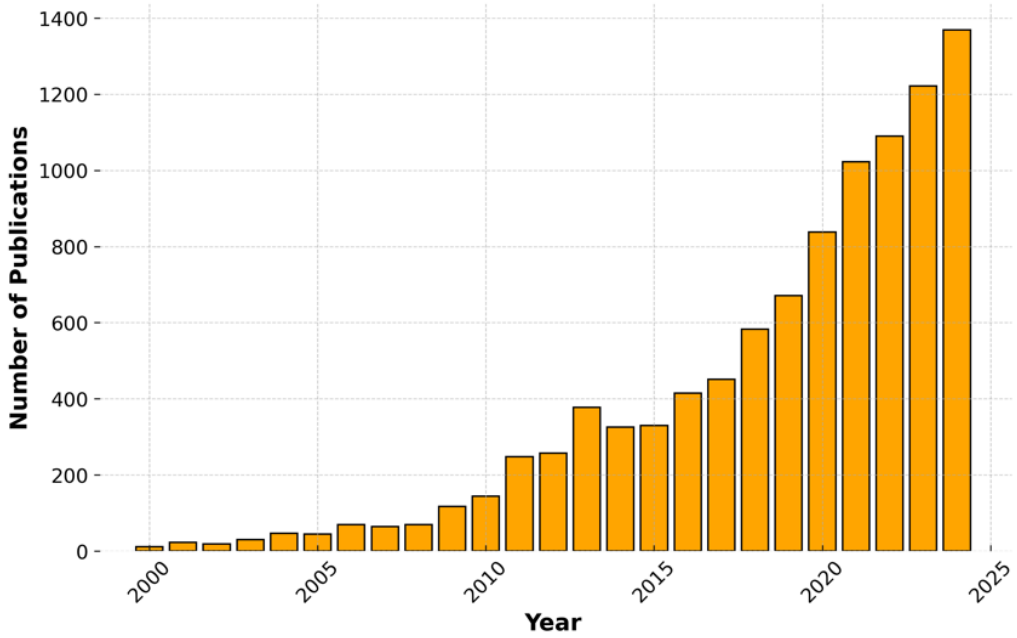

Figure 2. Trend of research publications on RCAs [16].

Few comprehensive reviews systematically synthesize these findings across mechanical and durability dimensions, alongside innovations in pretreatment methods and advanced mix designs. This gap in the literature limits the development of holistic strategies for optimizing RCAs in structural applications.

A key finding by Chauhan [17] indicates that the incorporation of metakaolin and lime powder in acid-mechanically treated recycled aggregate concrete significantly enhances its strength and durability. This is attributed to the improved pore structure and resistance to chloride ion permeability offered by the mineral admixtures used, which confer better mechanical properties to the concrete. Similarly, Islam [18] emphasizes that while the incorporation of polypropylene aggregates helps address the recycling of plastic waste, it also presents ecological concerns due to the low recycling rates of plastics. These studies underscore the critical balance between material innovation and environmental impact in the advancement of sustainable concrete solutions.

However, several treatment methods have been investigated to improve the modulus of elasticity in RCA concrete. Based on the study by Silva et al. (2016) [19], pretreatment techniques, such as acid washing, mechanical grinding, and polymer impregnation, have shown significant improvements in the modulus of elasticity. For instance, heating–scrubbing treatment resulted in a 42.92% increase in E-values, while mechanical grinding led to a 31.30% improvement [20]. Furthermore, bio-calcium deposition treatment increased the E-values by 32.8%, from 33.2 GPa for untreated RCAs to 44.1 GPa for treated RCAs [21]. Other methods, such as acetic acid immersion, also demonstrated improvements, with increases ranging from 12% to 29% depending on the treatment method and RCA replacement level [22]. These

findings suggest that pretreatment methods can effectively enhance the stiffness and overall mechanical performance of RCA concrete by reducing residual mortar content and improving the bond between RCAs and the cement matrix.

Mechanical and durability properties significantly deteriorate with a higher percentage of RCA replacement. Zia [23] reported that increased RCA content leads to notable reductions in compressive, tensile, and bending strengths, along with increased porosity and water absorption. This finding aligns with the work of Liu [24], who found that recycled coarse aggregate concrete exhibits excellent freeze-thaw resistance compared to natural aggregate concrete, thus highlighting an important advantage of RCA under certain conditions. This juxtaposition of qualities emphasizes the need for thoughtful integration of RCA in concrete formulations to optimize both sustainability and performance.

The impact of RCA on concrete properties can further be affected by parameters such as particle shape and size, as demonstrated in studies by Nithin [25]. They note that the strength and durability of recycled aggregates can vary significantly based on their physical characteristics, indicating that careful evaluation of aggregate properties is necessary during the mix design phase

Shang's exploration of wet carbonation with ethanol solutions reveals another promising treatment method for enhancing the microstructural and durability properties of RCA [26]. This process modifies the chemical composition of RCA, potentially improving its performance in concrete applications. Such innovative techniques are crucial in improving the mechanical properties of concrete while utilizing recycled materials, paving the way for sustainable construction practices.

Moreover, the incorporation of waste byproducts such as glass powder has gained traction, as evidenced by Singh's findings [27]. His studies demonstrate that when utilized as a partial cement substitute, waste glass powder can enhance the microstructural integrity and durability of fly ash-based alkali-activated concrete containing 100% RCA, thus suggesting new avenues for leveraging industrial waste in concrete production. This dynamic showcases the increasing potential of hybrid materials composed of recycled aggregate and various supplementary cementitious materials.

With rising concerns about sustainability and natural resource depletion, the use of recycled concrete aggregates (RCAs) from CDW is gaining momentum as a viable alternative to natural aggregates. However, the inclusion of RCAs often introduces variability due to the presence of adhered mortar, increased porosity, and higher water absorption compared to natural aggregates [28].

Durability is often a more critical concern than strength when using RCAs. The porous nature of recycled aggregates and the weaker interfacial transition zone (ITZ) between cement paste and aggregate typically result in reduced resistance to carbonation, chloride ingress, and freeze–thaw cycles [29]. Nevertheless, growing evidence suggests that when properly processed, RCAs can offer sufficient durability performance, especially for non-structural or moderately aggressive environments [30].

Among various durability indicators, oxygen permeability and chloride ion penetration are key parameters used to evaluate concrete's resistance to aggressive agents. Oxygen permeability, in particular, is closely associated with the microstructural quality of the concrete and provides a sensitive measure of its ability to resist gas ingress and subsequent reinforcement corrosion

[31]. Additionally, studies have shown that permeability-related parameters are often better indicators of long-term performance than compressive strength alone [32].

Carbonation represents a key durability concern in recycled aggregate concrete, since CO_2 penetration lowers the pore solution pH and may depassivate embedded steel reinforcement. Interestingly, some research highlights the potential benefits of using carbonated RCAs, which show lower water absorption and denser microstructures, thereby improving resistance to further carbonation [33]. This not only enhances durability but also aligns with carbon capture objectives through accelerated carbonation treatments [34].

Furthermore, the interplay between different durability mechanisms, such as carbonation depth, water permeability, and chloride ion penetration, can be complex. For example, concrete with low water permeability may still exhibit high carbonation due to the drying effect on pore structure [35]. Thus, evaluating correlations among durability indicators is essential for building comprehensive performance profiles for RAC.

Emerging predictive approaches, including probabilistic models and machine learning, have enabled better estimation of durability under variable exposure conditions. These techniques consider a wide range of input variables, from RCA properties to environmental exposure, and are proving useful for performance-based design and life-cycle analysis [36]. They also highlight the importance of multi-parameter durability assessments over isolated tests.

While numerous studies have examined the mechanical or individual durability properties of RAC, integrated experimental campaigns that simultaneously assess gas permeability, chloride transport, freeze–thaw resistance, and carbonation depth across different mix designs are still scarce. This gap limits the development of unified durability criteria tailored for RCA applications [37].

The mechanical performance of recycled aggregate concrete is being thoroughly investigated [38]. Previous studies on RCA report on reduced compressive strength but enhanced interfacial bonding due to rougher surfaces [39]. Recently, it has been investigated the fracture behavior of environmentally-friendly building materials such as rubberized steel fiber reinforced recycled aggregate concrete (RSRAC), which incorporates waste concrete and tires [40]. Very promising results indicate that RSRAC exhibits reduced brittleness and improved ductility with crumb rubber, while steel fiber enhances strength but increases brittleness, and recycled aggregate negatively affects both strength and ductility

From this perspective, the composite concrete steel solutions (Figure 3), like slabs, can provide interesting research results, see [41] and [42]. Composite steel concrete slabs combining steel and concrete, offer a synergistic effect by leveraging the tensile strength of steel and the compressive strength of concrete, resulting in enhanced structural performance and durability. These systems are particularly advantageous in construction, providing increased load-bearing capacity and efficient material usage.

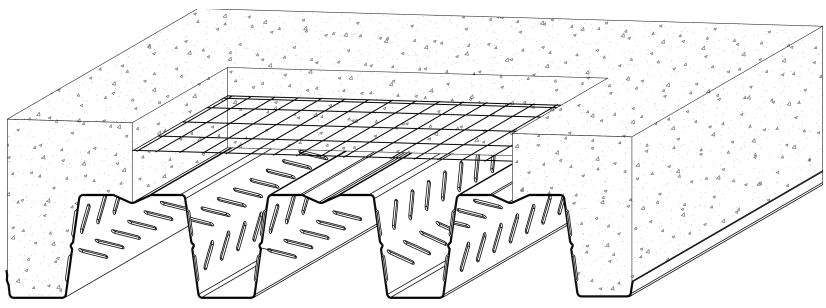

Figure 3. A standard steel-concrete slab incorporating a trapezoidal metal deck.

The response of such structures is governed by the tangential behaviour of the interface, i.e. the bond between the two materials, and for this reason the roughness of the concrete became more important than its ultimate strength [43,44]. The longitudinal shear strength (τ_u) stress, which governs the design of a composite slab, can be assessed by using the interaction domain proposed by the EN 1994-1-1 [45], together with the experimental results of a four point bending test procedure, i.e. by following the so-called partial shear connection (PSC) method. The main assumptions of the method are: i) at the ultimate limit state, the steel sheet response is always in the plastic range independently of the effective strain value reached at the various levels of the cross-section; ii) the contribution of the concrete inside the ribs is always neglected.

These simplified assumptions affect the resistance domain and could leads to an unreliable estimation of the level of interaction between concrete and steel. As already observed in ref. [46], it can be noted that once a limit strain ε_{lim} of the lower edge of the steel deck is reached, longitudinal shear collapse occurs, with a large part of the steel deck in the elastic range. For this reason more refined design methods are still under investigation [47].

Composite steel-concrete slabs have gained significant attention for their structural efficiency, particularly when combined with RCA. In this context their name is RACCS (Recycled Aggregate Concrete Composite Slabs), see Fig. 1. These hybrid systems leverage the tensile strength of steel and the compressive resistance of concrete, enhancing load-bearing capacity and durability [48,49]. Stochino et al. (2024) [50] conducted an experimental study on 12 RACCS, analyzing ultimate resistance and longitudinal shear strength. Their results indicate that increased RCA content weakens flexural performance, though enhanced bonding techniques can mitigate strength loss. Similarly, Chen et al. (2023) [51] performed longitudinal shear tests on corrugated steel-concrete composite slabs with RCA, concluding that the RCA-to-steel interface plays a critical role in shear performance, necessitating optimized bonding methods. Furthermore, Ferreira et al. (2024) [52] analyzed the punching strength of slab-column connections using RCA, confirming that well-graded RCA aggregates can maintain punching shear capacity comparable to conventional concrete, making RCA viable for high-load applications. A comprehensive review of the longitudinal shear behaviour of the RACCS has been recently proposed in [53]. This paper highlights material–geometry interactions in RACCS and discusses the variation of m–k method parameters for sustainable structural design

Another critical aspect of RCA-based composite structures is their performance under extreme conditions. Kefyalew et al. (2024) [54] reviewed the behavior of RCA-based composite metal decks under elevated temperatures, reporting that adhered mortar in RCA reduces thermal resistance, though modified aggregate treatments can improve fire resistance. Neupane et al. (2023) [55] studied RCA use in Southeast Asia, revealing that 100% RCA slabs exhibit lower flexural strength than natural aggregate slabs. Their findings suggest that hybrid mix designs incorporating silica fume significantly improve mechanical properties. In addition, Wattanapanich et al. (2024) [56] applied machine learning models to optimize RCA mix designs for extreme environments, providing predictive tools for enhancing durability and structural integrity.

With advancements in digital construction technologies, RCA has also been explored in 3D-printed concrete structures. Aslani & Zhang (2024) [57] investigated RCA applications in

automated construction, demonstrating that high-quality secondary raw materials enhance both printability and structural stability, paving the way for innovative RCA utilization in prefabricated and on-site printing applications.

Despite this growing body of research, the literature on RACCS remains fragmented. Most available studies have focused on small-scale specimens or single-span configurations, often overlooking the combined influence of RCA content and span length on the flexural and longitudinal shear behavior of full-scale slabs. Furthermore, existing design provisions, such as those in EN 1994-1-1 [45], were primarily developed for conventional concretes and may not adequately capture the altered interfacial behavior introduced by RCA. Consequently, systematic experimental evidence is still limited, particularly regarding the influence of geometry and aggregate type on composite action, ductility, and residual load-bearing capacity.

For these reasons, the development of composite slabs incorporating RCA represents a promising and necessary area of investigation. Achieving satisfactory resistance and stiffness does not necessarily require high-strength concrete but rather an efficient mechanical and chemical bond with the steel sheeting. In this context, concrete made with recycled aggregates offers a sustainable and technically feasible solution for the next generation of composite structural systems.

This study presents a comprehensive experimental and analytical investigation into the mechanical and durability performance of recycled aggregate concrete (RAC), as well as its structural application in composite concrete–steel systems. The research was developed within the framework of the SARCOS project [58], funded by the Italian Ministry, through a close collaboration between the University of Cagliari and the Politecnico di Milano. The project aims to promote the sustainable use of recycled aggregates in structural concrete, reducing the environmental impact associated with natural aggregate extraction and construction waste disposal.

To achieve these objectives, two extensive experimental campaigns were carried out between 2023 and 2024, focusing on both material-level and structural-scale investigations. The 2023 campaign involved four concrete mixes with different RCA replacement levels—0%, 30%, 50%, and 100%—identified as M0-0, M30-30, M50-50, and M100-100. These mixes were characterized in terms of mechanical and durability properties and subsequently used in composite slabs tested at three span lengths (2400, 2800, and 3200 mm). The 2024 campaign expanded this research by introducing additional mixes with replacement levels of 0%, 20%, 70%, and 100% (M0-0, M20-20, M70-70, and M100-100), again tested under identical span configurations.

A total of 48 full-scale Recycled Aggregate Concrete Composite Slabs (RACCS) were produced using RCA derived from construction and demolition waste. Each mix was tested across the three spans, with three specimens per configuration. The experimental program assessed a wide range of parameters, including compressive, tensile, and flexural strength, modulus of elasticity, creep, oxygen and water permeability, carbonation resistance, chloride ingress, and freeze–thaw durability. The structural program focused on the evaluation of ultimate load-bearing capacity and longitudinal shear resistance to better understand the interaction between concrete and steel in composite systems incorporating RCA.

The results obtained provide one of the most extensive and statistically robust datasets currently available for RCA-based concretes and composite slabs. By correlating mechanical and durability properties with structural behavior, this research contributes to a deeper

understanding of how recycled aggregates influence both material performance and composite action. Ultimately, the outcomes of this work support the feasibility of using RCA as a sustainable alternative to natural aggregates in modern concrete structures, offering valuable insights for the refinement of design provisions and the advancement of circular construction practices.

1.2. Thesis Structure

This thesis is organized into six chapters that progressively develop the research context, experimental work, and findings. Chapter 1 introduces the study by outlining the background, motivation, and objectives, followed by a brief description of the adopted methodology. It also presents the overall structure of the thesis to guide the reader through the subsequent chapters.

Chapter 2 provides a comprehensive state-of-the-art review of recycled concrete aggregates (RCA), beginning with the recycling of construction and demolition waste and the production of RCA. It then discusses the mechanical and durability properties of RCA concrete, as well as pretreatment methods aimed at enhancing aggregate quality. Recent developments related to CO_2 capture and life cycle assessment are also addressed, allowing the identification of knowledge gaps that motivate and shape the experimental program of this research.

Chapter 3 presents the experimental results concerning the mechanical characterization of RCA concrete. The investigation includes compressive strength, tensile and flexural strength, modulus of elasticity, and creep. The influence of different replacement levels of fine and coarse RCA is examined and compared with natural aggregate concrete, offering insight into how RCA affects fundamental mechanical behavior.

Chapter 4 focuses on the durability assessment of RCA concrete. It evaluates oxygen permeability, water permeability, carbonation depth, and freeze–thaw resistance, Chloride ion penetration, and Chloride migration coefficient, which are key indicators of long-term performance. The analysis also considers how this durability parameters relate to the mechanical properties, providing a more holistic understanding of RCA concrete behavior.

Chapter 5 shifts the attention from material characterization to structural application, reporting on the composite slab investigations carried out within the framework of the SARCOS project. Two experimental campaigns, conducted in 2023 and 2024, are presented, each involving composite steel–concrete slabs with varying RCA replacement levels and span lengths. The results are analyzed in terms of ultimate resistance, longitudinal shear resistance, and overall structural performance, thereby demonstrating the practical potential of RCA in structural concrete applications.

Finally, Chapter 6 draws together the main conclusions of the thesis, emphasizing both scientific contributions and practical implications for sustainable construction. Recommendations for the use of RCA in concrete structures are provided, along with suggestions for future research, particularly in relation to cyclic loading and dynamic applications. The thesis concludes with a full list of references documenting the sources consulted throughout the research.

2. State-of-the-Art

2.1. Recycling of construction of demolition waste for producing the aggregates

The recycling of CDW for producing aggregates has gained significant attention as a sustainable practice in the construction industry. CDW comprises various materials, including concrete, bricks, tiles, asphalt, wood, and metals, generated from construction, renovation, and demolition activities [59]. Recycling CDW not only reduces the burden on landfills but also conserves natural resources and reduces energy consumption associated with conventional aggregate production. Moreover, incorporating recycled aggregates from CDW in concrete offers potential economic benefits by lowering material costs and reducing the need for landfill disposal [60].

The quality of recycled aggregates obtained from CDW depends on several factors, including the type and composition of the original materials, the degree of contamination, the efficiency of the recycling process, and the quality control measures implemented [61]. Proper sorting, crushing, and screening techniques are essential to produce recycled aggregates with desirable properties for use in concrete production [62]. However, challenges such as variability in material composition, presence of contaminants, and limitations in processing technology can affect the quality and consistency of recycled aggregates, influencing the performance of concrete mixtures [15].

Despite the challenges, numerous studies have investigated the feasibility and effectiveness of using recycled aggregates from CDW in concrete applications. Research efforts have focused on evaluating the mechanical properties, durability performance, and long-term behavior of concrete incorporating recycled aggregates from CDW [63]. Additionally, advancements in recycling technologies and quality control measures have contributed to improving the quality and reliability of recycled aggregates, further enhancing their suitability for use in concrete production [64].

2.1.1. Recycled concrete aggregates (RCA)

RCAs obtained from construction and demolition waste are produced by crushing and processing demolished concrete structures, resulting in coarse and fine aggregates that can be used as substitutes for natural aggregates in concrete mixtures [65]. Figure 4 provides an example of RCAs, illustrating their typical particle size and texture.

Figure 4. Recycled concrete aggregates (RCAs).

The properties of RCAs significantly influence the performance of concrete mixtures. The quality of RCAs is affected by factors such as the quality of the original concrete, the degree of contamination, the crushing process, and the particle size distribution [11]. RCAs may contain residual mortar adhered to the aggregate particles, which can affect the workability, strength, and durability of concrete [5]. Therefore, proper characterization and quality control measures are essential to ensure the consistent and reliable performance of concrete containing RCAs.

Regional variations play a crucial role in influencing the performance of RCAs, primarily due to differences in CDW characteristics. Factors such as the age and type of demolished structures, local construction materials, and recycling practices contribute to these differences. For instance, RCAs obtained from regions with older buildings often contain higher proportions of masonry or plaster, which can negatively impact compressive strength and durability compared to RCAs derived from newer, concrete-rich demolitions. Moreover, areas with more regulated and advanced recycling systems, such as parts of Europe, tend to produce more consistent and higher-quality RCAs. These regional disparities underscore the need to consider local CDW characteristics when evaluating the suitability and performance of RCAs in concrete applications [66].

Research on RCAs has focused on evaluating their effects on various properties of concrete, including mechanical strength, durability, shrinkage, and permeability. Numerous studies have investigated the optimal replacement levels of natural aggregates with RCAs to achieve desired concrete performance while minimizing potential drawbacks [67]. Additionally, research efforts have explored different techniques to enhance the properties of recycled aggregate concrete, such as pre-soaking RCAs to reduce their water absorption and improve their compatibility with cement paste [68].

The influence of the quality of parent concrete on RCA properties remains a topic of debate in the literature. While several studies emphasize that the characteristics of the original concrete significantly impact the mechanical performance of recycled aggregate concrete, others suggest that factors such as mix design and curing conditions may play a more dominant role. For instance, Pani et al. (2020) [69] argue that the quality of parent concrete

does not substantially affect the compressive strength of recycled concrete, highlighting that mix proportions and other parameters have a greater influence on the final properties of RCA-based concrete. This divergence in findings underscores the complexity of RCA behavior and the need for further research to reconcile these varying perspectives.

RCAs have been extensively studied for their potential to mitigate the environmental impact of concrete production. The use of RCAs reduces the need for landfill space, conserves natural resources, and lowers greenhouse gas emissions associated with traditional aggregate mining and transportation [70]. Furthermore, incorporating RCAs into concrete mixtures aligns with sustainable development goals by promoting resource efficiency and waste reduction [71]. However, challenges such as variability in RCA properties, uncertainty regarding long-term performance, and potential durability issues remain areas of concern [72].

2.1.2. Pretreatment methods on RCA

The quality and performance of RCA are influenced by factors such as residual mortar content, contaminants, and particle size distribution. Effective pretreatment methods are crucial to enhance the properties of RCA and optimize their suitability for concrete production.

Mechanical pretreatment methods involve physical processes such as crushing, screening, and sieving to break down demolished concrete structures and segregate RCA into desired particle sizes [73]. Proper crushing techniques are essential to remove adhered mortar effectively and minimize the generation of fines. Screening and sieving processes further refine RCA into uniform aggregates suitable for concrete production.

Chemical pretreatment methods utilize solutions to dissolve or weaken the bond between aggregate particles and residual mortar, facilitating separation and improving RCA cleanliness [74]. Acid washing and alkali treatment are common chemical techniques employed. Acid washing removes calcium carbonate in the mortar matrix, while alkali treatment breaks down the bonds between aggregate particles and residual mortar. These methods enhance the quality of RCA but require careful handling to mitigate environmental impacts [75].

Thermal pretreatment involves heating and drying RCA to remove moisture and contaminants, improving their compatibility with cement paste and concrete performance [74,75]. Thermal treatment eliminates organic contaminants and weakens the bond between aggregate particles and residual mortar. However, it may alter the mineralogy and microstructure of RCA, necessitating careful consideration.

Pretreatment effectiveness depends on factors including the quality of the original concrete, contaminant type and concentration, and desired properties of recycled aggregates [15,76]. High-quality RCA can be obtained from well-maintained structures, while older or heavily contaminated sources may require more intensive pretreatment. Selection of pretreatment methods should align with concrete mix designs and intended RCA application. Comprehensive testing is crucial to assess pretreated RCA suitability for concrete production. Research aims to optimize recycling processes, improve recycled aggregate quality, and enhance concrete performance [5]. Studies like [74] have shown that chemical pretreatment significantly reduces residual mortar content in RCA, leading to improved concrete strength and durability. Experimental testing evaluates mechanical strength, durability, shrinkage, and permeability of concrete with pretreated RCA. Advancements in pretreatment technologies,

such as automated sorting and washing systems, streamline recycling processes and increase efficiency [77].

Pretreatment methods are vital for enhancing the quality and performance of RCA in sustainable concrete production. Mechanical, chemical, and thermal pretreatment techniques effectively address challenges associated with residual mortar, contaminants, and particle size distribution in RCA. However, their efficacy depends on various factors, necessitating comprehensive characterization and testing. Continued research and development efforts are crucial to optimize pretreatment methods and promote widespread adoption of recycled aggregates in the construction industry.

2.2. Mechanical properties of concrete with RCA

2.2.1. Compressive strength

The compressive strength is the most critical factor in evaluating concrete. Numerous studies have explored how recycled aggregates influence the compressive strength of recycled aggregate concrete (RAC). Silva et al. (2014) [78] reviewed 236 papers on RAC, with 119 focused specifically on compressive strength. However, reaching consistent conclusions has been challenging due to various factors. First, comparisons are often made between RAC and conventional concrete using natural aggregates, but the quality of these natural aggregates greatly influences the outcomes. The impact of recycled aggregates can vary depending on whether they replace natural aggregates with strong or weak mechanical properties. Second, different approaches were used to compare RAC, such as maintaining a consistent total water/cement ratio, an equivalent effective water/cement ratio, or the same workability, each of which can affect the effective water/cement ratio differently. Lastly, the results also depend on the specific properties of the recycled aggregates, such as their shape, size, and mechanical characteristics.

To better illustrate the influence of RCA content on compressive strength, a statistical analysis was conducted based on normalized values from multiple published studies. The results are shown in Figure 5, where the compressive strength of RAC is expressed as a ratio relative to that of conventional concrete and plotted against the percentage of RCAs used as replacements for natural aggregates.

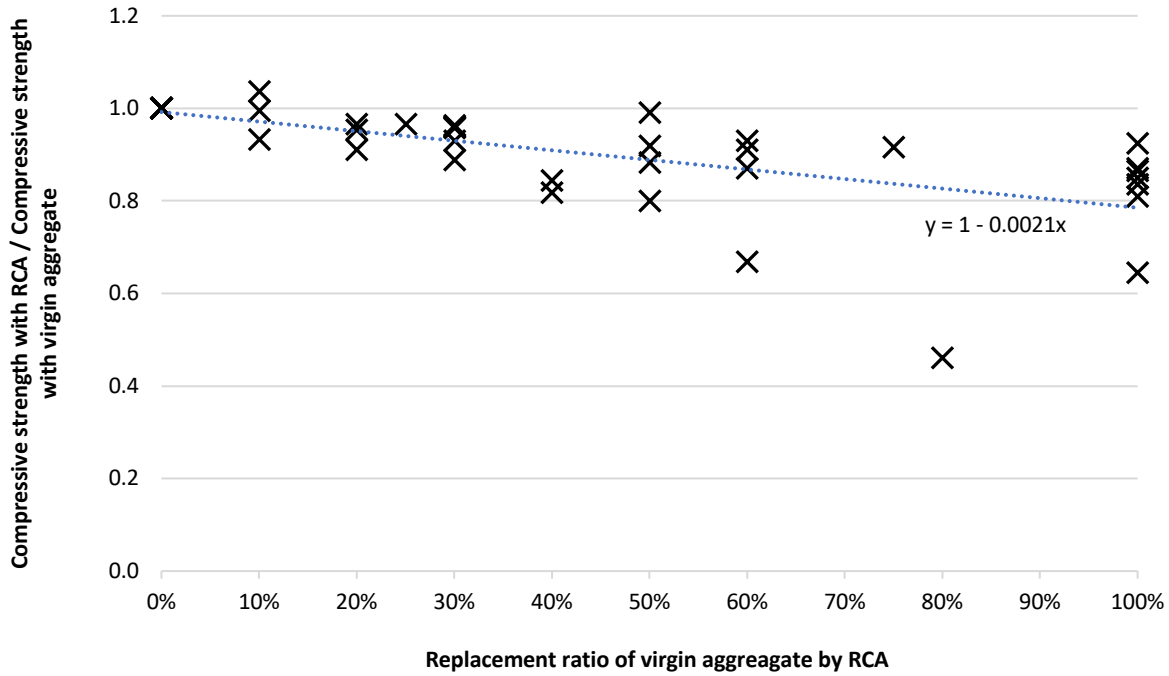

Figure 5. Normalized compressive strength of concrete with RCAs vs. replacements [79–90].

As seen in the figure, there is a clear downward trend: As the replacement level increases, compressive strength generally decreases. The data follow a linear trend, described by the equation $y = 1 - 0.0021x$, indicating that a full replacement (100%) could lead to about 79% of the compressive strength compared to concrete made entirely with virgin aggregates. This reduction is largely attributed to the higher porosity and lower mechanical quality of RCAs, which often contain residual mortar and form weaker interfacial transition zones (ITZs). These characteristics compromise the density and overall strength of the concrete matrix.

The compressive strength reduction is primarily due to the weaker adhered mortar present in the RCAs, which compromises the new concrete matrix's overall integrity. For instance, Silva et al. (2016) [19] observed that the compressive strength of RCA concrete could be approximately 10–30% lower than that of conventional concrete, depending on the RCA quality and the original concrete's properties.

The compressive strength of RCA concrete is strongly influenced by the RCA quality, which can be improved through proper pretreatment methods, such as acid washing or mechanical treatment. As mentioned in Section 2.2, these methods help reduce the residual mortar content, which can lead to better interfacial bonding and improved compressive strength.

Another critical factor affecting the compressive strength of RCA concrete is the mix design. Adjustments in the mix proportions, such as increasing the cement content or using supplementary cementitious materials (SCMs) like fly ash or silica fume, can mitigate the strength reduction caused by RCAs. A study by Kurda et al. (2019) [91] demonstrated that incorporating fly ash in RCA concrete mixes could enhance compressive strength by improving the interfacial transition zone between the RCAs and the cement paste. Their findings indicate that with optimal mix design, RCA concrete can achieve compressive strengths comparable to those of traditional concrete.

Curing conditions also play a crucial role in the development of compressive strength in RCA concrete. Proper curing can enhance the long-term strength of RCA concrete, despite initial lower strengths. Zhang et al. (2021) [73] reported that while RCA concrete exhibited lower early-age compressive strength, its long-term strength, particularly after 90 days, was comparable to that of natural aggregate concrete when subjected to appropriate curing practices. Their study emphasizes the importance of extended curing times to allow the RCA concrete to develop its full-strength potential.

With advancements in RCA processing techniques and optimized mix designs, the compressive strength of RCA concrete can be effectively managed to meet structural requirements. For instance, research by Wang et al. (2018) [92] highlights that incorporating RCAs in structural concrete is feasible and practical, provided that the mix design is tailored to account for the specific properties of the RCAs used.

2.2.2. Tensile strength

The tensile strength of concrete is a fundamental property that influences its behavior under various loading conditions, especially in scenarios involving flexure or cracking. The introduction of RCA into concrete mixes has been shown to impact tensile strength differently than compressive strength. Silva et al. (2015) [93] found that the tensile strength of RAC tends to decrease with an increase in RCA content, primarily due to the weaker interfacial transition zone (ITZ) in RAC compared to natural aggregate concrete. This weaker ITZ is often characterized by micro-cracks and increased porosity, which contribute to the reduced tensile strength.

The source and processing of RCA play crucial roles in determining the tensile strength of the resulting RAC. Yang et al. (2023) [94] conducted a study comparing the tensile strength of RAC produced with RCA from different sources. Their research indicated that RCA from high-strength concrete had a less detrimental effect on tensile strength than RCA sourced from lower-quality concrete. This finding emphasizes the importance of selecting high-quality RCA and possibly enhancing it through pre-treatment processes, such as washing and mechanical scrubbing, to remove adhered mortar and other contaminants.

Modifications in the mix design can also influence the tensile strength of RAC. Adding supplementary cementitious materials (SCMs) like fly ash or silica fume has been shown to improve tensile strength by refining the microstructure of the ITZ and enhancing the bond between the RCA and the new cement paste. Incorporating silica fume in RAC mixes improved tensile strength by reducing ITZ porosity and increasing the cohesion between RCA particles and the cement matrix. This modification is particularly effective in mitigating the reduction in tensile strength typically associated with higher RCA content [95,96].

Curing practices significantly affect the tensile strength development of RAC, as they do with compressive strength. Proper curing can enhance the tensile strength, even when using high levels of RCA. Dimitriou et al. (2018) [97] demonstrated that RAC subjected to extended curing times showed significant improvements in tensile strength, almost reaching that of natural aggregate concrete. This improvement was more pronounced in mixes where SCMs were used, highlighting the combined effect of optimal curing and mix design on tensile strength.

2.2.3. Elastic modulus

Elastic modulus is a critical mechanical property of concrete that defines its stiffness and ability to deform elastically under load. The modulus of elasticity is influenced by the composition of the concrete mix, particularly the quality of aggregates used. When RCAs replace natural aggregates in concrete, the elastic modulus is often observed to decrease due to the inferior quality of RCAs compared to natural aggregates. This reduction is attributed primarily to the quality of the recycled aggregates, which typically have a lower stiffness due to the presence of old adhered mortar and increased porosity. RCA particles contain old mortar and microcracks, which reduce the overall stiffness of the concrete, making it more susceptible to deformation under stress. Various studies have reported a reduction of up to 30% in the elastic modulus of concrete containing 100% RCA compared to natural aggregate concrete (NAC) [98,99]. Understanding how RCAs affect the elastic modulus is essential for ensuring that structural designs maintain adequate stiffness and serviceability.

Table 1 presents the modulus of elasticity of RCA concrete at different replacement levels, based on experimental results from a previous study [58]. The results indicate a clear reduction in the elastic modulus as the RCA content increases. The reference mix (M0-0) with natural aggregates exhibited the highest modulus of elasticity (34.7 GPa), whereas the 100% RCA mix (M100-100) recorded the lowest value (16.7 GPa), confirming the negative impact of RCAs on concrete stiffness. In the mix designation “M100-100,” the first “100” refers to the percentage of natural fine aggregate replaced with RCAs, and the second “100” refers to the percentage of coarse aggregate replaced with RCAs.

Table 1. Effect of RCA replacement on the modulus of elasticity of concrete.

Mix	Average [GPa]	CoV (%)
M 0-0	34.7	13.43
M 30-30	22.5	0.53
M 50-50	23.7	1.45
M 100-100	16.7	0.03

It is worth noting that, in some cases, the coefficient of variation (CoV) associated with the natural aggregate concrete (NAC) appears higher than that obtained for mixes incorporating recycled aggregates. Although this result may seem counterintuitive, it can be reasonably explained by a combination of statistical and material-related factors. First, the limited number of tested specimens makes the CoV particularly sensitive to small fluctuations in measured strength, especially for NAC mixes, which exhibit higher absolute strength levels. Second, recycled aggregate concretes tend to display more uniform failure mechanisms due to their more porous microstructure and the presence of attached mortar, which may reduce the influence of localized cracking and aggregate interlock on strength variability. In addition, the internal curing effect associated with recycled aggregates can mitigate local curing differences, contributing to a more consistent mechanical response. Consequently, a higher CoV for NAC does not indicate inferior material quality, but rather reflects the inherent scatter typical of brittle materials tested on a limited statistical basis.

The reduction in the elastic modulus of RCA concrete can be attributed to the higher porosity and weaker ITZ between the RCAs and the new cement matrix. Studies have shown that the ITZ in RCA concrete tends to be more porous due to the presence of old mortar on the RCA surface, which hinders the bonding between new cement paste and aggregate [100]. As a result, RCA concrete often exhibits lower stiffness, especially at higher replacement ratios of

natural aggregates with RCAs. The degradation in elastic modulus becomes more pronounced as the replacement level of RCAs increases, necessitating adjustments in mix designs or additional treatments to the RCAs to mitigate this effect [101].

Several factors influence the elastic modulus of RCA concrete, including the quality of the original concrete from which the RCAs are derived, the RCA treatment methods, and the ratio of RCA replacement. High-quality RCAs derived from strong parent concrete may exhibit a smaller reduction in elastic modulus compared to RCAs from low-strength concrete [102]. Additionally, pretreating RCAs, such as by removing adhered mortar or improving the surface characteristics, has been shown to mitigate the reduction in elastic modulus. Various studies have explored methods such as mechanical rubbing, acid treatment, and thermal treatment to improve RCA properties, ultimately aiming to enhance the elastic modulus of RCA concrete [103].

While the elastic modulus of RCA concrete is generally lower than that of conventional concrete, it is still possible to achieve acceptable stiffness for many structural applications through optimized mix designs and careful selection of RCA quality. The use of supplementary cementitious materials (SCMs) like fly ash, silica fume, or slag in RCA concrete has been shown to enhance the elastic modulus by improving the bond between the RCAs and the cement matrix. These SCMs contribute to a denser microstructure and reduce the porosity of the ITZ, partially compensating for the lower stiffness of RCA concrete [44].

In conclusion, the use of RCAs in concrete has a significant impact on the elastic modulus, primarily due to the porous and weak nature of RCA particles and the associated ITZ. However, by optimizing the quality of RCAs and mix design and incorporating SCMs, the reduction in elastic modulus can be controlled. Further research is needed to develop standard guidelines for improving the elastic modulus of RCA concrete, ensuring its suitability for a wide range of structural applications while promoting sustainability in construction practices.

2.2.4. Bonding strength between concrete and steel

The bond strength between concrete and steel reinforcement is a critical factor influencing the mechanical performance of reinforced concrete and composites structures. Several studies have evaluated the bond strength behavior using RCA, and the findings reveal varied influences based on environmental conditions, mix proportions, and external factors like corrosion and temperature. Ashteyat et al. (2024) [104] examined RCA and recycled asphalt pavements, reporting a reduction in bond stress with increasing recycled material, especially when smaller diameter bars were used, leading to a bond reduction of 6% to 45% compared to natural aggregates (NA). Similarly, Abushanab and Alnahhal (2023) [105] investigated the effects of treated wastewater (TWW) and fly ash (FA) in RCA concretes subjected to corrosion. RCA reduced bond strength by 18%, although the addition of 20% FA improved it by 10%, indicating RCA's sensitivity to corrosion when combined with other recycled materials.

The performance of RCA concrete under elevated temperatures was explored by Yusuf et al. (2022) [106], who found that RCA exhibited adequate bond strength compared to NA, but with greater deformations. Temperature-induced damage was particularly linked to the deterioration of mechanical properties, such as tensile strength, resulting in higher bond slippage. Zou et al. (2020) [107] corroborated these findings, noting that as temperatures increased, bond strength between RCA concrete and steel bars significantly dropped,

particularly in the post-heating phase, with a flattening of bond-slip curves. Their study introduced a modified model to predict bond strength, aligning well with experimental data.

Alhawat and Ashour (2019) [108] observed that corrosion greatly influences bond strength in RCA concrete, where the bond initially improved with minimal corrosion before degrading as corrosion intensified. Notably, the higher porosity of the RCAs led to faster degradation compared to conventional concrete. Namarak et al. (2018) [109] studied the use of a calcium carbide residue and fly ash binder with RCAs, finding that while RCAs reduced bond strength compared to natural aggregates, they still performed better than ordinary Portland cement concrete with RCAs. The type of steel reinforcement also influenced bond strength, with deformed bars outperforming smooth bars.

Prince and Singh (2015) [110] evaluated high-strength RCA concretes, discovering that the normalized bond strength of RCA concretes exceeded that of normal-strength RCAs and even natural aggregate concretes. Their proposed bond stress–slip relationship model accurately predicted bond behavior for various RCA replacement levels.

Figure 6 shows the relationship between RCA replacement levels and normalized bond strength for different concrete mixes and studies. Specifically, it compares the results for 8 mm and 10 mm deformed steel bars embedded in Mix A and Mix B, with increasing RCA content at 0%, 25%, 50%, 75%, and 100%. The trend lines demonstrate a general increase in normalized bond strength as RCA replacement levels rise. Notably, Mix B (high-strength RCAs) exhibited higher normalized bond strength than Mix A, suggesting that increasing RCA content in high-strength concrete enhances the bond performance more effectively.

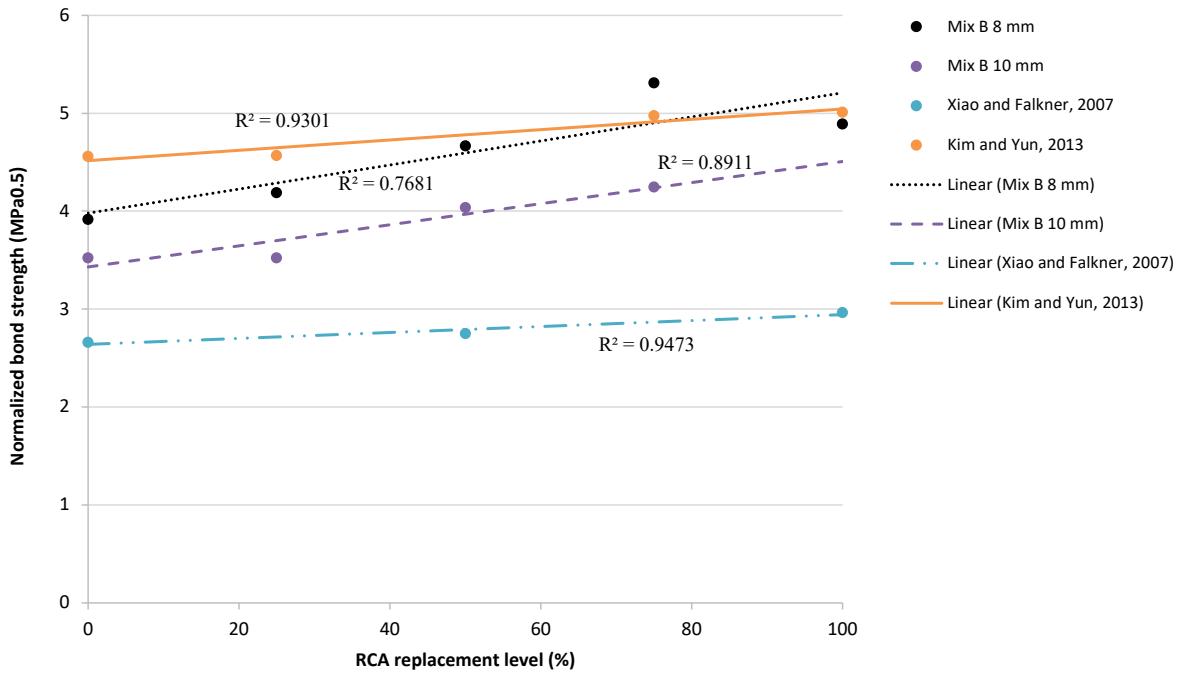

Figure 6. Normalized bond strengths corresponding to varying levels of RCA replacement [110].

In addition, the graph includes comparative data from studies by Xiao and Falkner (2007) [111] and Kim and Yun (2013) [112]. These comparisons reveal that the bond strength behavior observed in this experiment aligns closely with established trends in the literature. The R^2 values, which represent the strength of correlation between RCA replacement levels and

normalized bond strength, further validate this finding. A higher R^2 value indicates a stronger correlation, with the highest $R^2 = 0.968$ observed for Xiao and Falkner (2007) [111].

2.2.5. Creep

The creep behavior of recycled aggregate concrete (RAC) is one of the least studied aspects of its performance, leaving a critical gap in understanding its long-term deformation characteristics. While the mechanical and durability properties of RAC have been extensively investigated, limited research has addressed the influence of recycled aggregates on creep. This gap hinders the development of predictive models and design standards, particularly for applications requiring stringent long-term performance criteria.

The formulation of creep models has been significantly advanced through large experimental databases, particularly the NU-ITI database, which contains approximately 1,400 creep curves natural aggregate concrete. These curves are evenly divided between basic and drying creep, offering a comprehensive foundation for model development. When reporting experimental results on concrete creep, several metrics are used, including creep strain, ε_{cc}, experimental creep coefficient $\varphi_{exp} = \frac{\varepsilon_{cc}}{\varepsilon_{ci}}$ here ε_{ci} represents the initial strain at loading), specific creep $\frac{\varepsilon_{cc}}{\sigma_c}$, (i.e., creep strain per unit stress), and creep compliance J_c. Of these, creep compliance is the most general and optimal method of reporting, particularly for linear creep behavior (i.e., exposure to stresses below approximately 40–50% of compressive strength). The relation is defined as:

$$\varepsilon_{c\sigma}(t, t_0) = J_c(t, t_0) \cdot \sigma_c(t_0) \tag{1}$$

where $\varepsilon_{c\sigma}$ is the stress-dependent strain, and t_0 is the age of concrete at loading. This formulation enables the derivation of various creep coefficients, such as the one proposed in the *fib* Model Code 2010:

$$\varepsilon_{c\sigma}(t, t_0) = \left(\frac{1}{E_c(t_0)} + \frac{\varphi(t, t_0)}{E_{ci}}\right) \cdot \sigma_c(t_0) \tag{2}$$

where $E_c(t_0)$ and E_{ci} represent the modulus of elasticity at the age of loading and at 28 days, respectively. However, it is crucial to note that the creep coefficient derived from the *fib* Model Code 2010 does not directly match the experimental creep coefficient $\varphi_{exp} = \frac{\varepsilon_{cc}}{\varepsilon_{ci}}$ his distinction is important when comparing experimental results with code-based predictions [113].

Despite the extensive data available, including nearly 800 creep curves for concretes with various admixtures or additives, the NU-ITI database lacks specific information on the creep behavior of recycled aggregate concrete (RAC). The adhered mortar on recycled aggregate (RA) particles influences creep in several ways, from an internal curing effect to less restraint against creep, and even creep of the adhered mortar itself. In subsequent sections, experimental results on RAC creep are reviewed, and both new and modified models for predicting RAC creep are discussed [113].

A comprehensive literature review by Lye et al. (2014) [114] identified 100 publications on RAC creep from 27 countries, spanning 30 years. The experimental data covered a wide range of recycled materials, including RCAs, recycled masonry aggregates (RMAs), mixed recycled aggregates (MRAs), and fine and coarse RA.

The results consistently showed that creep increases with higher coarse RCA content, mirroring trends. For example, the average increase in creep for RAC with 20% and 100% coarse RCA content was 12% and 32%, respectively. These findings align with other studies, which report increases in the range of 10–50%. Additionally, compressive strength plays a key role in the relative increase in creep. For RAC with 100% coarse RCA, the increase in creep was found to be 35%, 30%, and 25% for f_{cm} in the ranges of 15–40 MPa, 41–50 MPa, and 51–70 MPa, respectively.

Gomez-Soberon (2002) [115] found that, as shown in Figure 7, under permanent stress at 40% of the compressive strength, the creep of RAC with replacement ratios of recycled aggregate (where factor r represents the replacement ratio) between 20% and 100% was higher by 35% to 51%, compared to that of NAC. While basic creep is not significantly affected by recycled aggregate replacement, drying creep is clearly impacted, particularly when the replacement ratio exceeds 30%. Fan et al. (2014) [116] attributed this increase in creep to the characteristics of the old mortar adhered to recycled aggregates, which contributes to the overall creep behavior of RAC.

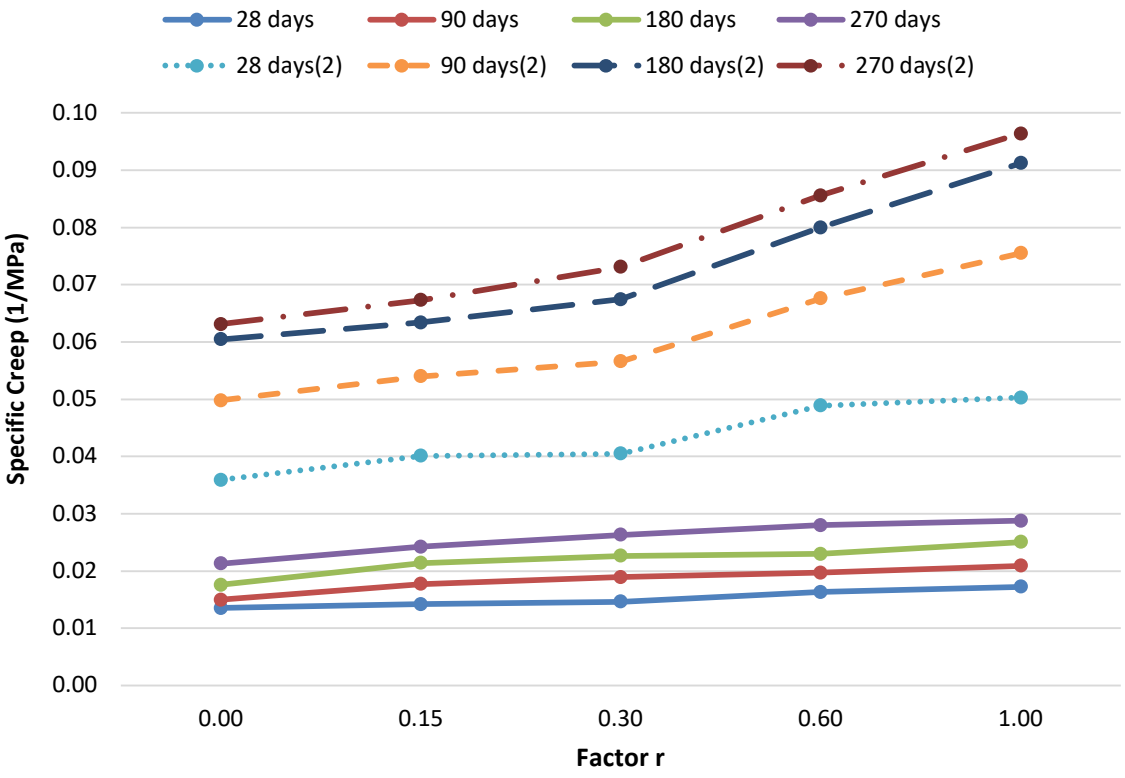

Figure 7. Specific creep for various recycled concretes at different replacement ratios of RCAs [115].

Overall, the mechanical performance of RCA concrete, while influenced by replacement ratios and material quality, can be effectively optimized through mix design and treatment strategies. However, ensuring the long-term serviceability of such concrete requires equal attention to its durability characteristics. In this context, the following section explores key

durability concerns, starting with carbonation, which plays a significant role in the long-term performance and sustainability of RCA-based concrete.

2.3. Durability properties of concrete with RCA

2.3.1. Carbonation

The carbonation of concrete made with RCA is an important concern for long-term durability, as the material's porosity tends to increase carbonation depth. Studies show that untreated RCA, when incorporated into concrete, can lead to an increase in carbonation depth due to the higher water absorption and porosity of RCA compared to natural aggregates [117,118]. For instance, untreated RCA increases the porosity of the concrete matrix, facilitating the ingress of carbon dioxide (CO_2) and leading to a faster rate of carbonation, which can impact the pH of concrete and promote the risk of steel reinforcement corrosion. Carbonation depth can increase by up to 20-30% in untreated RCA concrete compared to natural aggregate concrete.

Conversely, carbonation treatment of RCA has been shown to improve durability properties. The accelerated carbonation of RCA effectively reduces its porosity, leading to increased carbonation resistance in the resulting concrete [119]. For example, carbonated RCA (cRCA) has demonstrated reduced carbonation depth compared to untreated RCA due to the clogging of micro-pores by calcium carbonate deposits formed during carbonation [120]. The reduction in porosity can improve the density of the interfacial transition zone between the aggregates and the cement matrix, which is critical for enhancing concrete's resistance to environmental degradation.

The combination of carbonation and other treatments shows promising results for improving the mechanical and durability properties of RCA concrete. For instance, Malysz et al. (2022) [121] observed that combining air jigging technology and carbonation treatment significantly reduced carbonation depth in RCA concrete. Air jigging removes impurities such as mortar and ceramics from RCA, enhancing its mechanical strength and reducing its susceptibility to carbonation. However, despite these improvements, carbonation-treated RCA still exhibits lower carbonation resistance compared to natural aggregates, indicating the need for further optimization of treatment processes [122].

The variability of RCA characteristics presents challenges for maintaining consistent carbonation resistance. In repeated recycling cycles, RCA demonstrates progressively poorer resistance to carbonation, as shown in studies on second and third-generation RCA [118,123]. The loss of quality in RCA with each recycling cycle leads to increased porosity, and under freeze-thaw conditions, carbonation depth can increase further, making the concrete more vulnerable to environmental degradation.

In addition to mechanical improvements, accelerated carbonation can offer environmental benefits by sequestering CO_2 within the concrete matrix. The FastCarb project [124] has demonstrated the feasibility of storing significant amounts of CO_2 within RCA through accelerated carbonation processes. This approach not only improves the quality of RCA but also contributes to CO_2 mitigation, a crucial factor in reducing the carbon footprint of concrete production. Results from large-scale industrial trials show that up to 50 kg of CO_2 per ton of RCA can be captured through carbonation, significantly enhancing the sustainability of RCA-based concrete.

Finally, the impact of environmental conditions on carbonation treatment must be considered. Gholizadeh-Vayghan et al. (2020) [125] found that optimal carbonation conditions, such as controlled moisture levels and relative humidity, are crucial to achieving significant reductions in porosity and enhancing the mechanical and durability properties of RCA. However, suboptimal carbonation conditions can lead to limited improvements in durability, indicating the importance of precise control over the carbonation process to maximize the benefits for RCA concrete.

2.3.2. Chloride attack

Chloride ion attack is a critical durability concern for concrete, particularly in marine environments or regions exposed to de-icing salts. Wang et al. (2024) found a relationship between the chloride diffusion coefficient (a measure of how easily chloride ions penetrate concrete) and the recycled aggregate (RA) replacement ratio. The trend shows a generally linear increase in the chloride diffusion coefficient as the RA content increases, indicating that a higher proportion of recycled aggregates tends to facilitate chloride ion penetration into the concrete. This is primarily because recycled aggregates contain adhered mortar and interfacial transition zones (ITZs) that have higher porosity compared to natural aggregates, making the concrete more permeable. The slope of the increase is steeper in cases where the RA replacement ratio is closer to 100%, showing a more significant impact on chloride penetration at higher RA contents. This linear relationship is essential for understanding the durability concerns in recycled aggregate concrete (RAC), as higher chloride ion penetration could accelerate the corrosion of steel reinforcement in such structures, especially in aggressive environments like coastal areas or where de-icing salts are used. This research underscores the importance of treatments and modifications to recycled aggregates to mitigate this increased permeability [126].

The use of RCA in concrete has been increasingly promoted for sustainability; however, its vulnerability to chloride penetration due to higher porosity compared to natural aggregates poses challenges for long-term durability. Research shows that chloride ions penetrate more easily into RCA concrete, leading to reinforcement corrosion and a decrease in structural integrity [118,127].

To mitigate chloride ion penetration, carbonation treatments have emerged as an effective solution. Jiang et al. (2024) [128] showed that carbonated recycled coarse aggregate concrete (CRCAC) exhibited significantly reduced chloride penetration depths compared to untreated RCA concrete. The carbonated aggregates help to clog micro-pores, slowing chloride ingress and providing better protection for reinforcement in chloride-rich environments. In marine infrastructure, this treatment has been shown to extend the structure's durability life by up to 28%.

Adding supplementary cementitious materials such as fly ash, silica powder, and ground granulated blast furnace slag (GGBS) also enhances the chloride resistance of RCA-based concrete. Studies like those by Pandey & Rajhans (2023) [127] demonstrate that incorporating these materials in quaternary blends significantly reduces chloride permeability. Rapid Chloride Permeability Test (RCPT) results showed that quaternary blends containing RCA exhibited lower chloride ion ingress, improving the durability of the concrete in aggressive environments.

Other innovative methods for chloride resistance include surface treatments of RCA. Sasanipour & Aslani (2020) [77] investigated silica fume slurry coatings on RCA and observed enhanced resistance to chloride ion penetration. The treated RCA mixes showed reduced charge passed during RCPT, indicating less chloride migration through the concrete matrix. Such treatments also improved the concrete's overall strength and electrical resistivity, further contributing to better durability.

Incorporating fibers into RCA-based concrete offers another avenue for improving chloride resistance. Research by Lu et al. (2020) [129] demonstrated that adding basalt fibers and polypropylene fibers enhances the dynamic properties and chloride resistance of RCA concrete. The fibers contribute to a more compact microstructure, reducing chloride penetration and improving durability under cyclic loading and environmental exposure.

Chloride transport models play a key role in predicting the long-term durability of RCA concrete in chloride environments. Chen et al. (2020) [118] developed models based on chloride ion diffusion through RCA concrete, highlighting the importance of assessing the long-term chloride ingress behavior. These models help in designing mixes with optimal resistance to chloride attack, especially in infrastructure exposed to aggressive environments.

The use of calcined layered double hydroxides (LDOs) to capture chloride ions is another promising technique. Gao et al. (2024) [130] found that LDOs could significantly reduce chloride ion diffusion in RCA concrete. The LDOs function by adsorbing chloride ions, preventing them from migrating through the concrete matrix. This innovative approach enhances both mechanical performance and durability, offering a sustainable solution to chloride-induced degradation.

While these advancements improve chloride resistance in RCA concrete, the quality of RCA remains a challenge. The porosity of RCA, which arises from the attached mortar, is a primary pathway for chloride ions to penetrate. Strategies such as carbonation treatment, surface coatings, and the incorporation of supplementary materials offer substantial improvements, but further research is required to optimize these methods for widespread use.

2.3.3. Oxygen permeability

Oxygen permeability is a crucial parameter in assessing the durability of RCA as it significantly impacts the long-term performance of structures by allowing the ingress of harmful agents. Various studies have evaluated the effects of RCA on oxygen permeability, highlighting that due to the presence of old adhered mortar, RCA-based concrete tends to have higher porosity and permeability compared to natural aggregate (NA) concrete. This increased porosity can reduce the resistance to oxygen ingress, leading to accelerated carbonation and reinforcement corrosion [131,132]. However, methods such as partial RCA replacement and the addition of supplementary cementitious materials can mitigate this issue by refining the microstructure and reducing pore connectivity [133].

The porosity of RCA is a significant contributing factor to its higher oxygen permeability. As RCA is composed of both old mortar and aggregate, the attached mortar increases the interconnected pore structure, facilitating the movement of oxygen and other gases [134]. Kapoor et al. (2018) [135] reported that concrete containing RCA had higher oxygen permeability coefficients than concrete with natural aggregates, correlating this with the

higher porosity of RCA. The residual mortar in RCA can create weak zones in the concrete, which act as pathways for oxygen diffusion.

A comparison of the oxygen permeability between RCA and natural aggregate concretes conducted by Mahmood et al. (2022) [136] revealed that the permeability of RCA concrete is typically higher, especially at higher levels of RCA replacement. At 50% RCA replacement, oxygen permeability increases by nearly 30%, indicating a strong dependence on the quantity of RCA used. Similar findings were observed by Ismail et al. (2017) [133], who noted that higher RCA content correlates with greater oxygen permeability due to the increased volume of permeable voids within the RCA concrete matrix.

Thomas et al. (2013) illustrated the relationship between compressive strength and oxygen permeability of concrete with varying percentages of recycled aggregate replacement (0%, 20%, 50%, and 100%) in Figure 8 [137]. As the compressive strength increases, oxygen permeability decreases exponentially across all replacement levels, indicating that denser concrete resists gas penetration more effectively. The exponential models fit the data well, as indicated by high R^2 values (ranging from 0.89 to 0.99), suggesting strong predictive accuracy. The slope of the curves shows that higher recycled aggregate content slightly reduces the rate of permeability decrease.

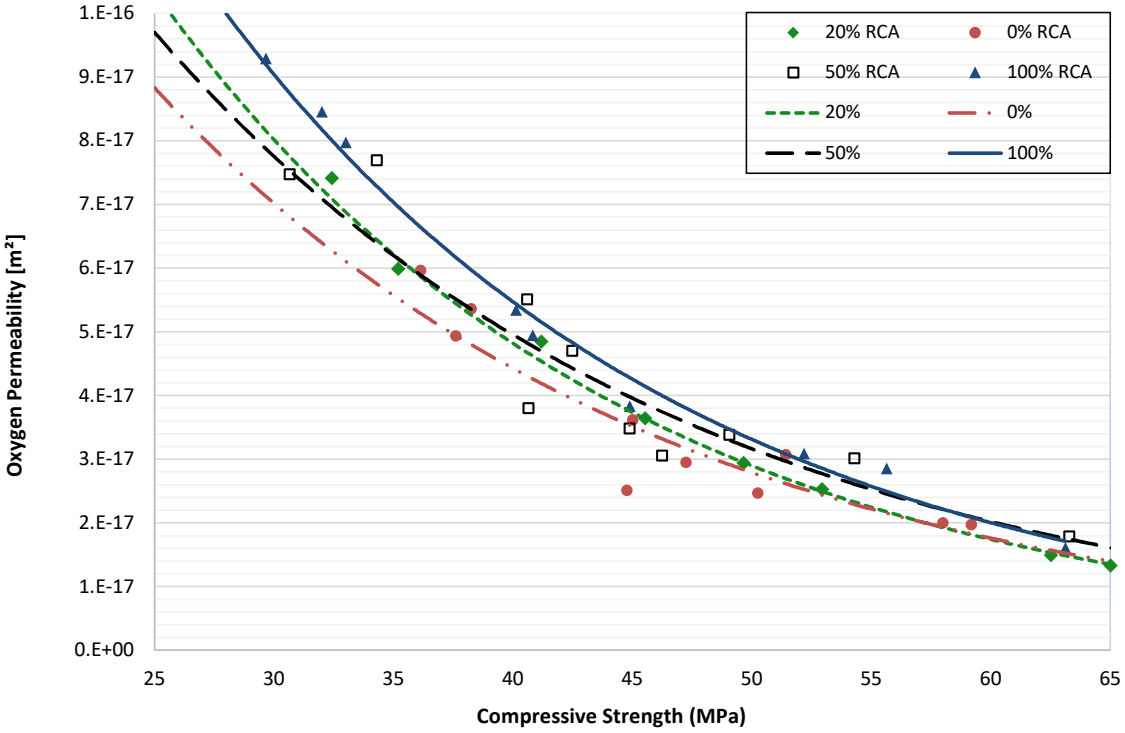

Figure 8. Relationship between oxygen permeability and compressive strength of recycled aggregate concrete (RAC) [137].

Various techniques have been proposed to mitigate the high permeability of RCA concrete. Studies by Safiuddin et al. (2013) [138] and Zhan et al. (2019) [139] suggest that the use of supplementary cementitious materials (SCMs) such as fly ash and silica fume can significantly reduce the oxygen permeability of RCA concrete. SCMs work by refining the pore structure and reducing the permeability of the cement matrix. For instance, Paul et al. (2013) [132] found that the use of 30% fly ash in RCA concrete reduced the oxygen permeability by up to 40%.

In addition to SCMs, pre-treatment of RCA has also shown promise in improving its performance with respect to oxygen permeability. Cantero et al. (2021) [134] investigated the use of recycled cement fines to coat RCA particles, thereby reducing their porosity and enhancing the overall durability of the concrete. Their results demonstrated a marked reduction in oxygen permeability, suggesting that surface treatment of RCA could be an effective strategy for reducing permeability in concrete applications.

The influence of oxygen permeability is further emphasized in RCA concrete under different curing conditions. Studies show that untreated RCA concrete exhibits higher oxygen permeability when exposed to open-air curing, compared to water curing. This permeability difference is due to the higher pore volume and the weaker interfacial transition zones (ITZ) in RCA concrete. However, treating RCA with carbonation or surface pretreatment methods like silica fume slurry can significantly reduce oxygen permeability, improving durability [140].

Research by Xuan et al. (2017) [141] found that carbonated RCA substantially reduces oxygen and gas permeability, enhancing the overall impermeability of the concrete matrix. These findings suggest that carbonation curing of RCA enhances the durability of concrete by filling micro-cracks and reducing pore volume, thereby impeding the transport of oxygen and other aggressive agents into the concrete.

Finally, the type and size of RCA particles used in concrete also influence oxygen permeability. Fine RCA tends to contribute more significantly to permeability than coarse RCA due to the higher specific surface area and greater volume of attached mortar [142]. Moreover, selective crushing methods that reduce the amount of adhered mortar on RCA have been shown to lower permeability, as demonstrated in studies by Kubissa et al. (2016) [143].

2.4. CO_2 Capturing in RCA

The integration of RCA in construction is gaining attention for its sustainability and potential for CO_2 capture through carbonation. This section explores recent scientific insights on CO_2 capture mechanisms in RCA, their efficiency, and their impact on the environment and material properties.

RCA capture CO_2 through a process called carbonation, where CO_2 reacts with calcium compounds in the concrete to form stable calcium carbonates. This reaction primarily occurs in porous areas of RCA, which increases its potential for carbon sequestration [144]. Additionally, accelerated carbonation processes enhance the CO_2 uptake capacity by increasing reaction rates [145].

It should be noted that several carbonation approaches reported in the literature are based on aqueous or slurry-phase processes, which promote enhanced CO_2 uptake by recycled aggregate particles due to improved gas–solid contact. However, despite their effectiveness at the laboratory scale, these aqueous carbonation techniques are currently of limited applicability at the industrial level. This limitation is mainly related to the need for additional water management, complex processing steps, and higher operational costs, which hinder their implementation in large-scale recycling plants. Consequently, although such methods demonstrate a high carbonation potential, their practical use in industrial RCA production remains challenging, and dry or semi-dry carbonation processes are generally considered more feasible for large-scale applications.

RCA can store significant amounts of CO_2, particularly when subjected to accelerated carbonation methods. Braymand et al. (2024) [146] employed a calcimetric method to measure CO_2 capture rates, highlighting that RCA sequestered 15-20% more CO_2 compared to natural aggregates under similar conditions. Additionally, Jiang et al. (2025) [147] showed that optimized aggregate grading and particle size distribution further enhanced CO_2 capture efficiency.

A life cycle assessment conducted by Ang et al. (2024) [148] demonstrated that using RCA with CO_2 capture reduced the carbon footprint of concrete production by 25-30% over the entire cradle-to-gate cycle. Similarly, Goh et al. (2025) [149] highlighted the techno-economic feasibility of mineralizing CO_2 within RCA, achieving both carbon capture and material performance enhancement.

Carbonation not only captures CO_2 but also strengthens the RCA by densifying its microstructure. Zhu et al. (2024) [150] analyzed the structural properties and found a 17.6% reduction in porosity, which improved compressive strength and reduced water absorption. However, carbonation reduces the alkalinity of concrete (see [145]), posing a risk for steel reinforcement corrosion by lowering the pH and diminishing the passive protection provided to rebars.

Several innovative carbonation techniques have been proposed to enhance CO_2 capture efficiency. Tham et al. (2024) [151] developed an integrated CO_2 capture and mineralization process with lower energy consumption, which reduced operational costs while maintaining high capture efficiency. Additionally, Chong et al. (2024) [152] introduced an aqueous CO_2 sequestration method suitable for ready-mix concrete containing RCA, demonstrating its industrial scalability. Despite promising results, some challenges remain. Jiang et al. (2025) [147] pointed out that the efficiency of CO_2 capture in RCA decreases over time as the surface becomes saturated with carbonates.

Future research should focus on optimizing carbonation conditions, such as temperature, pressure, and humidity, to maximize CO_2 uptake. Additionally, combining RCA carbonation with other sustainable construction practices, such as using cement substitutes, can further reduce the carbon footprint [153]. Life cycle assessments should continue to guide the development of eco-friendly construction practices [148].

2.5. Life Cycle Assessment (LCA) in RCA

The application of Life Cycle Assessment (LCA) in RCA has become a critical tool in evaluating its environmental, economic, and sustainability aspects. With increasing efforts to adopt sustainable construction materials, understanding RCA's full lifecycle impact is essential for optimizing its use while minimizing its carbon footprint. Recent studies have provided valuable insights into the benefits, challenges, and comparative assessments of RCA versus natural aggregates, emphasizing the importance of a holistic LCA approach in construction.

One of the fundamental advantages of RCA, as highlighted by Ang et al. (2024) [148], is its reduction in carbon footprint compared to natural aggregates. Their study demonstrated that incorporating RCA in concrete mixtures can reduce CO_2 emissions by 30-40%, depending on factors such as processing techniques and transportation distances. Similarly, Huang & Wang (2024) [154] assessed geopolymer concrete incorporating RCA and found a 25% lower global

warming potential (GWP) compared to conventional concrete, further validating its sustainability potential.

Another key component in RCA's life cycle is its energy and water consumption. The crushing and processing of RCA require less energy compared to virgin aggregates, making it a more energy-efficient option. A study conducted by Huang et al. (2025) [155] on LC3 concrete (limestone calcined clay cement) with RCA found that its embodied energy was 18% lower than traditional concrete, primarily due to lower heat requirements in processing.

The economic viability of RCA is also an important aspect of LCA studies. While RCA offers significant environmental advantages, its cost-effectiveness depends on transportation distances, processing costs, and mix design optimizations. Research by Manan et al. (2025) [156] found that transportation distance was the most significant cost factor in RCA utilization. However, when sourced locally, RCA could be 15-20% more cost-effective than virgin aggregates, making it a viable solution for sustainable construction projects. On the other hand, Ma et al. (2025) [157] conducted an LCA comparing RCA blended with Supplementary Cementitious Materials (SCMs) and found that CO_2 emissions were reduced by 40-50%, further strengthening the case for RCA in sustainable concrete production.

Future research in RCA life cycle assessment should focus on digital modeling and optimization tools that allow for more accurate impact predictions. Pradhan et al. (2024) [158] proposed the use of digital twin models and machine learning algorithms to simulate long-term environmental benefits of RCA-based structures, providing better data-driven decisions for sustainability. With continued advancements in carbon capture, material optimization, and LCA standardization, RCA is set to play an even more critical role in reducing the construction sector's environmental impact.

In conclusion, LCA studies confirm that RCA presents a viable, sustainable alternative to natural aggregates, offering substantial reductions in carbon emissions, energy use, and environmental degradation. Although economic and regional barriers still exist, ongoing research and policy support can further improve its adoption. As industries continue to seek greener alternatives, RCA when optimized through LCA frameworks, offers a promising path toward truly sustainable construction.

3. Materials and Methods

In this study, CEM II A-LL 42.5 R (Portland limestone cement) was used for the preparation of all concrete mixtures. This cement complies with the chemical requirements of sulphates (as SO_3) ≤ 4.0% and chloride content ≤ 0.10%. Potable water conforming to ASTM C1602 [159] specifications free of any impurities or additives, was employed for mixing. A superplasticizer (CHRYSO® Quad 890) was and aggregates were characterized in terms of maximum particle size, water absorption, and dry density. Table 2 presents the detailed physical properties of the aggregates used in both the 2023 and 2024 campaigns.

Table 2. Specifications of the aggregates.

Component	Agg. Size [mm]	Wat. Absorption [%]	Dry density [kg/m³]
2023 Campaign			
Coarse Natural	[5-12.5]	0.9	2690
Fine Natural	[0.063-5]	1.5	2830
Coarse Recycled	[5-12.5]	6.4	2460
Fine Recycled	[0.063-5]	12.9	2240
2024 Campaign			
Coarse Natural	[5-12.5]	0.63	2780
Fine Natural	[0.063-5]	1.3	2750
Coarse Recycled	[5-12.5]	5.8	2450
Fine Recycled	[0.063-5]	10.6	2320

The recycled concrete aggregates (RCA) used in this study were obtained from commercial recycling facilities processing construction and demolition waste (CDW) and were not produced by crushing laboratory-made concrete specimens. The aggregates therefore reflect the characteristics of real recycled materials currently available on the construction market. According to the information provided by the supplier, the RCA consisted predominantly of crushed concrete particles, with minor fractions of masonry-related materials (such as brick fragments) and negligible amounts of other constituents (e.g., glass or asphalt).

A detailed particle-by-particle compositional analysis was not performed; however, visual inspection and supplier documentation confirmed that concrete-derived particles represented the dominant fraction of the recycled aggregates. This is consistent with typical RCA obtained from structural concrete demolition, as widely reported in the literature. The presence of attached mortar on the surface of the recycled aggregates was evident and represents a key distinguishing feature compared to natural aggregates. Although the attached mortar content was not quantitatively measured, its influence is indirectly reflected in the higher water absorption, lower density, and reduced stiffness observed for mixes with higher RCA replacement levels.

The parent concrete from which the RCA originated was not characterized in terms of compressive strength; however, given the source from conventional building demolition, it is reasonable to assume that it corresponds to normal-strength concrete, typically ranging between C25/30 and C35/45. This assumption is consistent with values commonly reported for recycled aggregates sourced from commercial CDW recycling plants and provides a

realistic basis for interpreting the mechanical and durability performance observed in this study.

To examine the influence of recycled aggregate replacement on concrete performance, four concrete mix designs were formulated for each campaign. These are summarized in Table 3. The notation of each mix (e.g., M 30-30) reflects the replacement percentage of fine and coarse natural aggregates with recycled aggregates. For instance, M 30-30 denotes a mixture with 30% replacement of both fine and coarse aggregates by recycled ones.

Table 3. Mix compositions.

Mix	Cement [kg/m³]	Water/Cement	Fine RA (%)	Coarse RA (%)	Fine NA [kg/m3]	Coarse NA [kg/m3]	Fine RA [kg/m3]	Coarse RA [kg/m3]
2023 Campaign								
M 0-0	366	0.51	0	0	893	893	0	0
M 30-30	366	0.51	30	30	536	536	223	223
M 50-50	366	0.51	50	50	370	370	400	350
M 100-100	366	0.51	100	100	0	0	700	700
2024 Campaign (Sarcos)								
M 0-0	366	0.51	0	0	1002	903	0	0
M 20-20	366	0.51	20	20	801	720	157	155
M 70-70	366	0.51	70	70	300	270	552	542
M 100-100	366	0.51	100	100	0	0	789	775

All concrete mixes were designed with a fixed water-to-cement (w/c) ratio of 0.51. However, due to the higher water absorption capacity of the recycled aggregates, all aggregates were pre-saturated prior to mixing. This approach ensured that the effective water available for cement hydration remained consistent across all mixtures. Consequently, the total mixing water varied depending on the quantity of recycled aggregates in the mix.

Figure 9 and Figure 10 present the granulometric distributions of the aggregates employed in the experimental campaigns conducted in 2023 and 2024, respectively. Figure 9 shows the particle size distribution curves of both natural and recycled aggregates used in the 2023 mixes, highlighting the differences in gradation among the various aggregate types. These variations in particle size distribution directly affect the mechanical performance and workability of the concrete, as they influence packing density, water demand, and overall mix compactness.

Similarly, Figure 10 illustrates the granulometry curves for the aggregates utilized in the 2024 campaign. The comparison between natural and recycled aggregates reveals consistent differences in grading trends, particularly in the finer fraction of RCA, which tends to increase due to the presence of residual mortar. Such discrepancies in gradation play a crucial role in determining the fresh and hardened properties of the resulting concrete, ultimately influencing both its mechanical strength and durability.

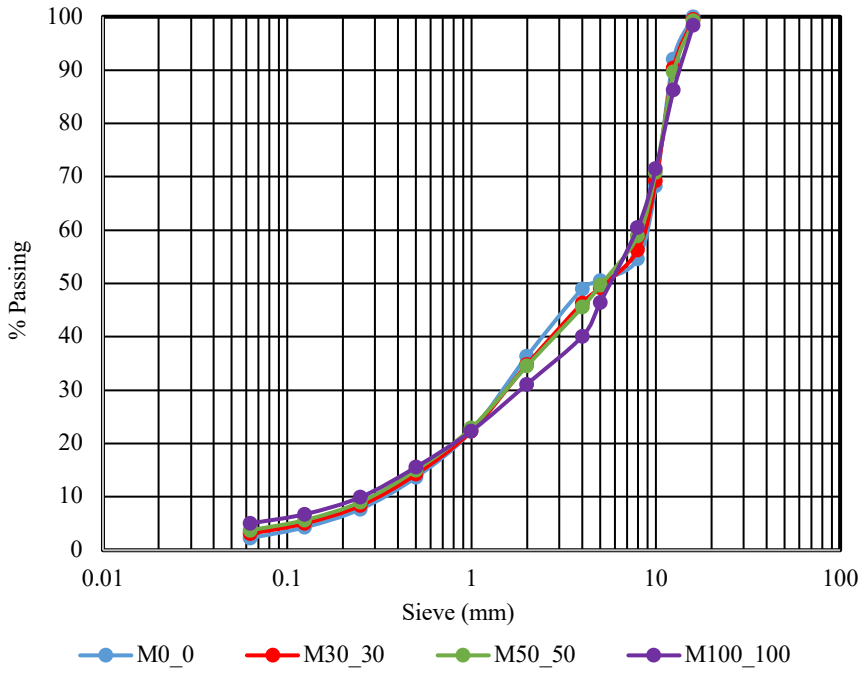

Figure 9. Particle size distribution of natural and recycled aggregates used in the 2023 campaign.

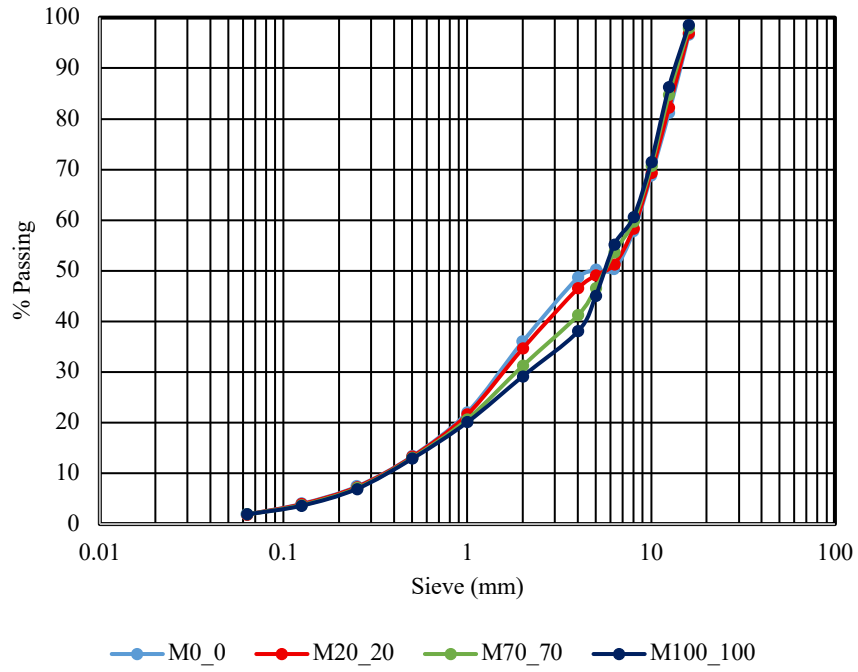

Figure 10. Particle size distribution of natural and recycled aggregates used in the 2024 campaign.

After casting, all specimens were stored under standard laboratory conditions (23 ±2°C) for 24 hours, after which they were demolded. The demolded specimens were then wrapped in plastic sheets and stored for curing until the designated testing age.

4. Mechanical Characterization of RCA Concrete

4.1. Compressive and Tensile Strength

This chapter presents the experimental program developed to investigate the mechanical performance of concrete incorporating fine and coarse recycled concrete aggregates (RCA), as well as the structural behavior of composite slabs produced with these materials. The experimental campaign was conceived with reference to typical composite slab applications, where concrete works in combination with profiled steel sheeting. Starting from this baseline, different replacement ratios of natural aggregates with recycled concrete aggregates were investigated to assess their influence at material and structural scale.

In this study, cubic samples were also prepared using 150 × 150 × 150 mm cube molds for mechanical tests. The cubic samples were kept in standard laboratory conditions for 24 hours (at a temperature of 23 ± 2 °C) and then removed from the molds. Subsequently, the samples were cured by being wrapped in plastic covers. The cube samples underwent curing for 7, 28, and 90 days.

The compressive strength of concrete cube specimens was evaluated in accordance with EN 12390-3 [160]. Tests were performed using a hydraulic compression machine (Controls Testing Equipment Ltd.) with a maximum capacity of 3000 kN, equipped with a digital load control system. A uniform loading rate of 0.4 MPa/s was applied until failure. For each mix and curing age, at least three specimens were tested, and the average compressive strength was recorded. Prior to testing, samples were removed from curing, surface-dried, and inspected for defects to ensure data reliability.

Additionally, a 28-day splitting test was conducted, according to the standards outlined in EN 12390-6 [161]. In this case, the same load-controlled machine was used, along with a suitable steel frame design, to subject the concrete cubes to a splitting tensile test at a constant load rate of 0.04 MPa/s. The impact of replacing recycled concrete aggregates on the compressive strength of cube concrete samples at 7 and 90 days of 2023 campaign is presented in Figure 11. Furthermore, Figure 12 depicts the results obtained from the compression and the tensile test after 28 days. The M0-0 mix, which contains 0% RCA, exhibited a 28-day compressive strength of 43 MPa. This value is consistent with the performance of C30/37 concrete, in accordance with EN 206 [162] standard, which is commonly used in composite slab applications. The compliance with industry standards ensures that the control specimen provides a reliable baseline for comparing the effects of RCA on the mechanical properties of composite slabs.

The presented results indicate that an increase in the replacement of recycled concrete aggregates leads to a reduction in the compressive strength at 7, 28, and 90 days, as well as the tensile strength at 28 days. Specifically, for the M100-100 mix design with complete replacement of fine and coarse recycled concrete aggregates, as compared to the M 0-0 mix design with natural aggregate, there is a decrease in compressive strength of approximately 17 MPa for the 90-day compressive strength. This phenomenon can be attributed to the weaker nature of the recycled concrete aggregates in the interfacial transition zone (ITZ) compared to natural aggregate. The presence of mortar adhered to the recycled aggregate contributes to this weakness.

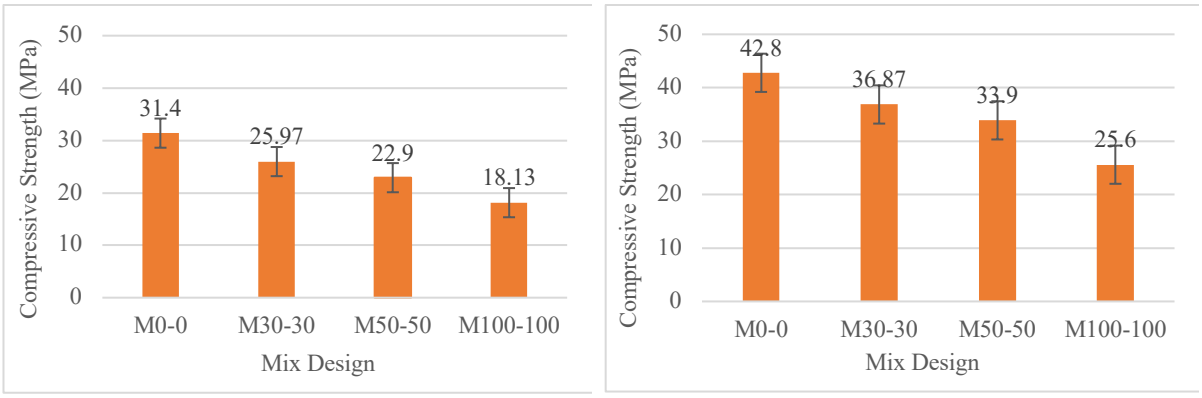

Figure 11. 2023 Campaign. Effect of recycled concrete aggregates replacement on compressive strength: a) 7 days, b) 90 days.

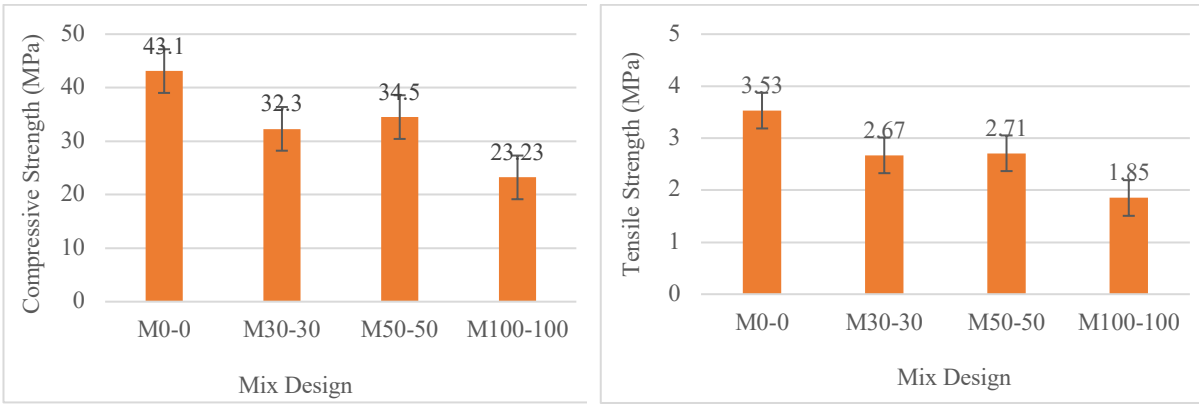

Figure 12. 2023 Campaign. Effect of recycled concrete aggregates replacement after 28 days of curing: a) compressive and b) tensile strength.

The influence of RCA replacement on compressive strength at 7 and 90 days of 2024 campaign is presented in Figure 13, while the results for compressive and tensile strength at 28 days are shown in Figure 14 at 7 days, compressive strength ranged from 28.3 MPa for M100-100 to 34.0 MPa for M70-70. After 90 days of curing, strength development was observed across all mixes, with M70-70 achieving the highest value of 46.2 MPa, slightly higher than the control M0-0 (43.8 MPa) and M20-20 (44.2 MPa). In contrast, the fully recycled mix M100-100 exhibited the lowest value, with 36.1 MPa.

At 28 days, compressive strength results indicated similar performance for M0-0 (38.2 MPa), M20-20 (38.1 MPa), and M70-70 (39.9 MPa), whereas M100-100 recorded a reduced strength of 32.9 MPa. The corresponding tensile strength results demonstrated a comparable trend. The control mix M0-0 reached 2.91 MPa, while M20-20 and M70-70 slightly improved performance, showing 3.21 MPa and 3.11 MPa, respectively. On the other hand, M100-100 achieved only 2.37 MPa, confirming the negative effect of complete RCA substitution.

Overall, the 2024 campaign results suggest that partial replacement of natural aggregates with 20–70% RCA can maintain, or even slightly enhance, both compressive and tensile strength relative to conventional concrete. However, complete replacement led to a marked reduction in mechanical performance, mainly due to the higher porosity and weaker interfacial transition zone associated with RCA.

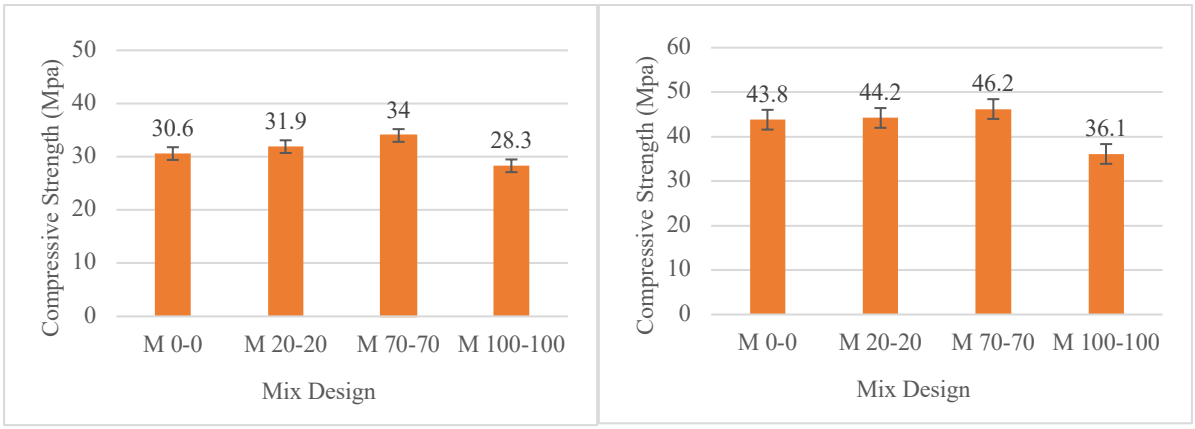

a) b)

Figure 13. 2024 Campaign. Effect of recycled concrete aggregates replacement on compressive strength: a) 7 days, b) 90 days.

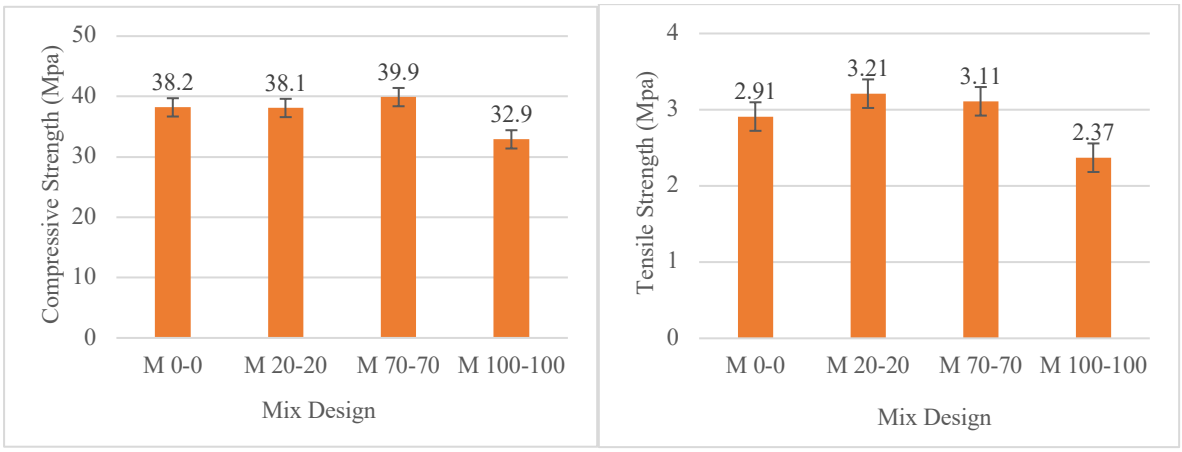

a) b)

Figure 14. 2024 Campaign. Effect of recycled concrete aggregates replacement after 28 days of curing: a) compressive and b) tensile strength.

The results in Figure 15 illustrate a clear decline in compressive strength with increasing replacement levels of RCA across both the 2023 and 2024 experimental campaigns. In the 2023 series, the 28-day strength dropped from approximately 41.6 MPa at 0% RCA to 24 MPa at 100%, reflecting a sharp regression slope of −0.1837 MPa per percent RCA. At 90 days, strength values ranged from approximately 42.4 MPa to 27 MPa, following a slightly less steep slope of −0.1701 MPa per percent RCA.

In contrast, the 2024 campaign used the same mix design but employed different recycled aggregates. As a result, strength retention improved significantly. At 28 days, the strength declined more gradually from around 40 MPa to 35 MPa, with a regression slope of −0.0576 MPa per percent RCA. At 90 days, the variation was even smaller, with strength decreasing from 45.3 MPa to 40 MPa (slope: −0.0378), indicating better long-term performance.

The reduction in compressive strength with increasing RCA content is primarily attributed to the intrinsic deficiencies of recycled aggregates. These include higher porosity, adhered mortar, and a weaker ITZ, which compromise internal bonding and load transfer. However,

the improved performance in the 2024 campaign highlights the pivotal role of aggregate quality, even when the mix proportions are identical. The better results may be linked to lower water absorption, improved gradation, or reduced contamination in the 2024 RCA batch.

Furthermore, strength gains observed at 90 days in both campaigns demonstrate the benefit of extended curing, which likely enhances hydration and supports improved microstructural development within the concrete matrix. Regression trends confirm that compressive strength loss was more pronounced in the 2023 campaign, especially at early ages. In comparison, the flatter slopes in the 2024 data suggest that RCA type and processing quality significantly influence long-term mechanical behavior.

These findings support the conclusion that although higher RCA contents can reduce early-age strength, optimizing RCA quality and allowing for sufficient curing can effectively mitigate such losses. Therefore, recycled aggregate concrete with well-characterized RCA has potential for structural applications in sustainable construction, provided that performance requirements are met.

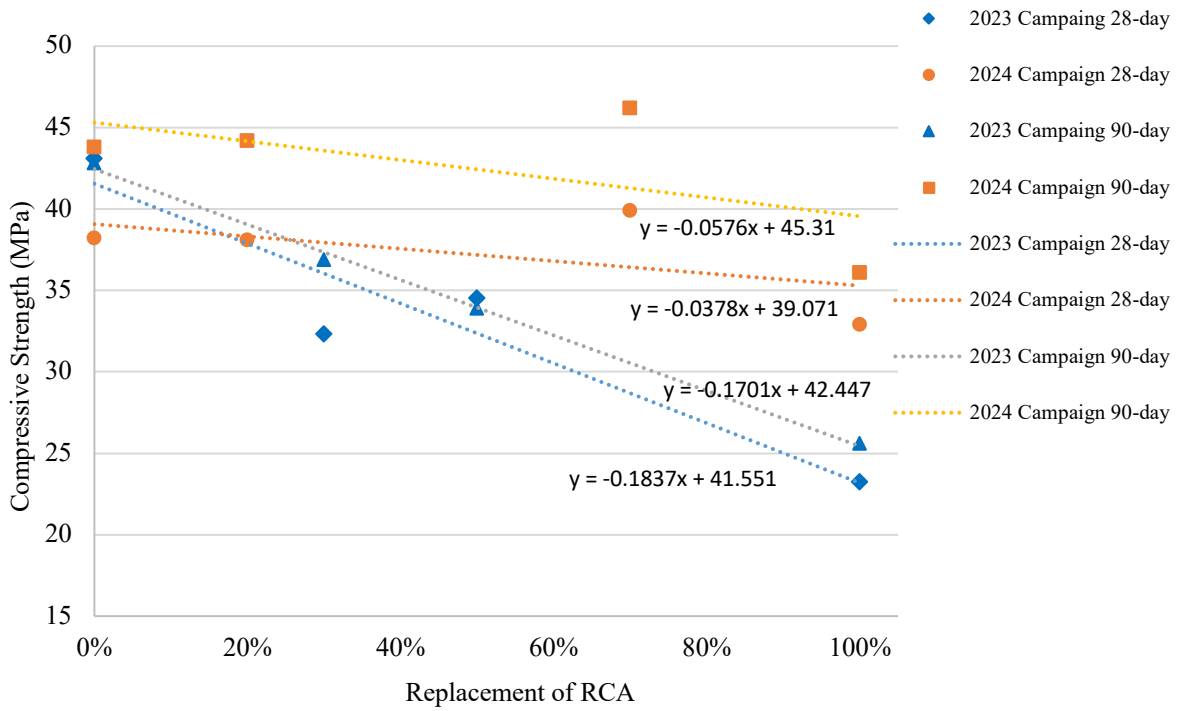

Figure 15. Evolution of compressive strength at 28 and 90 days as a function of RCA replacement ratio for the 2023 and 2024 campaigns.

4.2. Modulus of Elasticity

The Modulus of Elasticity in compression was determined in accordance with UNI-EN 12390-13:2013 [163] For each concrete type, two cylindrical specimens with diameters of 150 mm and heights of 300 mm were fabricated and tested. A servo-controlled compression testing machine equipped with Linear Variable Differential Transformers (LVDTs) was used to record axial strain during loading. The load was applied gradually, reaching up to 40% of each specimen's compressive strength to ensure the measurement was taken within the elastic range. The secant modulus was calculated based on the linear portion of the stress-strain curve. The average result from two specimens was recorded for each mix.

Figure 16. Modulus of Elasticity test.

Table 4 presents the average Modulus of Elasticity values and the corresponding coefficient of variation (CoV) for each mix in the 2023 and 2024 campaigns. A consistent reduction in stiffness was observed as the RCA replacement level increased. In the 2023 series, the modulus dropped from 34.7 GPa for the control mix (M 0-0) to 16.7 GPa for the fully recycled mix (M 100-100). Intermediate values included 22.5 GPa for M 30-30 and 23.7 GPa for M 50-50. In the 2024 campaign, the results followed a similar trend but with slightly higher values at partial replacement levels. The modulus decreased from 34.4 GPa for M 0-0 to 18.2 GPa for M 100-100. Notably, M 20-20 and M 70-70 achieved values of 30.1 GPa and 25.2 GPa, respectively, indicating improved stiffness compared to their 2023 counterparts.

Table 4. Average Modulus of Elasticity and Coefficient of Variation (CoV) for Concrete Mixes with Varying RCA Replacement Levels in 2023 and 2024 Campaigns.

2023 Campaign			**2024 Campaign**		
Mix	**Average [GPa]**	**CoV (%)**	**Mix**	**Average [GPa]**	**CoV (%)**
M 0-0	34.7	13.43	**M 0-0**	34.4	14.69
M 30-30	22.5	0.53	**M 20-20**	30.1	1.56
M 50-50	23.7	1.45	**M 70-70**	25.2	3.36
M 100-100	16.7	0.03	**M 100-100**	18.2	4.81

As illustrated in Figure 17, both campaigns demonstrated a clear linear relationship between RCA content and modulus reduction. The regression slopes were −0.1626 GPa per percent RCA for 2023 and −0.1497 GPa per percent RCA for 2024. These results reflect the lower stiffness of recycled aggregates, which is typically influenced by factors such as residual mortar, higher porosity, and weaker interfacial bonding. However, the RCA used in 2024 showed more favorable behavior. This improvement may be due to better aggregate gradation, reduced impurities, or lower water absorption. Across both campaigns, the CoV values remained within acceptable ranges, confirming the repeatability and reliability of the testing.

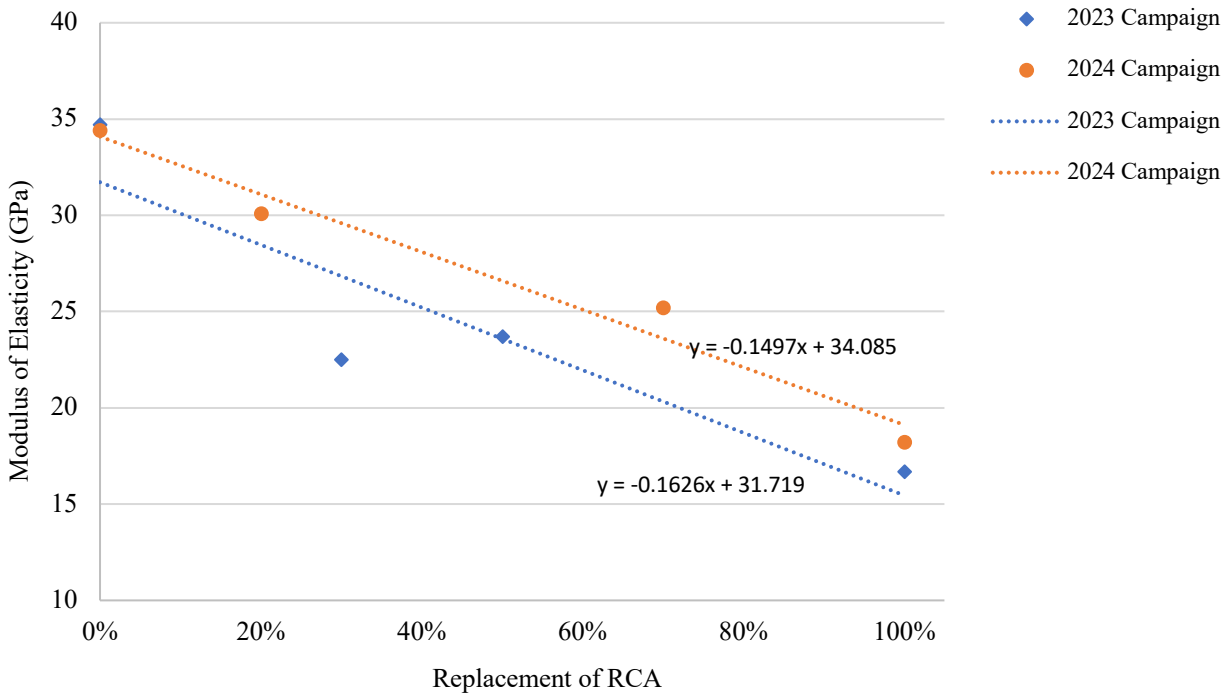

Figure 17. Variation of Modulus of Elasticity with RCA Replacement Level for 2023 and 2024 Campaigns at 28 Days.

These results confirm that the Modulus of Elasticity is significantly affected by RCA content and aggregate quality. Although stiffness decreases with increased RCA usage, proper selection and processing of recycled aggregates can reduce this negative effect. This insight is particularly important for structural applications where elastic behavior and long-term deformation control are critical.

5. Durability Assessment

5.1. Oxygen Permeability

The oxygen permeability coefficient was determined in accordance with the UNI 11164:2005 standard [164], which evaluates the ability of concrete to resist oxygen diffusion, a critical factor in assessing long-term durability and the risk of reinforcement corrosion. For each mix, three cylindrical specimens with a diameter of 150 millimeters and a height of 50 millimeters were tested after 28 days of curing. The test involved applying a controlled oxygen pressure gradient across the specimen in five incremental levels ranging from 1.50×10^5 to 3.50×10^5 pascals. The permeability coefficient, expressed in square meters, was calculated based on the steady-state gas flow rate through the concrete. The average value from the three specimens was recorded as the representative coefficient for each mix.

Figure 18. Oxygen permeability test.

Table 5 presents the oxygen permeability coefficients for all mixes from the 2023 and 2024 campaigns. In the 2023 series, a significant and consistent increase in permeability was observed with increasing recycled concrete aggregate (RCA) content. The control mix (M 0-0) recorded the lowest value at 5.65×10^{-15} m², while the fully recycled mix (M 100-100) showed a value of 2.18×10^{-13} m². Intermediate mixes exhibited gradual increases, with M 30-30 reaching 2.53×10^{-14} m² and M 50-50 reaching 4.81×10^{-14} m².

The results from the 2024 campaign displayed more variability. The control mix (M 0-0) recorded a permeability of 3.55×10^{-14} m². While mixes M 20-20 and M 100-100 reached higher values of 1.03×10^{-13} m² and 1.28×10^{-13} m² respectively, the M 70-70 mix yielded a noticeably lower value of 2.31×10^{-14} m². This irregular pattern suggests a weaker correlation between RCA content and oxygen permeability in the 2024 mixes.

Table 5. Oxygen permeability coefficients of concrete mixes with varying recycled aggregate content in the 2023 and 2024 campaigns.

2023 campaign	Mix code	Oxygen permeability coefficient (m^2)	2024 campaign	Mix code	Oxygen permeability coefficient (m^2)
M0-0	0	5.65E-15	M 0-0	0	3.55E-14
M30-30	30	2.53E-14	M 20-20	20	1.03E-13
M50-50	50	4.81E-14	M 70-70	70	2.31E-14
M100-100	100	2.18E-13	M 100-100	100	1.28E-13

Overall, these findings confirm that oxygen permeability is governed not only by the proportion of RCA but also by its intrinsic physical characteristics, particularly porosity and the condition of the adhered mortar. Appropriately processed recycled aggregates can substantially mitigate the adverse effects commonly associated with RCA on gas transport behavior.

In general, mixtures exhibiting higher compressive strength showed lower oxygen permeability, reflecting a denser and more refined pore network. This indicates that, although strength is a useful indicator of gas resistance, inherent differences in aggregate source and quality continue to influence permeability.

These results are consistent with previous studies, which identified oxygen permeability as a reliable microstructural indicator of concrete compactness and overall durability [165].

5.2. Water Permeability

Water permeability was assessed according to the UNE-EN 12390-8 standard [166], which determines the maximum depth of water penetration under pressure as a measure of concrete's pore connectivity and resistance to fluid ingress. For each mix, three specimens were tested after 28 days of curing. A constant water pressure was applied for 72 hours, after which the specimens were split, and the maximum penetration depth was measured visually in millimeters.

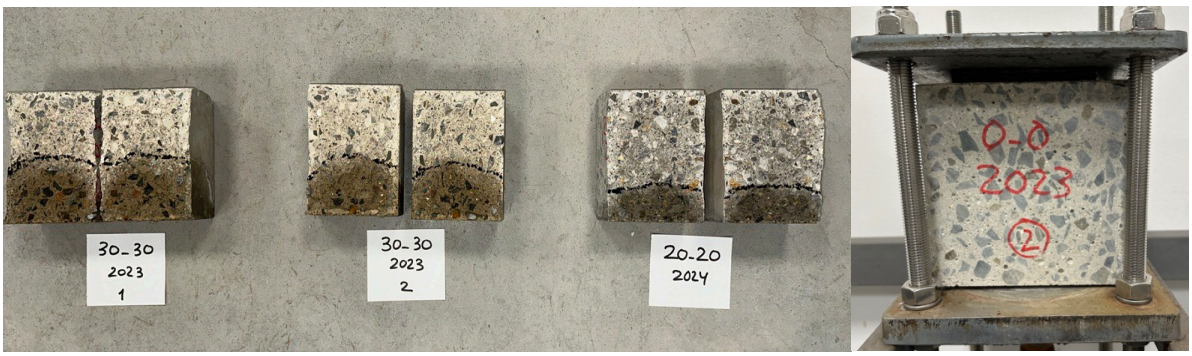

Figure 19. Oxygen permeability test.

The results are shown in Figure 20. In the 2023 campaign, penetration depth increased with higher RCA content. The control mix (M 0-0) recorded 57 millimeters, while M 30-30 and M 100-100 reached 74 and 78 millimeters respectively. In contrast, M 50-50 showed a lower

depth of 36 millimeters, indicating better performance at this intermediate level. This may be due to favorable particle packing or reduced permeability pathways at that replacement ratio.

In the 2024 campaign, the control mix (M 0-0) recorded 45 millimeters. Mixes M 20-20 and M 70-70 displayed similar depths of 43 and 40 millimeters, while M 100-100 showed a noticeable increase to 70 millimeters. These values suggest that partial use of 2024 RCA can retain or even improve water permeability performance, but full replacement still compromises durability.

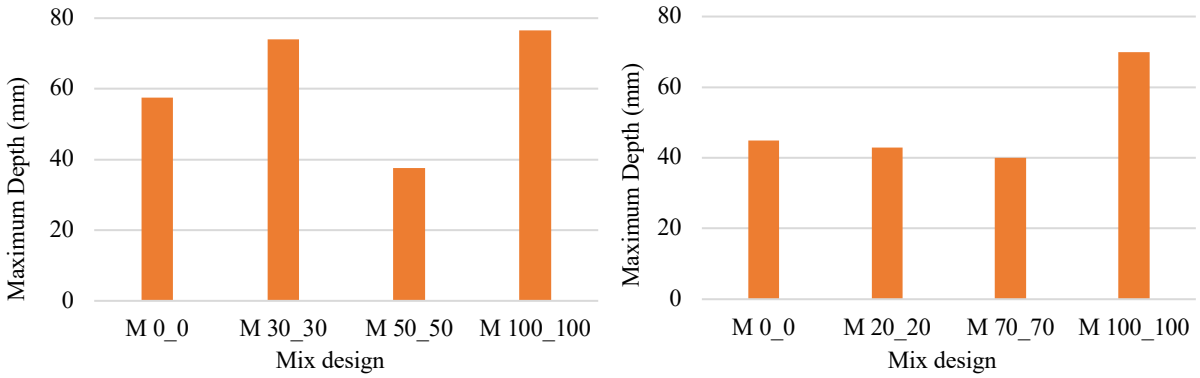

Figure 20. Maximum water penetration depths (mm) for concrete mixes from the 2023 (left) and 2024 (right) campaigns.

The greater water permeability observed in the 2023 mixes can be attributed to the higher porosity and weaker ITZ associated with the RCA batch used in that campaign. The adhered old mortar increases overall pore connectivity and facilitates capillary suction, which in turn accelerates water ingress. Conversely, the improved performance of the 2024 campaign suggests that its RCA possessed a denser matrix and lower absorption capacity, reducing the continuity of permeable pathways within the hardened concrete. This observation aligns with established findings in the literature, where improved RCA quality and pre-saturation treatments have been shown to significantly reduce permeability and enhance overall durability [165,167].

Overall, the water penetration results confirm that while increasing RCA content generally reduces water-tightness, the extent of this reduction is strongly governed by aggregate quality. Therefore, the 2024 campaign demonstrates that by selecting and processing recycled aggregates appropriately, RAC can achieve permeability levels suitable for use in moderate exposure classes, supporting its viability as a sustainable alternative to conventional concrete.

5.3. Carbonation Depth

The carbonation test was performed in accordance with UNE-EN 12390-12 [168], which evaluates the depth of carbon dioxide ingress into concrete. This test provides insight into the potential risk of reinforcement corrosion due to loss of alkalinity in the concrete matrix. For each mix, three specimens were exposed to accelerated carbonation conditions and split at designated intervals of 7, 14, and 28 days. The carbonation depth was measured using phenolphthalein indicator, and the average of three readings per specimen face was recorded.

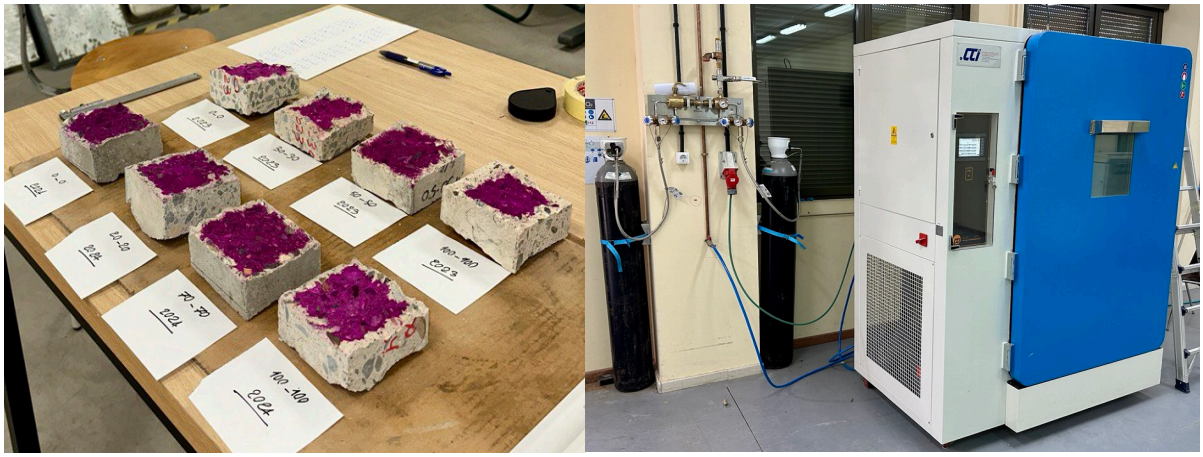

Figure 21. Carbonation test.

The absolute carbonation depths are presented in Figure 22. In the 2023 campaign, carbonation depth increased with both exposure time and RCA content. At 28 days, M 0-0 showed a depth of 11.96 mm, while M 30-30 and M 100-100 reached 15.42 mm and 20.92 mm, respectively. The M 50-50 mix exhibited a depth of 11.92 mm, similar to the control, suggesting improved microstructural performance at this intermediate level.

In the 2024 campaign, similar temporal and compositional trends were observed. The control mix (M 0-0) recorded 8.88 mm at 28 days, while M 100-100 reached 12.29 mm. Intermediate replacements such as M 20-20 and M 70-70 achieved values of 11.92 mm and 9.75 mm, respectively. Compared to the 2023 series, 2024 mixes showed lower carbonation depths at each replacement level, suggesting improved resistance due to better aggregate quality and matrix refinement.

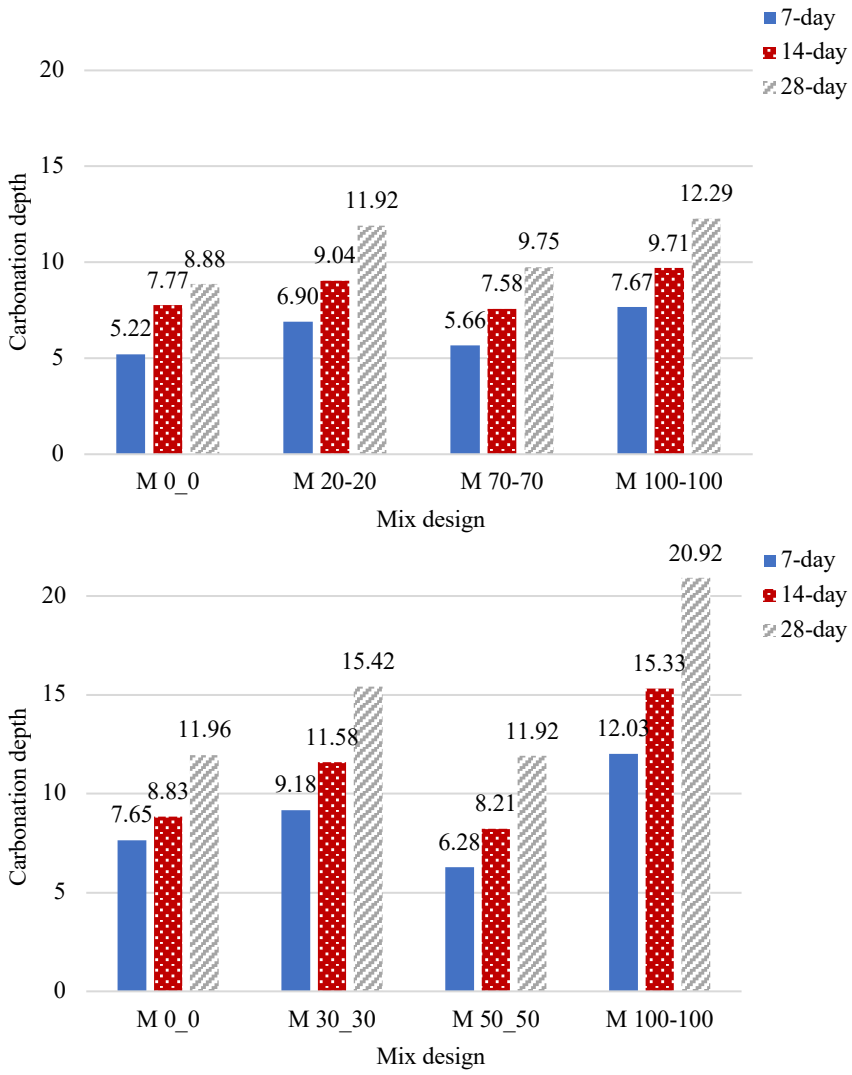

Figure 22. Carbonation depth at 7, 14, and 28 days for concrete mixes from the 2023 (top) and 2024 (bottom) campaigns.

To better isolate the effect of RCA content, Figure 23 presents carbonation depth normalized to the control mix for each campaign and exposure time. This allowed for direct comparison of the relative performance of RCA-based mixes. In both campaigns, a consistent increasing trend was observed with higher RCA content. However, the rate of increase was steeper in the 2023 series, especially at 14 and 28 days. The 2024 campaign exhibited flatter slopes across all time points, indicating that aggregate quality significantly influenced carbonation resistance beyond just the replacement ratio.

Together, the absolute and normalized results confirm that carbonation resistance decreases with increasing RCA content, particularly at full replacement. However, mixes incorporating high-quality RCA, such as those in the 2024 campaign, can achieve acceptable or even enhanced carbonation performance at partial replacement levels. These findings emphasize the importance of both RCA processing and optimal replacement levels in designing concrete for carbonation-critical environments.

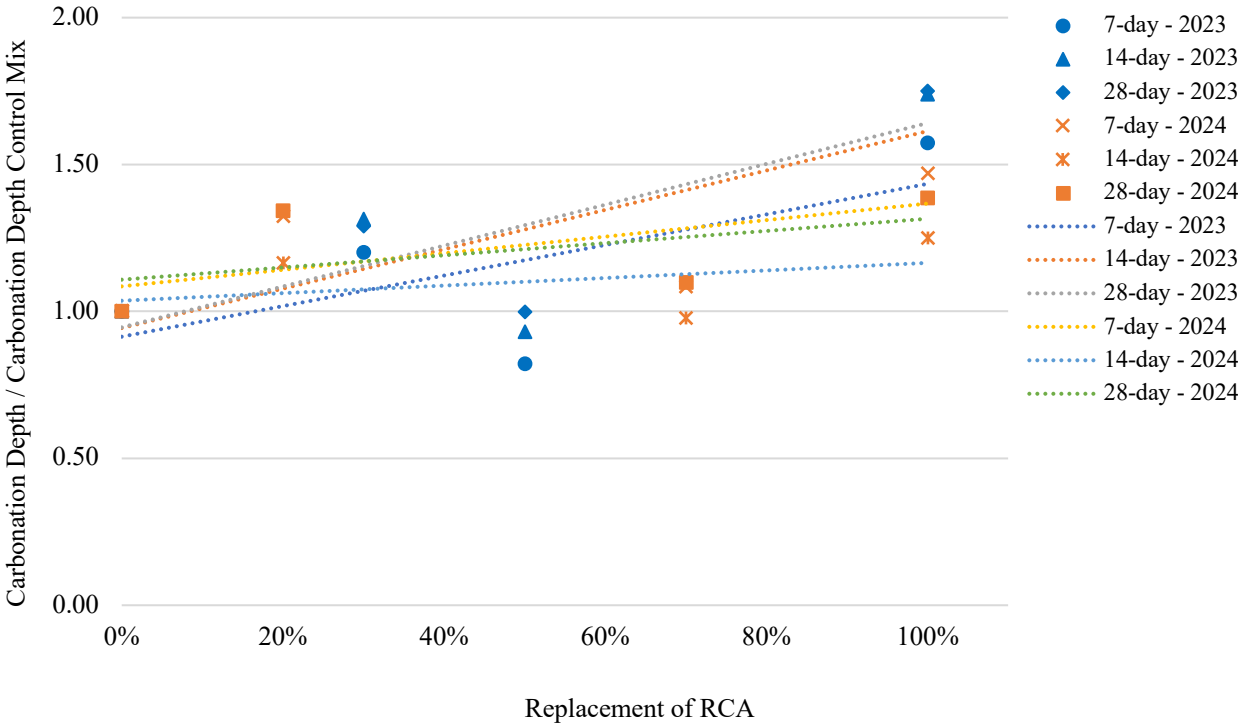

Figure 23. Normalized carbonation depth (relative to control mix) as a function of RCA replacement level for the 2023 and 2024 campaigns at 7, 14, and 28 days of exposure.

The observed increase in carbonation depth with RCA incorporation aligns with well-documented trends in RAC [165]. The higher porosity and weaker ITZ associated with RCA facilitate CO_2 ingress. Nonetheless, the superior performance of the 2024 campaign suggests that RCA quality plays a decisive role, as better-processed aggregates can substantially offset these deficiencies.

5.4. Freeze and thaw

The freeze–thaw resistance of concrete mixes was evaluated in accordance with CEN/TS 12390-9 [169], which assesses concrete durability under cyclic freezing and thawing conditions. For each mix, specimens were subjected to repeated freeze–thaw exposure, where each 24-hour cycle involved temperature fluctuation from +20 °C to −25 °C. The specimens were initially saturated, and mass measurements were taken at 7, 14, 28, and 56 days. The mass loss rate (%) was used as the primary durability indicator, reflecting surface damage and material degradation due to cyclic stress.

Figure 24. Freeze-thaw resistance test.

As shown in Figure 25, mass loss trends varied across campaigns. In the 2023 series, the control mix (M 0-0) maintained relatively stable weight through 28 days but dropped significantly at 56 days. M 30-30 and M 100-100 experienced major mass reductions after 28 days, with M 100-100 falling below 1200 g by day 56. Interestingly, M 50-50 showed the most stable performance, retaining higher mass across all time points.

In the 2024 series, the control mix and partial replacement levels (M 20-20 and M 70-70) retained mass well until day 28. However, at 56 days, M 70-70 and M 100-100 exhibited noticeable mass loss, especially in M 70-70, which fell below 700 g. These results confirm that RCA content affects freeze–thaw resistance, and performance is highly dependent on replacement level and aggregate source.

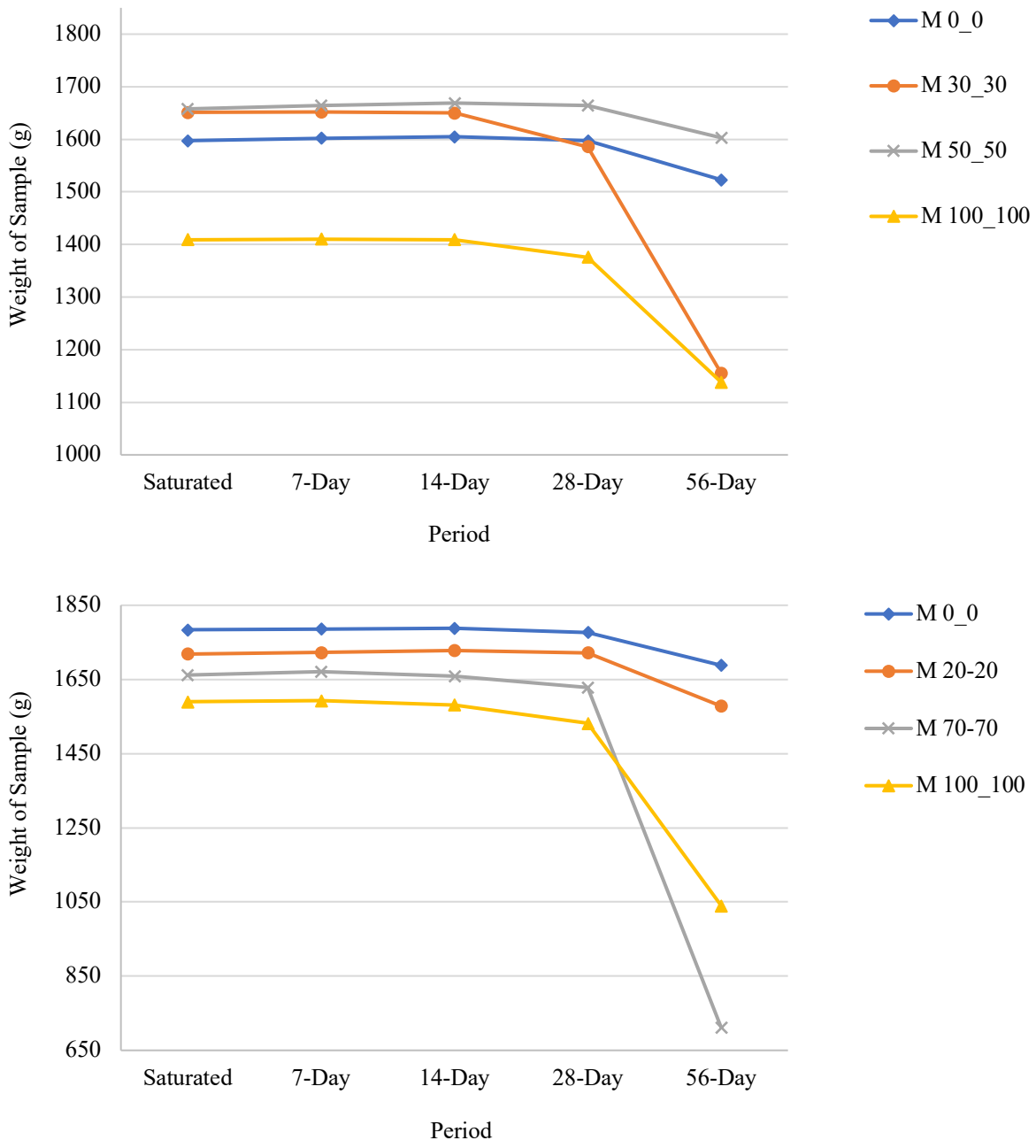

Figure 25. Weight evolution of concrete specimens subjected to freeze–thaw cycles, measured at saturated state and after 7, 14, 28, and 56 days of exposure. 2023 campaign (top), 2024 campaign (bottom)

The results confirm that RCA incorporation increases vulnerability to freeze–thaw damage, especially at full replacement. However, concretes containing moderate RCA levels (≤ 50%) maintained acceptable durability, particularly in the 2023 campaign. The improved performance of certain 2024 mixes at early stages may be attributed to variations in RCA source quality, though these effects were less pronounced at longer exposures.

Overall, the data demonstrate that freeze–thaw resistance is influenced by both the intrinsic mechanical strength of the mix and the microstructural characteristics of the recycled aggregates. The significant correlation between stiffness and durability further emphasizes the role of matrix integrity in mitigating freeze–thaw damage.

5.5. Chloride ion penetration

Chloride ion ingress was assessed using the Rapid Chloride Permeability Test (RCPT) in accordance with ASTM C1202 [170]. This test measures the total charge passed (in coulombs) across a concrete specimen over a 6-hour period under an applied voltage, offering a quantitative indication of the material's resistance to chloride transport. For each mix, cylindrical slices with a diameter of 100 mm and a thickness of 50 mm were tested after 28 days of curing, and the average charge passed was reported.

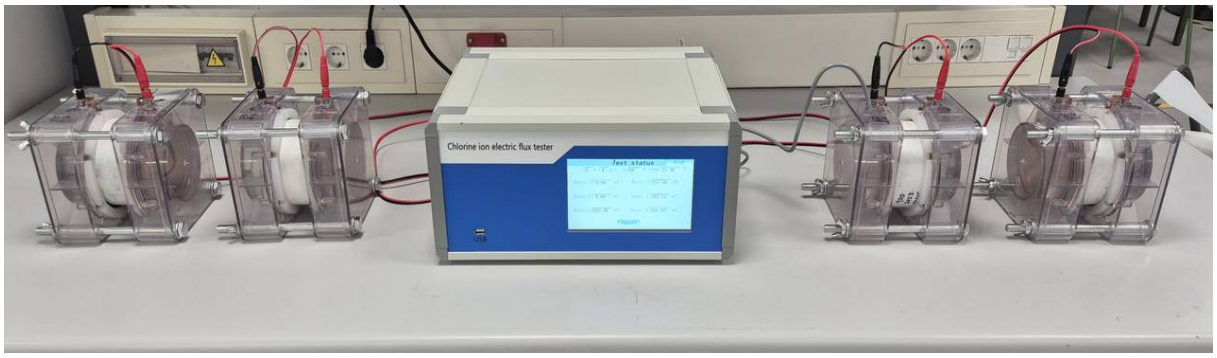

Figure 26. Chloride ion penetration test.

As illustrated in Figure 27, the results exhibit substantial variation between mixes and campaigns. In the 2023 series, the control mix (M 0-0) demonstrated a low charge passed value of approximately 900 coulombs, indicating very low chloride permeability. However, this resistance was significantly reduced in mixes with partial RCA replacement. M 30-30 and M 50-50 reached charge values of 3300 and 2900 coulombs, respectively, both falling within the moderate to high permeability range as per ASTM classification. Interestingly, the M 100-100 mix recorded the lowest value among the RCA mixes at only 600 coulombs, a result that deviates from expected trends and suggests anomalous refinement of the pore structure or surface densification effects in that batch.

In the 2024 campaign, the overall resistance to chloride penetration was lower. The control mix (M 0-0) started at a higher baseline of 2700 coulombs, with M 20-20 and M 100-100 reaching 3400 and 3800 coulombs, respectively. M 70-70 exhibited the highest charge passed at over 5000 coulombs, placing it in the high permeability category. These results point to weaker chloride resistance in the 2024 series, particularly at intermediate and high replacement levels, despite the generally better performance observed in other durability tests.

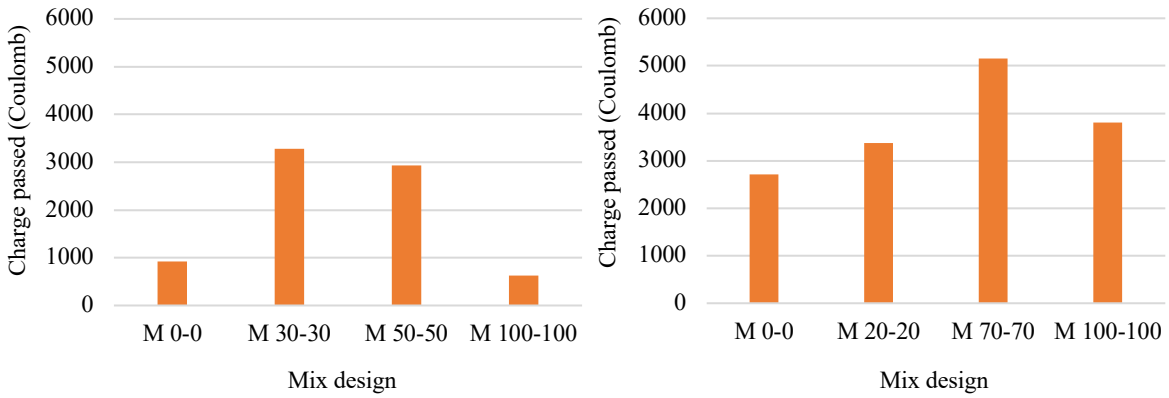

Figure 27. Total charge passed (coulombs) during Rapid Chloride Permeability Testing (ASTM C1202) for all concrete mixes in the 2023 and 2024 campaigns.

The RCPT results confirm that chloride resistance in RAC does not vary linearly with RCA content. Instead, performance depends strongly on the quality and morphology of the recycled aggregate, including porosity, absorption, and the integrity of the ITZ [171].

5.6. Chloride migration coefficient

The resistance of concrete to chloride penetration was further evaluated using the Chloride Migration Coefficient determined according to NT Build 492 [172]. This method estimates the non-steady-state migration coefficient based on chloride transport through a concrete specimen under an applied electrical field. The test was conducted on 28-day cured cylindrical slices, and the coefficient was calculated by measuring the depth of chloride ingress after a fixed exposure period.

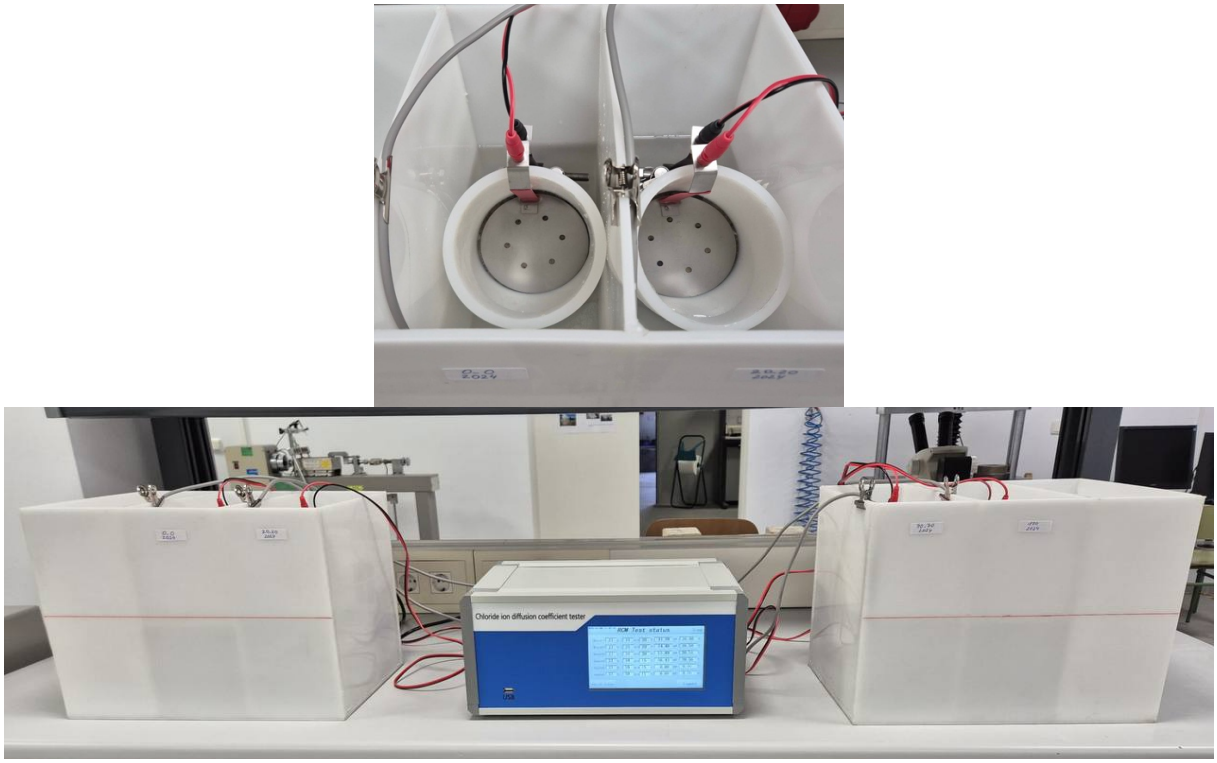

Figure 28. Chloride migration coefficient test.

The chloride migration coefficients obtained for both campaigns are presented in Fig. 39. In the 2023 series, values ranged from 28 × 10^{-12} to 50 × 10^{-12} m^2/s. The control mix (M0-0) showed a coefficient of 44 × 10^{-12} m^2/s, while M50-50 achieved the lowest value (28 × 10^{-12} m^2/s), suggesting improved transport resistance at moderate RCA content. However, the fully recycled mix (M100-100) reached 50 × 10^{-12} m^2/s, indicating reduced durability at complete replacement levels.

In contrast, the 2024 campaign exhibited a narrower and overall lower range, from 34 × 10^{-12} to 42 × 10^{-12} m^2/s. The fully recycled mix (M100-100) recorded the lowest coefficient (34 × 10^{-12} m^2/s), implying enhanced chloride resistance likely associated with the improved physical quality of RCA used in that campaign.

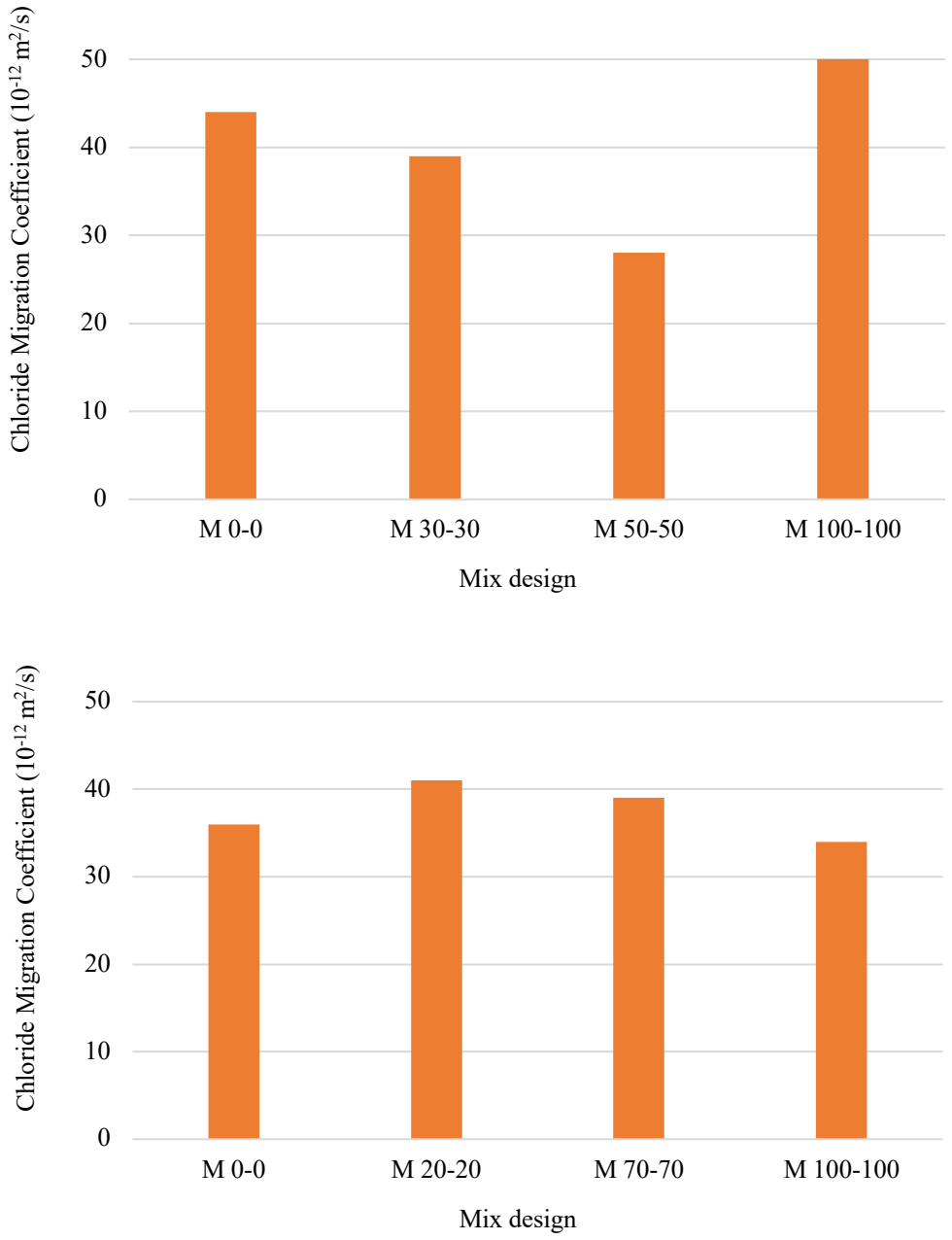

Figure 29. Chloride migration coefficients (10^{-12} m^2/s) for all mix designs from the 2023 and 2024 campaigns.

The results demonstrate that the chloride migration coefficient does not vary monotonically with RCA content but is strongly influenced by aggregate quality and ITZ refinement. The improved performance of the 2024 mixes, particularly at full replacement, suggests that high-quality, well-processed RCA can maintain adequate impermeability despite higher porosity at the aggregate level [171,173].

These findings are consistent with prior research showing that chloride transport in recycled aggregate concrete depends on both the mortar–aggregate interfacial properties and the pore connectivity of the matrix [29].

5.7. Correlations between Carbonation depth and Oxygen permeability

A clear positive correlation was observed between carbonation depth and oxygen permeability coefficient, as presented in Figure 30. This relationship reflects the shared dependence of both parameters on the internal pore structure and gas transport capacity of concrete. Mixes exhibiting higher oxygen permeability consistently showed greater carbonation depths, highlighting the increased susceptibility of porous concretes to both oxygen ingress and carbon dioxide diffusion.

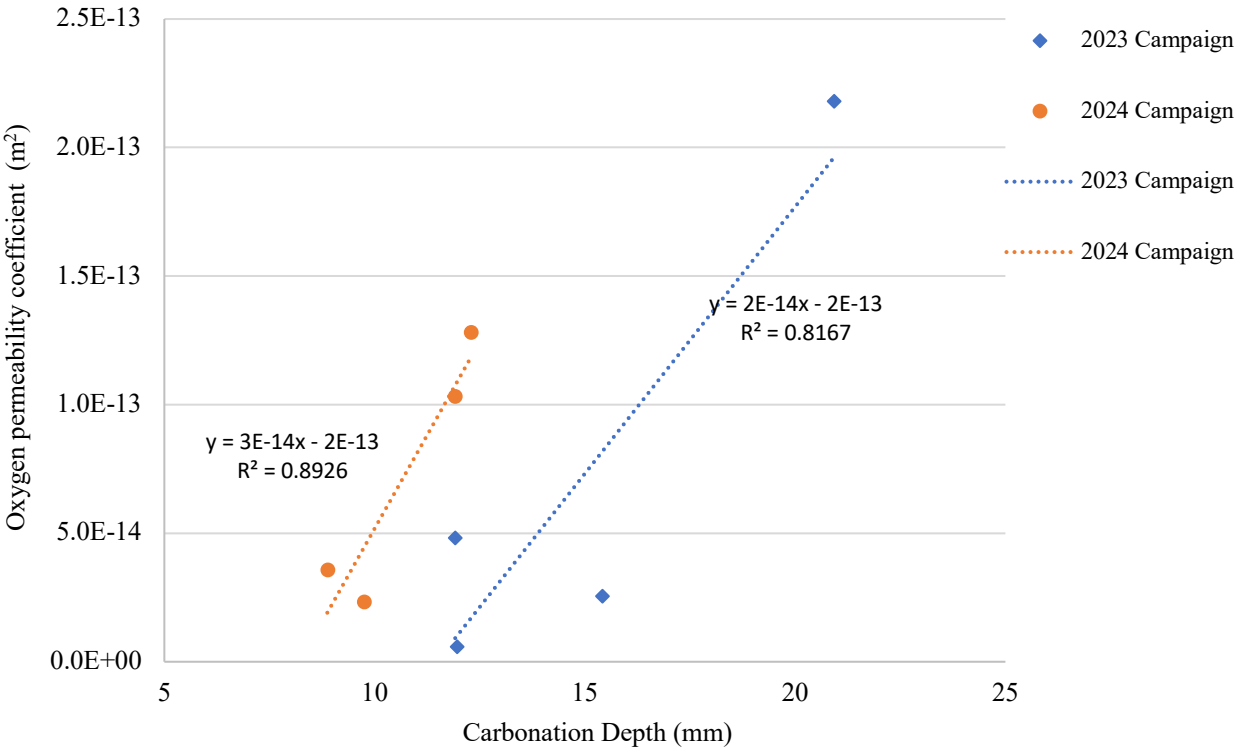

Figure 30. Correlation between carbonation depth and oxygen permeability coefficient.

The 2024 campaign demonstrated a steeper regression slope (3×10^{-14} m²/mm) and a higher coefficient of determination ($R^2 = 0.89$), indicating a strong and consistent relationship between gas transport and carbonation progression. In contrast, the 2023 campaign showed a slightly flatter slope (2×10^{-14} m²/mm) and a lower R^2 value (0.81), suggesting greater variability among the mixes, likely related to differences in recycled aggregate characteristics and pore network interconnectivity.

This trend implies that, although both campaigns exhibited similar mechanistic behavior, the concretes produced in 2024 had a more uniform and refined microstructure, leading to a tighter correlation between oxygen permeability and carbonation depth. These results are consistent with the literature, where permeability and carbonation depth are often reported to be closely related due to their shared dependence on effective porosity and connectivity of the capillary network [165,174,175].

Overall, the regression analysis reinforces that oxygen permeability serves as a reliable proxy for assessing carbonation susceptibility in RAC. Mixes with lower oxygen permeability coefficients generally exhibited shallower carbonation fronts, underscoring the critical role of microstructural densification and aggregate quality in enhancing long-term durability.

6. Composite Slabs

This chapter represents the final step of the experimental investigation, extending the analysis from the material and durability scale to the structural scale. While the previous chapters focused on the mechanical performance and durability characteristics of concretes incorporating fine and coarse recycled concrete aggregates, the present chapter aims to evaluate the implications of RCA use on the global structural behavior of composite slabs.

To this purpose, full-scale composite slabs were tested under four-point bending in order to investigate the longitudinal shear behavior, load–deflection response, failure mechanisms, and ultimate load capacity. The slab tests were designed to assess whether the material-level differences observed between natural aggregate concrete and RCA concrete translate into significant variations in structural performance, particularly in terms of steel–concrete interaction and partial shear connection behavior.

The experimental results are analyzed by comparing different RCA replacement ratios and span lengths, considering both the 2023 and 2024 experimental campaigns. Special attention is devoted to the evaluation of interface shear behavior, slip development, and collapse modes. Furthermore, the experimental collapse loads are compared with analytical predictions obtained using the Partial Shear Connection (PSC) method in accordance with EN 1994-1-1, with the aim of assessing the applicability and limitations of current design approaches when recycled aggregate concrete is employed.

Overall, this chapter provides a comprehensive assessment of the structural feasibility of composite slabs incorporating RCA concrete and establishes a direct link between material properties, durability performance, and structural behavior.

The composite slabs were casted and were kept in standard laboratory conditions for 24 hours (at a temperature of 23 ± 2 °C) and then removed from the molds. Subsequently, the samples were cured by being wrapped in plastic covers.

The steel material for the sheeting is a S280GD used for cold-formed profiles. The deck has been provided by Spinelli srl, named SG110-600, which is a special deck having a total height of the ribs equal to about 110mm, which is not usual for this type of profile Figure 31. The thickness of the sheeting is constant and equal to 0.75mm. It has been used the same identical profile for all the tested slabs. Tensile tests on four coupon samples identified a mean yielding tension equal to 338.18 MPa and a mean ultimate tension equal to 593.16 MPa. The mean value of the Young Modulus is equal to 195 GPa.

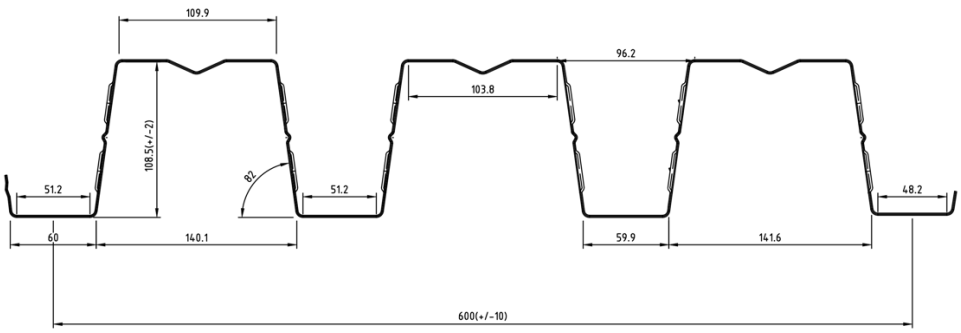

Figure 31. Steel sheet geometric characteristics from Spinelli srl, (named SG110-600), measures in mm.

Experimental tests were performed employing a loading machine outfitted with a hydraulic jack, facilitating precise loading on all slabs at two predetermined points at L/4 from midspan, where L denotes the span length of the slab. All the specimens were restrained with a simple support and an hinge at their ends. The displacement of the slabs was monitored at 8 distinct locations using linear displacement transducers (LVDTs) with a nominal displacement of 100 mm, nominal sensitivity 2 mV/V, sensitivity tolerance ± 0.1%, measure resolution 1 µm. In particular, 4 LVDTs were used to monitor the debonding of the slab, i.e. the lateral relative deformation between the steel and the concrete. The instrument position and the static scheme of the tests is reported in Figure 32.

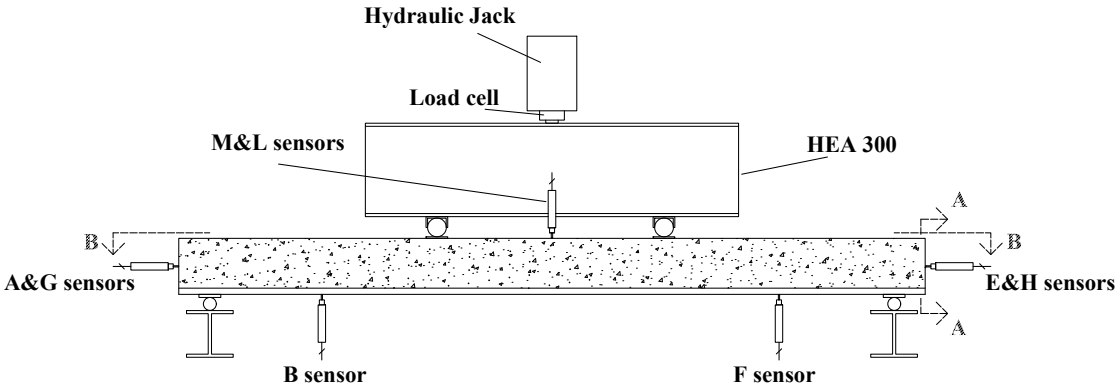

A-A Section

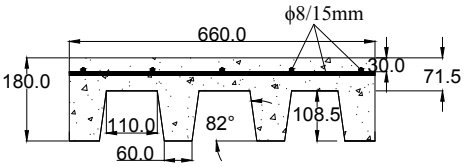

Figure 32. Experimental set-up of the composite slab test. Top: drawings and sensors location, bottom: pictures from the experimental tests.

The loading protocol involved two successive load cycles up to 30% and 50% of the theoretical collapse load, respectively. After these load cycles in the testing sequence, a third loading cycle was performed until reaching the peak load, corresponding to the debonding failure of each slab specimen. This kind of failure occurs when the bond between the concrete and the steel is compromised. Following this peak measurement, the slabs were subjected to additional loading until flexural failure that occurred at a lower load. This behavior was detected for each slab specimen showing an intrinsic *ductility* for this kind of structure.

6.1. 2023 Campaign

The structural response of the recycled aggregate concrete composite slabs (RACCS) was evaluated in terms of flexural and longitudinal shear behavior using four concrete mixes, namely M0, M30, M50, and M100, which reflect increasing levels of recycled aggregate replacement. Testing was carried out for three span lengths of 2.40 m, 2.80 m, and 3.20 m, with one slab specimen produced and tested for each combination of mix and span length. Load–displacement relationships were recorded for all specimens through the linear displacement transducers (LDTs) positioned along the span.

6.1.1. Load versus vertical displacement

For each test, LDT L and LDT M were positioned at the mid-span along the front and rear edges of the composite slab to capture vertical deflection in the regions most affected by flexural action. In addition, LDT E&H and LDT A&G were installed on the right and left sides of the slab to monitor horizontal displacements associated with potential longitudinal slip at the steel–concrete interface.

The applied vertical load is plotted in Figure 33-51 as a function of the middle displacement (M and L transducers, see figure 6 for their positions). Figures differ for the length of the slab, while the different mix design are grouped together in the same figure. This representation allows for a comprehensive understanding of how varying structural dimensions influence the response to the test. It can be noted that, for the 2400mm span, the M 30-30 mix design demonstrated the highest vertical load while for the 2800mm and 3200mm spans, the maximum vertical load is associated with the M 50-50 and the M 100-100 mix design, respectively.

Some patterns are common for all Figure 33-51: the initial linear portion is influenced by the elastic response of both materials, whereas post-peak behavior shows debonding and subsequent flexural deformation. The sudden drop in load post-peak is explained as a debonding failure, followed by a ductile phase characterized by progressive cracking and load redistribution.

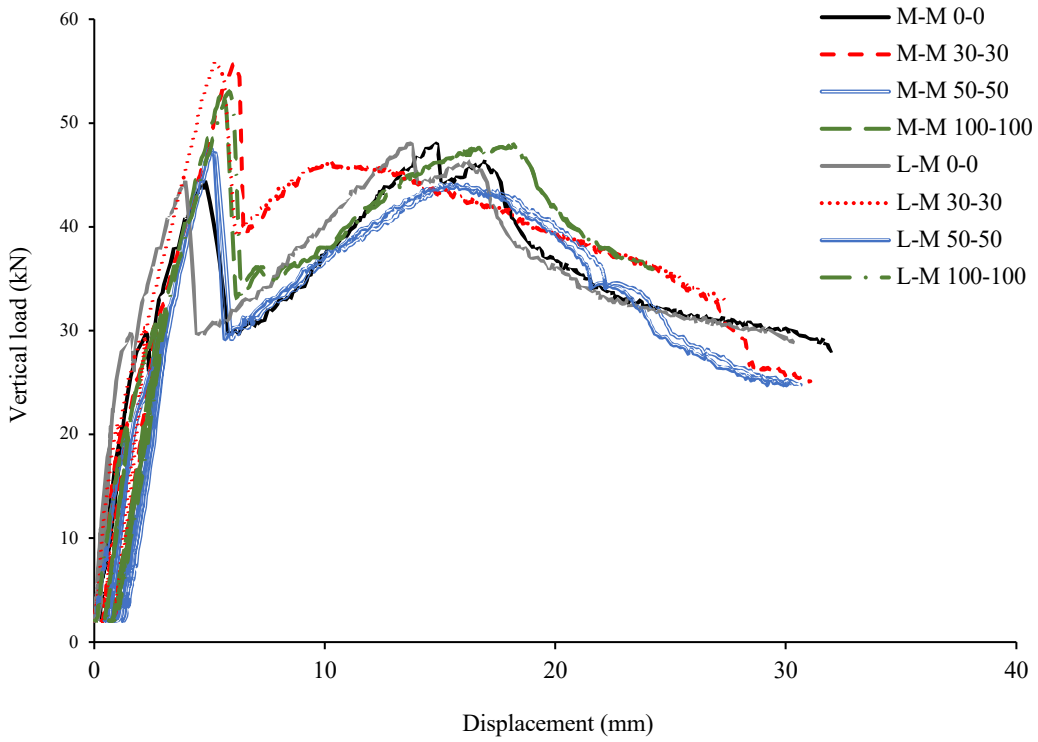

Figure 33. Load-displacement curves (M and L, LVTD) for 2400mm span.

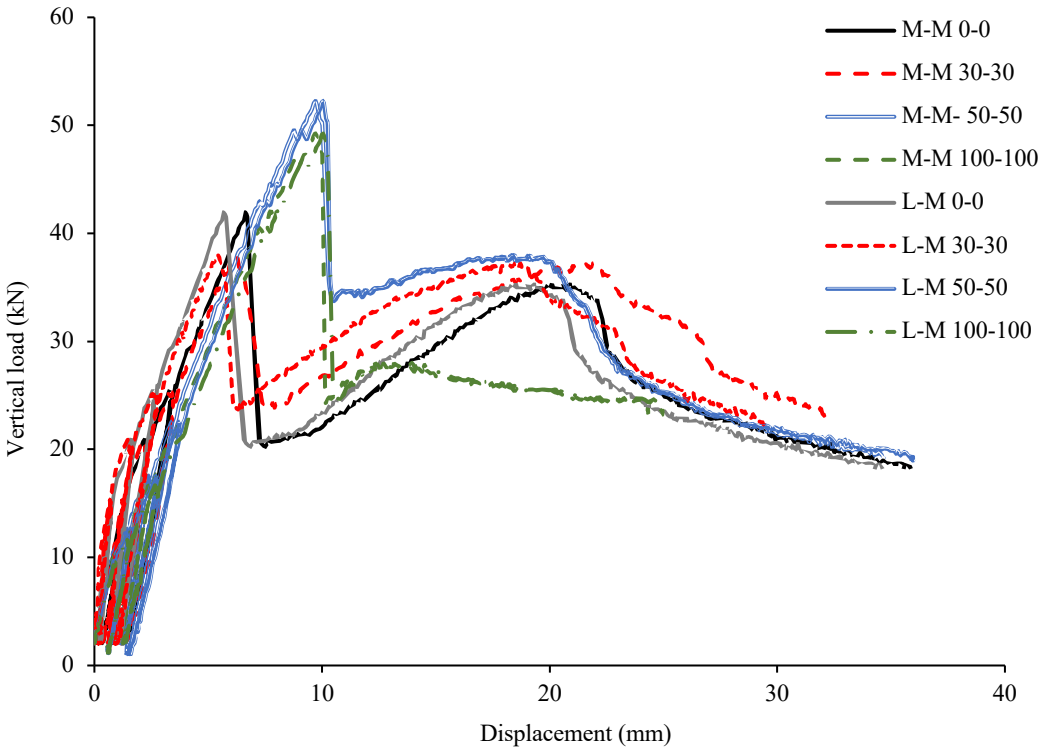

Figure 34. Load-displacement curves (M and L, LVTD) for 2800mm span.

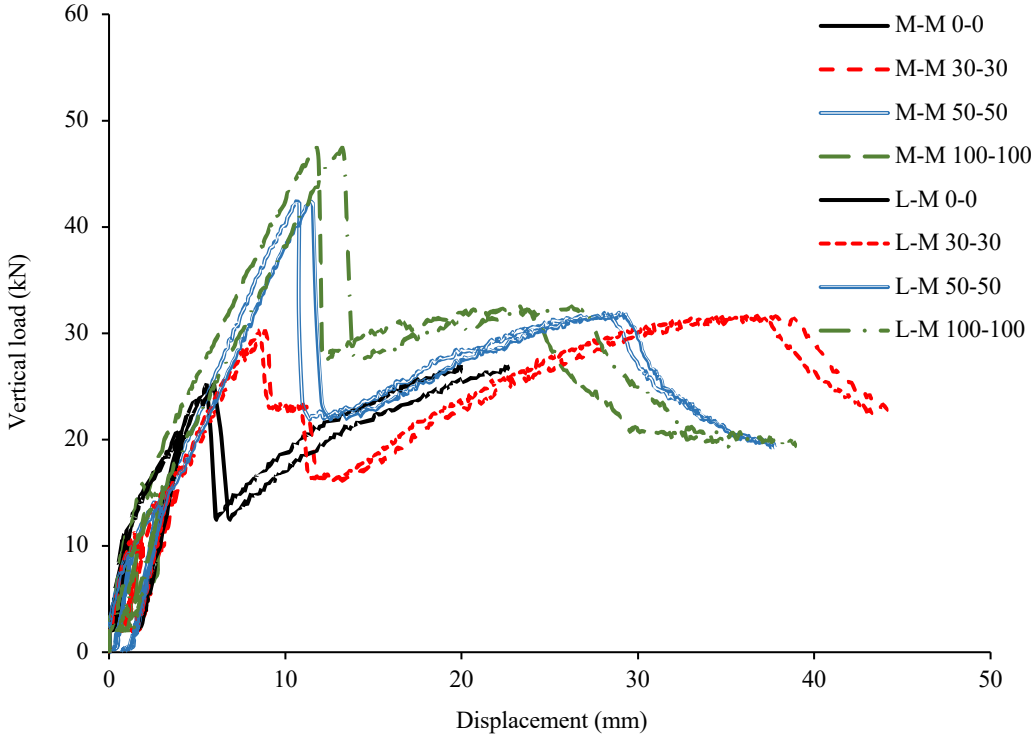

Figure 35. Load-displacement curves (M and L, LVTD) for 3200mm span.

The collapse mechanism exhibited uniformity across all slabs: upon reaching the maximum load, debonding initiates (as depicted in Figure 36), resulting in a sudden decline in the curves. This initial debonding phase is succeeded by a flexural mechanism, inducing substantial deformations despite minimal load variation. With the progression of cracking, the bond between the concrete and steel further deteriorates, facilitating the expansion of the debonded region. Ultimately, this enlarged debonded area compromises the structural integrity of the composite slab. Following debonding, a flexural mechanism ensues, redistributing loads within both the composite slab and its supporting structure. Once debonding transpires, the composite slab forfeits its complete composite action, necessitating load redistribution. While the remaining bonded sections continue to support a fraction of the loads, the distribution becomes uneven. Regions proximate to the debonded area undergo heightened stresses as they bear a larger portion of the load, potentially leading to localized overstressing and subsequent failure if unaddressed. The severity of debonding and the capacity of the remaining bonded areas determine whether the composite slab experiences flexural failure in localized regions, as illustrated in Figure 37. This failure mode can manifest through cracking, excessive deflection, or in extreme scenarios, complete collapse.

Figure 36. Typical relative displacements of the steel sheet with respect the concrete during the test.

Figure 37. Flexural crack at the end of the test.

The collapse load at the center of all composite slabs is provided in Table 6. Referring to Table 4, it can be noted that the increment in the percentage of recycled aggregate also corresponds to a load increment which is contrary to the previous results related to the mechanical properties of the mix designs. This implies that an increase in the replacement of recycled aggregates in composite slabs results in an enhancement of bonding strength. Augmenting the replacement of recycled concrete aggregates has heightened the friction between concrete and steel sheets, i.e. increasing the longitudinal shear strength. These results are in agreement to those presented in [38,176] and suggest that the use of recycled aggregates, with a focus on reducing environmental impacts and promoting a circular economy, can lead to improved structural performance in composite slabs and mechanical systems where bonding is critical.

The improved bond friction observed at the concrete–steel interface in RAC slabs can be attributed to several intrinsic features of recycled aggregates compared to natural aggregates. First, recycled aggregates are characterized by a rougher and more angular surface morphology due to the presence of adhered mortar from the parent concrete. This increased surface roughness enhances the mechanical interlock at the steel–concrete interface, leading to higher frictional resistance against longitudinal slip.

Second, the residual mortar attached to the recycled aggregates increases the overall porosity and micro-texture of the concrete matrix. While this may reduce the intrinsic strength of the concrete, it promotes localized penetration of cement paste into the embossments and ribs of the profiled steel sheeting, improving the frictional component of bond transfer.

Additionally, recycled aggregates typically exhibit higher water absorption than natural aggregates, which can locally modify the hydration process near the steel deck. This may result in a denser cementitious layer at the interface, further contributing to frictional resistance.

Stochino et al. (2024) investigated the mechanical behavior of composite slabs incorporating RCAs and found a notable enhancement in the bond strength between concrete and metal sheets. Their experimental study demonstrated that the presence of RCAs improves longitudinal shear resistance, suggesting a stronger mechanical interlock at the steel–concrete interface. This improvement is primarily attributed to the rougher surface texture of RCAs, which enhances friction and mechanical interlocking, ultimately leading to better load transfer mechanisms within the composite system. Notably, composite slabs with RCAs exhibited higher debonding resistance and sustained load-bearing capacity post-failure, reinforcing their potential for structural applications where bond performance is critical [50]. This result underscores the significant impact of RCA content on bond strength, reinforcing the notion that increasing RCA content improves the bond performance in reinforced concrete structures.

Finally, the combined effect of aggregate angularity, adhered mortar, and increased micro-scale roughness promotes a more tortuous slip path along the steel–concrete interface. This mechanism delays the onset of relative slip and enhances longitudinal shear resistance, as also observed experimentally through higher degrees of interaction and increased shear stress values in RAC slabs compared to NAC slabs.

These observations are consistent with previous studies reporting improved interfacial friction and mechanical interlock in recycled aggregate concretes when used in composite systems with profiled steel decking.

Table 6. Collapse load [kN] of the tested slabs

Mix design	2400 mm	2800 mm	3200 mm
M 0-0	48.20	41.96	26.98
M 30-30	55.91	38.01	31.67
M 50-50	47.53	52.24	42.41
M 100-100	53.05	49.23	47.45

An important observation emerging from both the 2023 and 2024 experimental campaigns is that, for a given span length, the maximum load does not systematically correspond to the same RCA replacement ratio. This behavior can be explained by the interaction of competing mechanical mechanisms governing the response of composite slabs.

On one hand, increasing the RCA content generally leads to a reduction in concrete compressive and tensile strength, which tends to penalize the flexural resistance of the slab. On the other hand, recycled aggregates are characterized by higher surface roughness and the presence of adhered mortar, which can enhance mechanical interlock and friction at the steel–concrete interface. At intermediate replacement ratios, this improvement in bond behavior may partially compensate for the reduction in concrete strength, leading to higher degrees of interaction and, consequently, to increased peak loads.

The observed variability in the RCA content corresponding to the maximum load within the same span length therefore reflects a balance between strength-related effects and interface-controlled mechanisms. Moreover, the governing failure mode may shift with RCA content, ranging from flexural-dominated behavior to longitudinal shear or mixed failure, further influencing the peak load.

To further investigate this aspect, the experimental peak loads were also examined in normalized form, for example as ratios of peak load to $\sqrt{f_{cm}}$ or to the tensile strength f_{ct}. While such normalization reduces part of the scatter, it does not fully eliminate the variability among mixes, confirming that the peak load of composite slabs incorporating RCA is not controlled solely by concrete strength parameters. Instead, it is strongly influenced by bond conditions, interaction degree, and span-dependent stress redistribution effects.

Overall, these results highlight that the optimal RCA replacement ratio in terms of peak load is not unique but depends on the combined effects of material properties, interface behavior, and structural configuration.

6.1.2. Load versus horizontal displacement

As previously discussed at the peak load the debonding is detected and the relative displacement between the sheeting and concrete occur. This relative displacement has been monitored by the use of E&H and G&A LVDTs. The output from these transducers have been plotted in Figure 38-56. It is important to note that, for clarity, only the most significant results are shown. Therefore, not all transducers are represented in every figure.

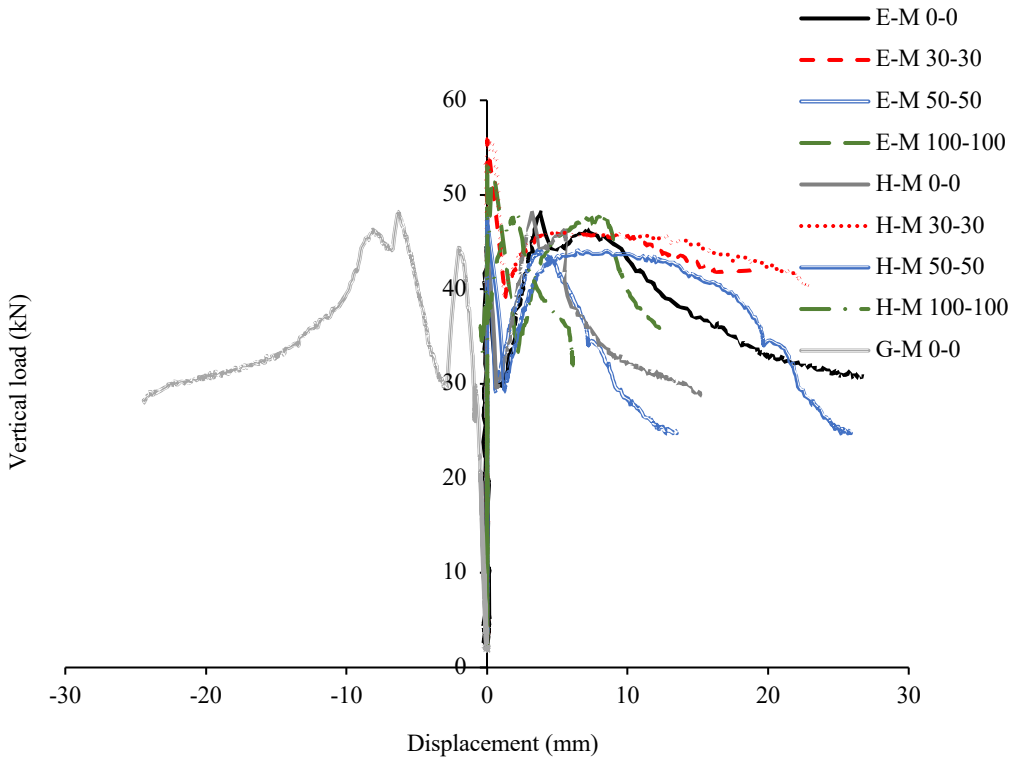

Figure 38. E&H&G and A sensors displacement versus the load, 2400mm slab.

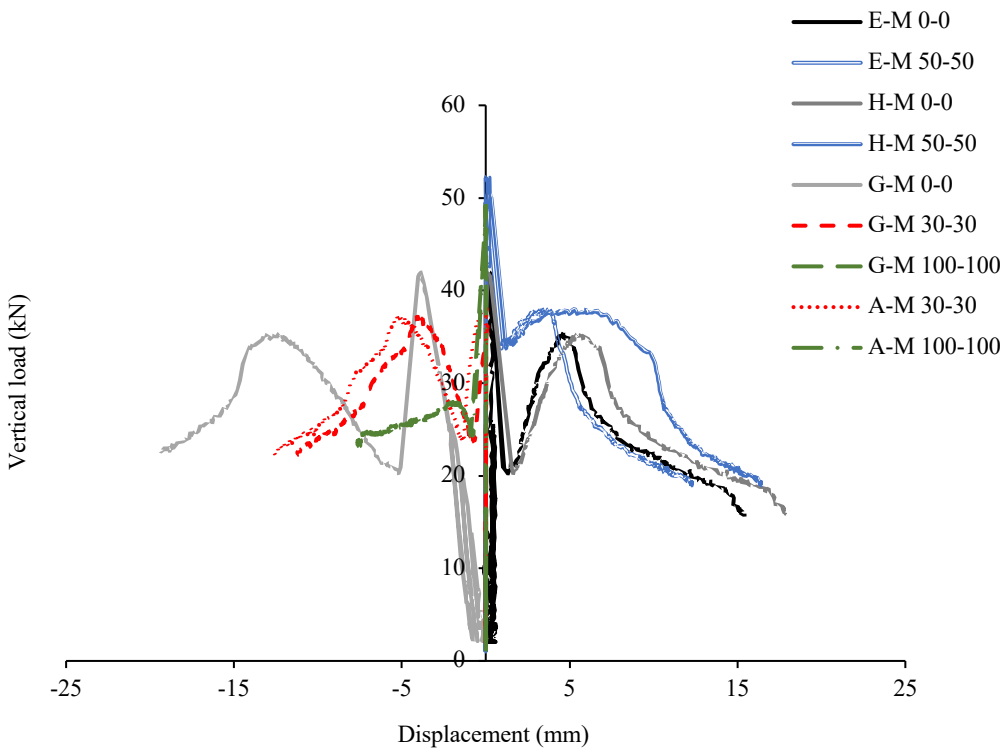

Figure 39. E&H&G and A sensors displacement versus the load, 2800mm slab.

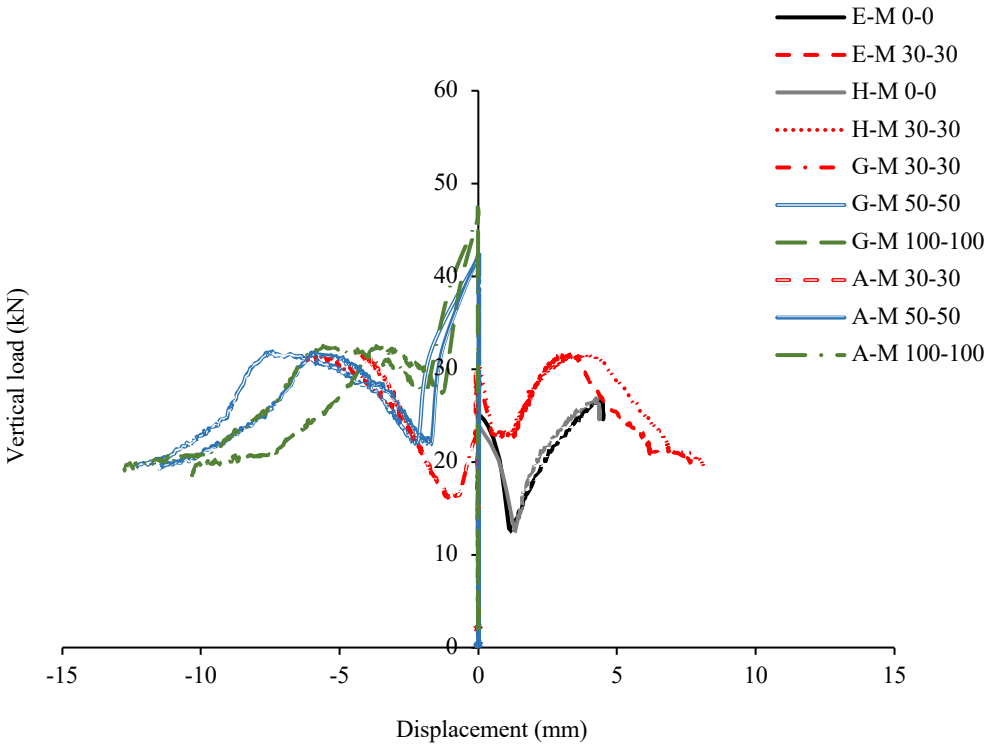

Figure 40. E&H&G and A sensors displacement versus the load, 3200mm slab.

It can be noted that until the debonding load is not reached the lateral displacement is almost equal to zero. At this load level the slab starts to deform laterally. These graphs confirm that the load level assumed as the debonding load is really associated with this lateral slippage of the slab. The position of the first movement seems to be quite casual, depending on

imperfections of the slab and of the load and supports positions. For this reason, is not easy also to find a rule to describe how the maximum displacement is influenced by the recycled aggregate percentage.

6.1.3. Estimation of the longitudinal shear strength

Starting from the experimental results, the degree of interaction (η) and then the longitudinal shear strength (τ_u) was evaluated by means of the use of the partial interaction domain (PSC) of the EC4-1-1 [177]. The main hypotheses of the procedure are: i) at the ultimate limit state (ULS) the thin steel deck works always in plastic range independently on the stress level reached in the cross-section. The position of the plastic axis of the steel sheet is identified by terms e_p; ii) the concrete inside the ribs gives no contribution to the final resistance; iii) when the degree of interaction is equal to zero (η =0), only the effective bending resistance of the steel sheeting is considered. The effective properties of the steel hi-bond under pure bending were evaluated following the prescriptions of EC3-1-3 [178] by properly considering the presence of stiffeners on the cross-section which produce also distortional buckling in addition to the local one. The obtained effective section is plotted in Figure 41.

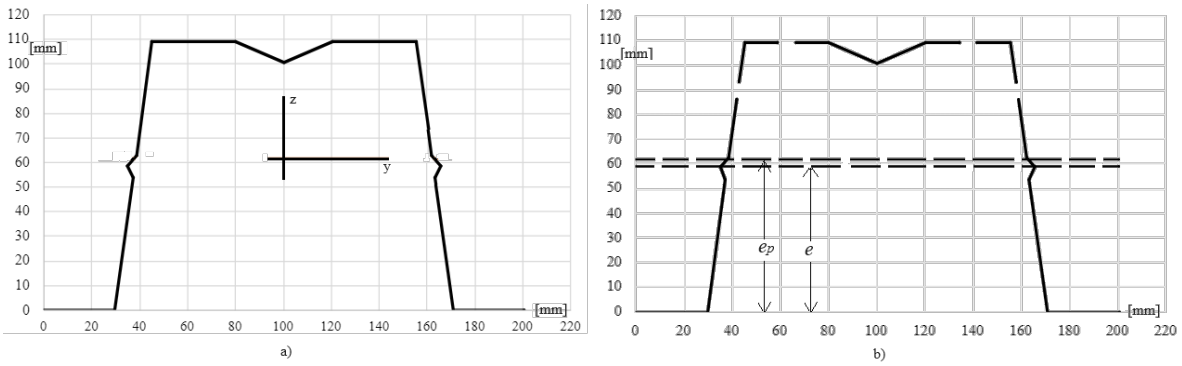

Figure 41. Gross (a) and effective (b) cross-section of the metal deck in bending.

The maximum compression, which is assumed to act on the concrete, N_{cf}, is equal to (Figure 42):

$$N_{cf} = b \cdot h_c \cdot 0.85 f_{cm} \tag{3}$$

where b is the width of the section, h_c is the height of the concrete slab above the steel sheeting and f_{cm} is the mean value of the cylindrical resistance of the concrete. It can be observed that the interaction domain is influenced by the mechanical properties of the concrete, for this reason we will obtain one different domain for each mix design.

From the equilibrium between the maximum compression on the concrete and the maximum tension on the steel, it is possible to evaluate the position of the neutral axis, x:

$$A_p \, f_{yp} = 0.85 \, f_{cm} b \, x \tag{4}$$

$$x = \frac{A_p \, f_{yp}}{0.85 \, f_{cm} \, b}$$

(5)

where A_p is the area of the steel sheeting and f_{yp} is the correspondent yielding, experimentally assessed.

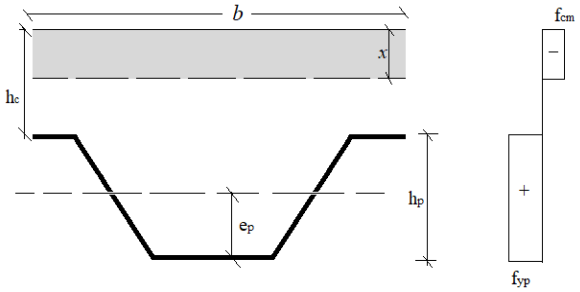

Figure 42. Stresses distribution on the composite section.

For the partial interaction (i.e., 0< η <1) the position of the neutral axis depends on the grade of interaction, $x' = \eta \, x$. It can be noted that when the grade of interaction is nil, the neutral axis coincides with the top axis of the section. As a consequence, also the force on the compressed part decreases with the decrement of η, $N_c = \eta \, N_{cf}$.

The bending resistance is then obtained considering the equilibrium to the rotation with respect to the neutral axis, ranging from the maximum value, $M/M_{p,Rm}$, obtained with η = 1 to the minimum one, i.e. the bending resistance of the steel sheeting. The non-dimensional M-η domain obtained from M0-0 slab is proposed in Figure 43 which can be assumed as significant for each mix design.

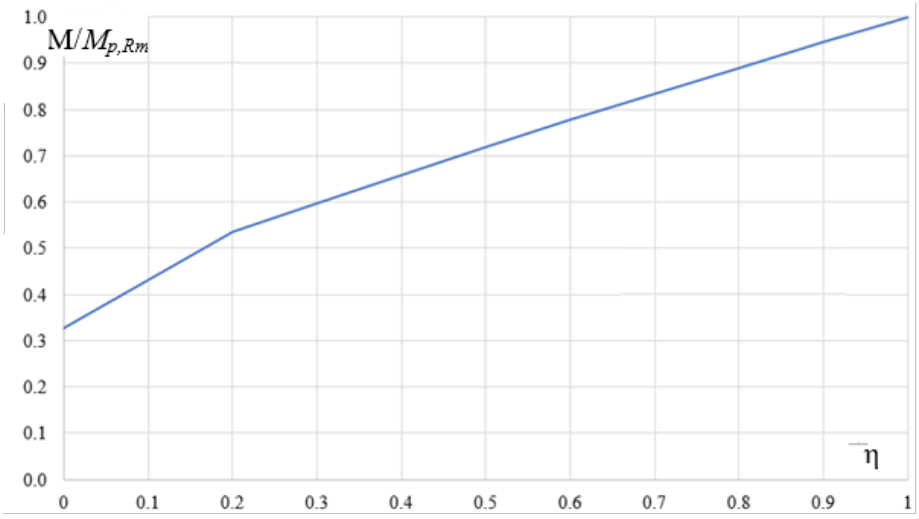

Figure 43. The M- η domain for the composite section with M0-0 mix design.

The value of the degree of interaction is obtained by entering with the experimental bending moment M_{test} into the domain (Figure 44).

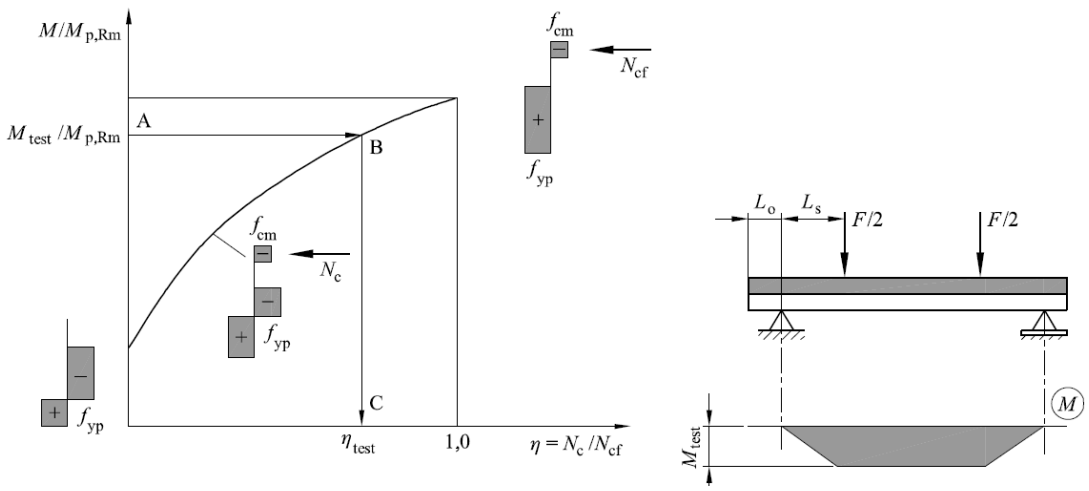

Figure 44. Approach for the determination of the degree of interaction (EC4).

Finally, the longitudinal shear strength, τ_u, is directly obtained from equation (6):

$$\tau_u = \frac{\eta\, N_{cf}}{b\ l_s} \qquad (6)$$

where l_s is the distance between the force and the support, equal to L/4.

The ratio between the longitudinal shear stress obtained from each slab, over the M0-0 mix design, i.e. $\frac{\tau_{u,i}}{\tau_{u,M0}}$, is reported in Table 7. The average value between each length and the covariation is reported too.

It is confirmed that the use of concrete made by recycled aggregates brings a non-negligible improvement in term of longitudinal adhesion between the two materials, the longitudinal shear is increased, in mean, up to 1.7 times.

The increased bond strength between RCA concrete and steel sheeting can be attributed to the enhanced roughness of RCA surfaces. The adhered mortar on recycled aggregates increases the friction coefficient and results in better mechanical interlock with the steel deck. We referenced studies (e.g., [176]) that report similar observations.

Table 7. Non-dimensional longitudinal shear strength.

	2400mm	**2800mm**	**3200mm**	**average**	**CoV**
$\frac{\tau_{u,M30}}{\tau_{u,M0}}$	1.59	0.70	0.64	0.98	0.19%
$\frac{\tau_{u,M50}}{\tau_{u,M0}}$	0.95	1.92	1.47	1.44	0.15%
$\frac{\tau_{u,M100}}{\tau_{u,M0}}$	1.30	1.57	2.14	1.68	0.13%

6.2. 2024 Campaign

The flexural and longitudinal shear behaviours of RACCS (Recycled Aggregate Concrete Composite Slabs) were characterized for each material configuration, identified by the mix codes M0, M20, M70, and M100 according to the percentage of recycled aggregate. Each configuration was tested through a total of nine experimental trials, distributed across three different span lengths: 2.40 m, 2.80 m, and 3.20 m. For each group of three specimens with the same span length, three load-displacement curves were obtained, each corresponding to the linear displacement transducers (LDTs) used for measurement.

6.2.1. Average Load-Displacement curve from LDTs

To obtain an average curve, a common interpolation domain was defined using displacement as the interpolating variable, as it generally increases monotonically throughout the test. Unlike load, which may experience sudden drops due to damage and progressive failure, displacement allows for consistent alignment across curves, even when measurement points do not perfectly match. The common domain was created by merging and sorting all displacement values from the three specimens, removing duplicates, and truncating the range at the average of the maximum displacements recorded. Load values were then matched to these displacements, where direct matches were missing, linear interpolation was applied between the two nearest experimental points– one immediately before and one after- were identified. The corresponding load was then calculated using the equation of the straight line passing through those two points, by applying a proportion based on the relative distances between the known displacements. Once the corresponding load value had been identified for each curve at every point of the common domain, the average load was calculated, and the load-displacement curve along with the corresponding standard deviation was computed and graphically represented.

A similar method was applied for the horizontal displacement data from LDT E&H and A&G. Since longitudinal slip may develop on either both sides or just one side of the slab, the analysis was adapted accordingly. In cases where not all specimens exhibited slip, the average load corresponding to the mean of the maximum loads reached by the curves before the loss of load-bearing capacity and the onset of slip in the specimen where the phenomenon did occur was first evaluated. For the remaining displacement response, only the curve of the specimen that showed slip was included, ensuring that the mechanical behaviour associated with the phenomenon was not distorted by data from specimens without slip.

The resulting average curve offers a robust and statistically reliable representation of the flexural and longitudinal shear behaviour of RACCS, accounting for variations in span length, material composition, and LDT positioning. Full individual curves for each specimen, including those from LDT F and LDT B, placed under the loading points to monitor local vertical displacements, are provided in the **Appendix**.

6.2.2. Load versus vertical displacements

In Figure 45-Figure 47 are shown the average load-displacement curves are recorded by LDT L and LDT M at mid-span for three different spans (2.40 m, 2.80 m, and 3.20 m). The result compares four mix designs (M0, M20, M70, and M100), each incorporating a different percentage of recycled concrete aggregates in place of natural ones. In general, all curves exhibit a three-phase response: an initial elastic phase with linear behaviour, a debonding

failure phase marked by a sudden drop in load, and a post-peak flexural phase dominated by progressive cracking and load redistribution. After the peak, the curves typically display a sudden loss of load-bearing capacity followed by a plateau or slowly descending branch, indicating ductile deformation. This post-peak segment is more evident in mixes containing RCA, suggesting a more gradual degradation of the steel-concrete bond. Oscillations in the load signal following the initial linear segment may reflect the progressive loss of bond integrity. These fluctuations are particularly pronounced in M70 and M100, suggesting a more irregular debonding evolution in those mixes. Once the debonding process stabilizes, the curve tends to evolve more smoothly at large displacements and nearly constant load levels, indicating the activation of the flexural failure mechanism.

For the 2.40 m span configuration, M20 achieved the highest peak load. This result suggests that, under short-span conditions, a moderate replacement rate of natural aggregates with recycled aggregates can provide structural efficiency, likely due to a favourable combination of good interface bonding and still-sufficient mechanical stiffness. This finding is consistent with the result reported in a previous study by Stochino et al. [179], where a 30% replacement level resulted in the highest peak load under similar conditions. Of particular interest is the performance of mix M100, which reached a peak load very close to that of M0. This indicates that even in the presence of reduced mechanical properties of concrete, the interface behaviour between RCA concrete and steel sheeting is effective in ensuring adequate global resistance.

When the span increases to 2.80 m, a general decrease in peak load is observed for all mixes, and M20 again records the highest peak load. A distinctive feature of this configuration is the progressive and nearly linear recovery of load-bearing capacity observed in the M20 slabs following the initial load drop. Unlike other mixes, which tend to exhibit irregular oscillations or plateau behaviour, the M20 curve gradually regains strength smoothly and consistently. This suggests that, following debonding, the degradation of the interface may be less abrupt, allowing the slab to activate an effective flexural mechanism that progressively restores structural performance. In contrast, M70 and M100 show delayed peaks, occurring after the elastic phase, possibly due to slower interface mobilization.

For the 3.20 m span, mixes M0, M20, and M70 exhibit similar structural responses and nearly identical peak load values, indicating that up to 70% RCA replacement ratio does not compromise load-bearing capacity even in longer spans. In contrast, mix M100 registers a noticeably lower peak load but shows a more stable and prolonged post-peak response. While the other mixes display three or more significant load drops, M100 experiences only two, suggesting a more continuous and controlled redistribution of internal stresses. This smoother evolution reflects the development of a sustained flexural regime, in which the slab retains load-bearing capacity over a wider deformation range, despite its lower initial stiffness. The behaviour suggests that, although M100 is more fragile in terms of strength, it may exhibit a form of ductile resilience under large deformations due to its ability to maintain a coherent failure mode. At the 3.20 m span, it is also observed that both M20 and M70 exhibit a more extended linear-elastic phase compared to M0, despite showing a similar initial stiffness. This behaviour is particularly evident in M70, which displays the most prolonged elastic branch among all mixes.

The average collapse load reported in Table 8 refers to the mean of the peak loads obtained from the individual tests conducted for each mix configuration, as presented in the **Appendix**. It should be clarified that this value does not correspond to the peak of the average load–

displacement curve, which instead reflects the global structural behaviour of the composite slab.

Table 8. Average collapse load [kN] of the tested slab.

Mix design	2400 mm	2800 mm	3200 mm
M0-0	48.23	41.96	36.56
M20-20	54.69	41.97	36.59
M70-70	42.12	40.36	35.58
M100-100	46.37	42.40	32.17

Figure 48-Figure 50 provides a comprehensive overview by illustrating the average load–displacement curves for all mix designs combined into a single graph for each span—2.40 m, 2.80 m, and 3.20 m, respectively—thus enabling direct visual comparison of the overall structural performance across different replacement levels.

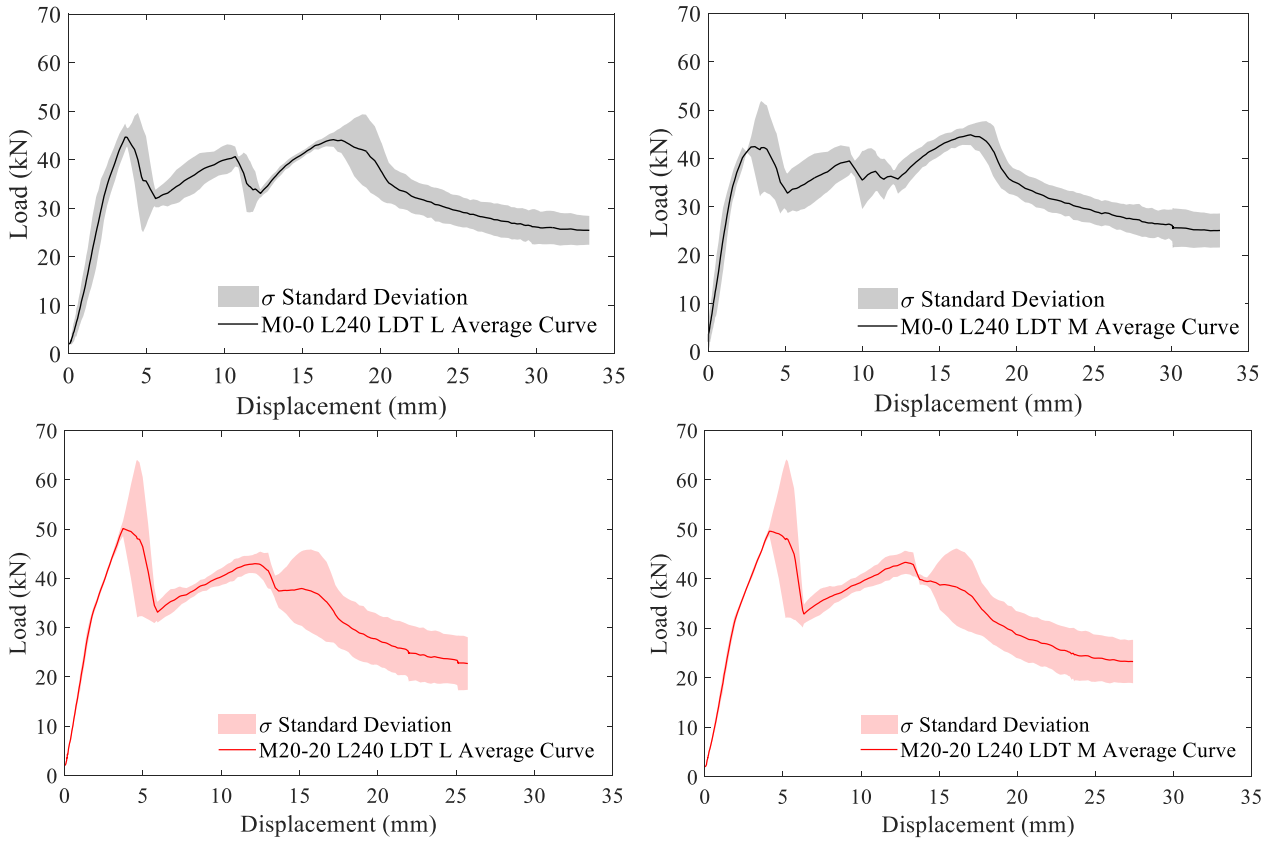

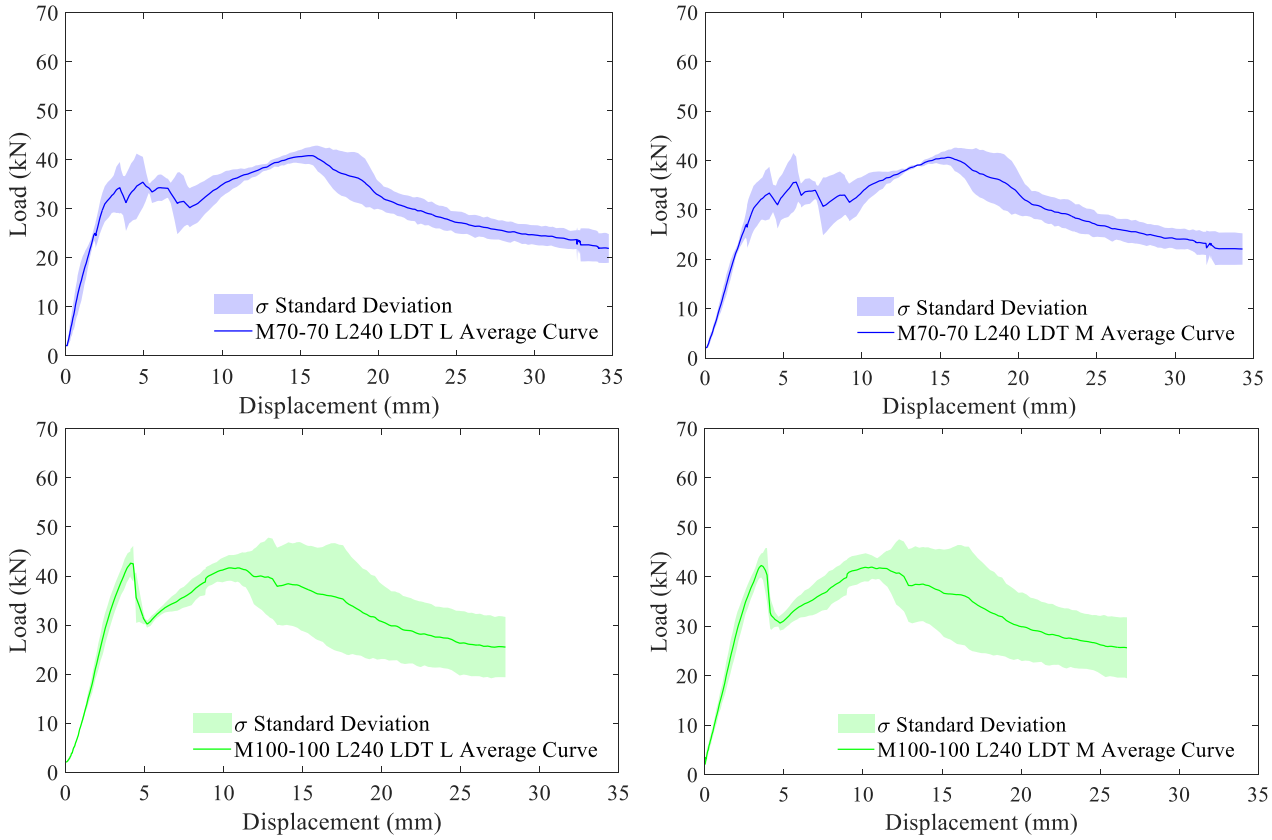

Figure 45. Average load-displacement curves for M0-0 (black), M20-20 (red), M70-70 (blue) and M100-100 (green) with a span of 2.40 m, recorded using LDT L (left) and LDT M (right).

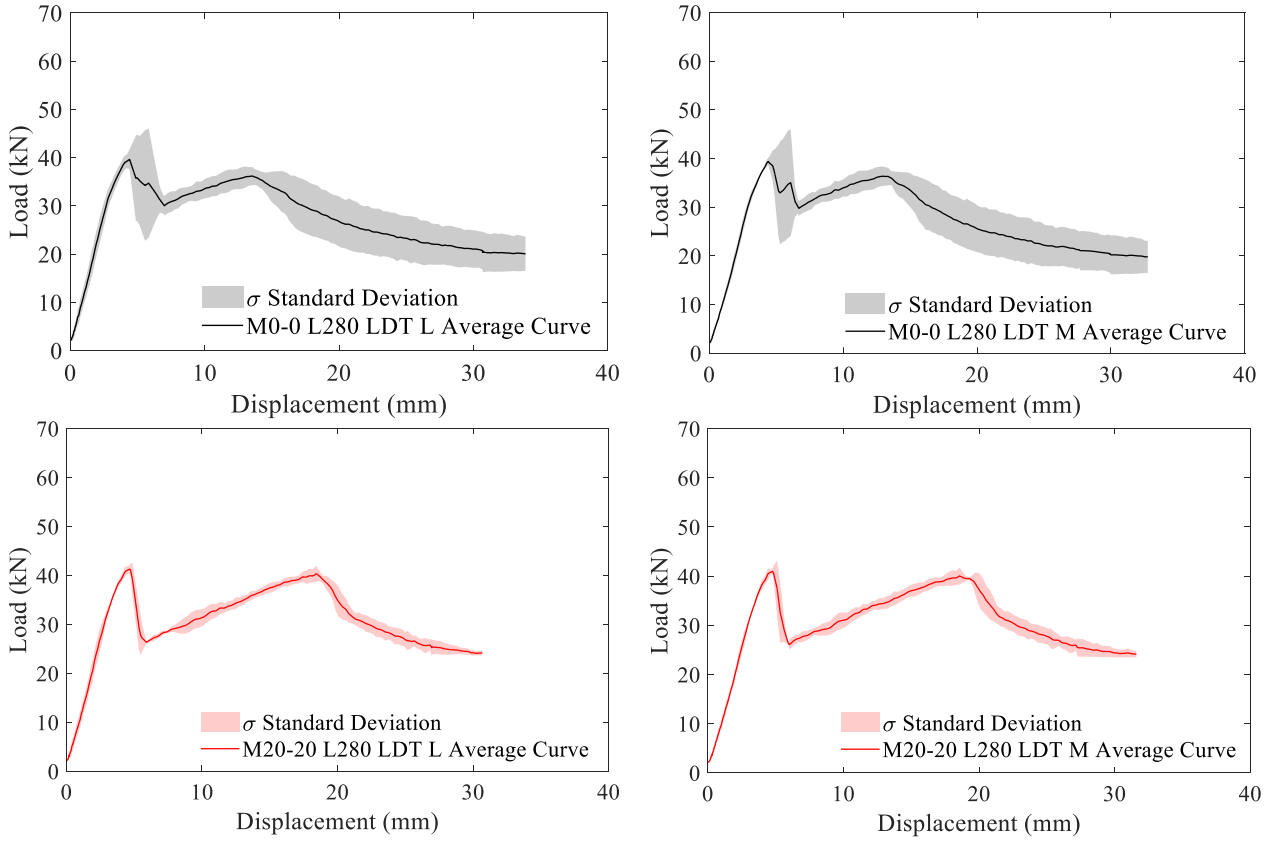

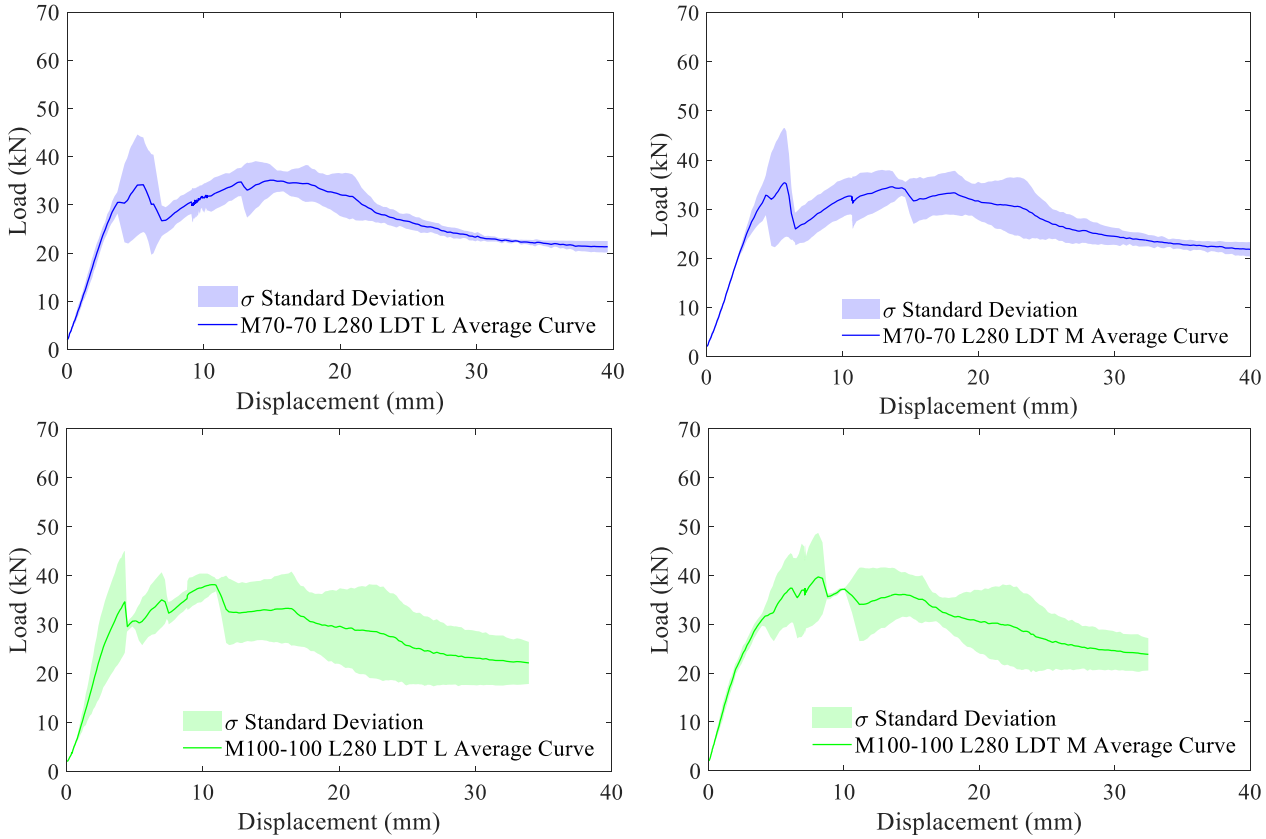

Figure 46. Average load-displacement curves for M0-0 (black), M20-20 (red), M70-70 (blue) and M100-100 (green) with a span of 2.80 m, recorded using LDT L (left) and LDT M (right).

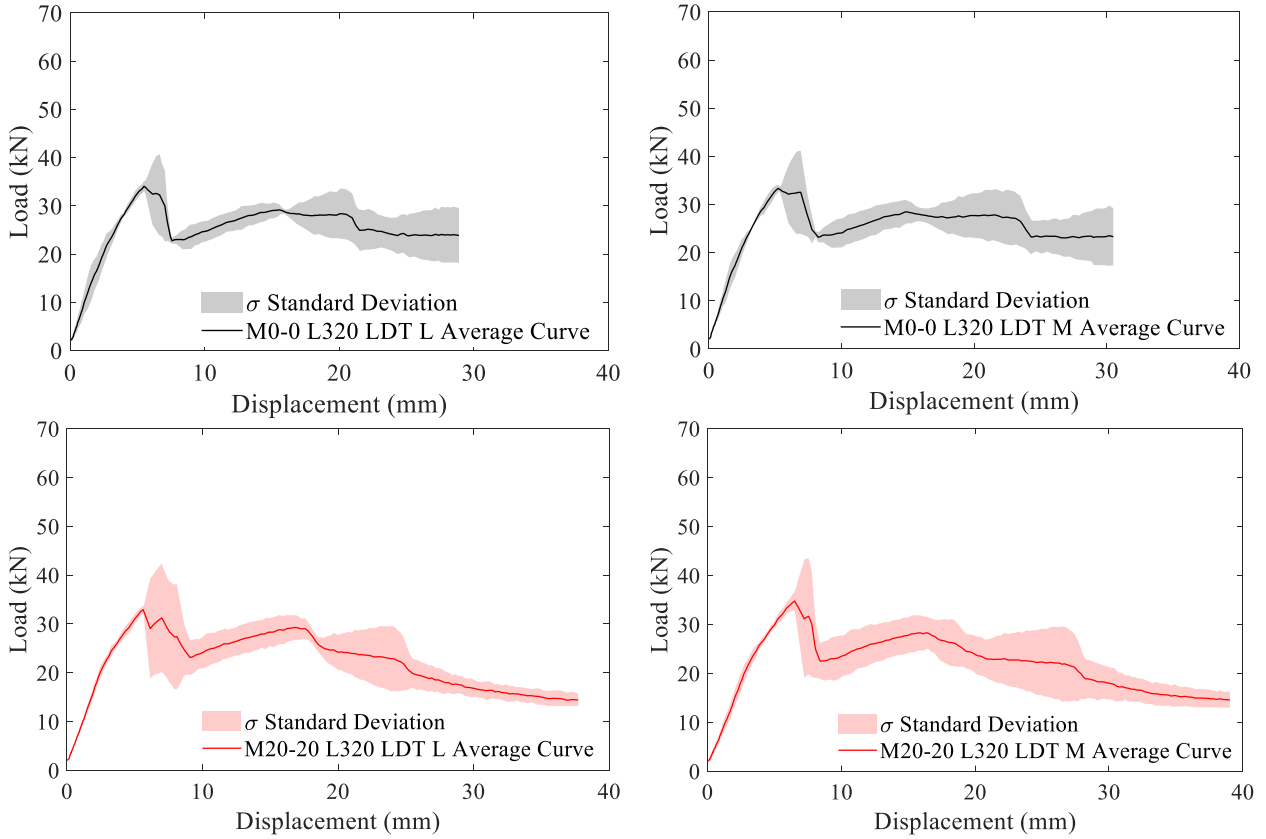

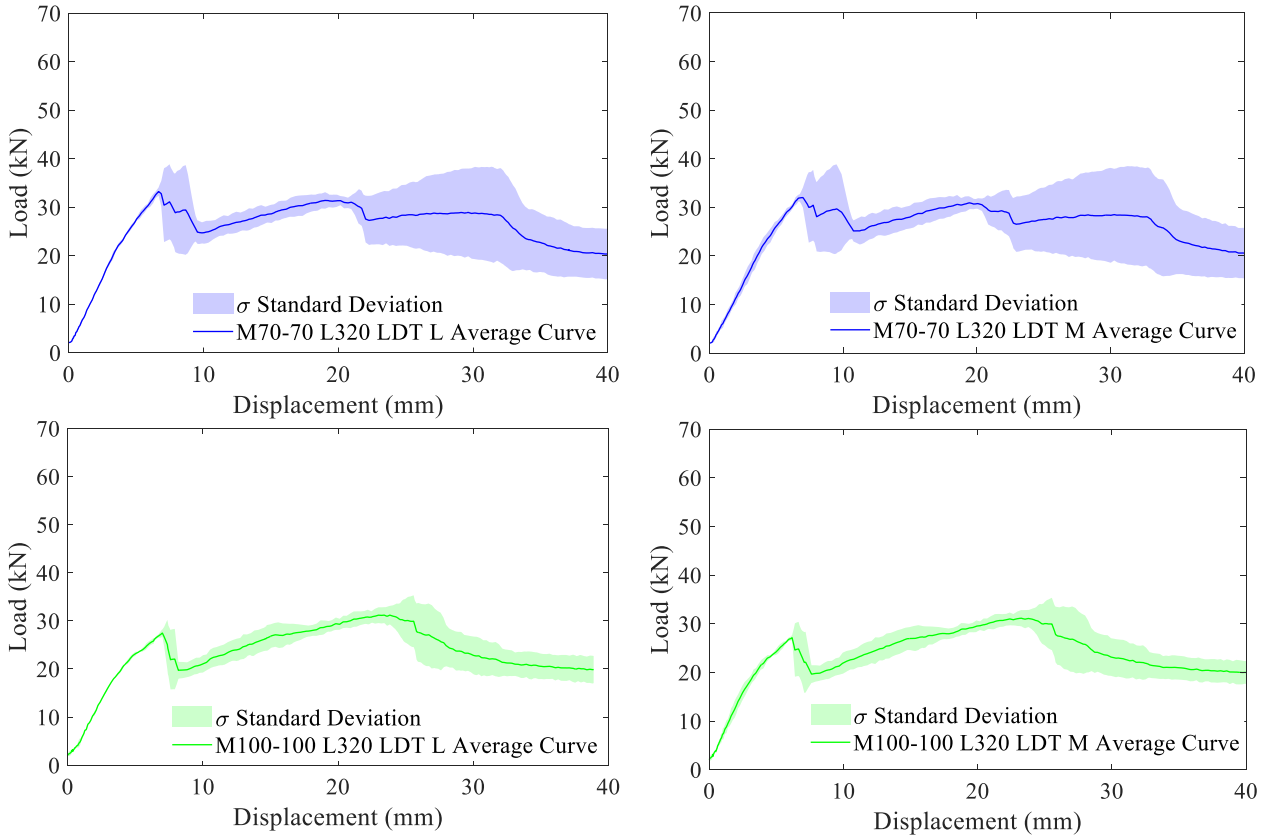

Figure 47. Average load-displacement curves for M0-0 (black), M20-20 (red), M70-70 (blue) and M100-100 (green) with a span of 2.80 m, recorded using LDT L (left) and LDT M (right).

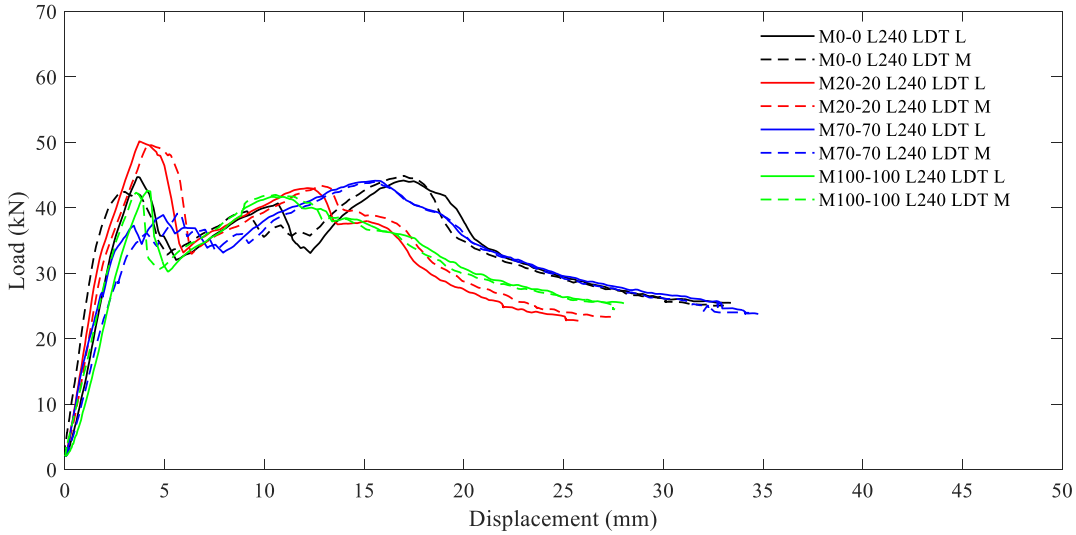

Figure 48. Average load-displacement curves for all mix designs with a span of 2.40 m, recorded using LDT L and LDT M.

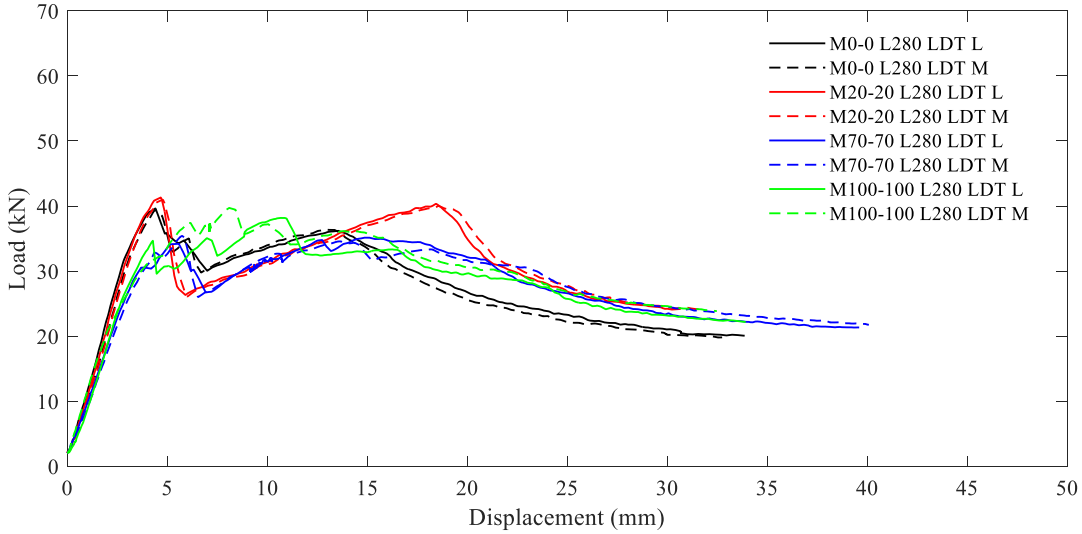

Figure 49. Average load-displacement curves for all mix designs with a span of 2.80 m, recorded using LDT L and LDT M.

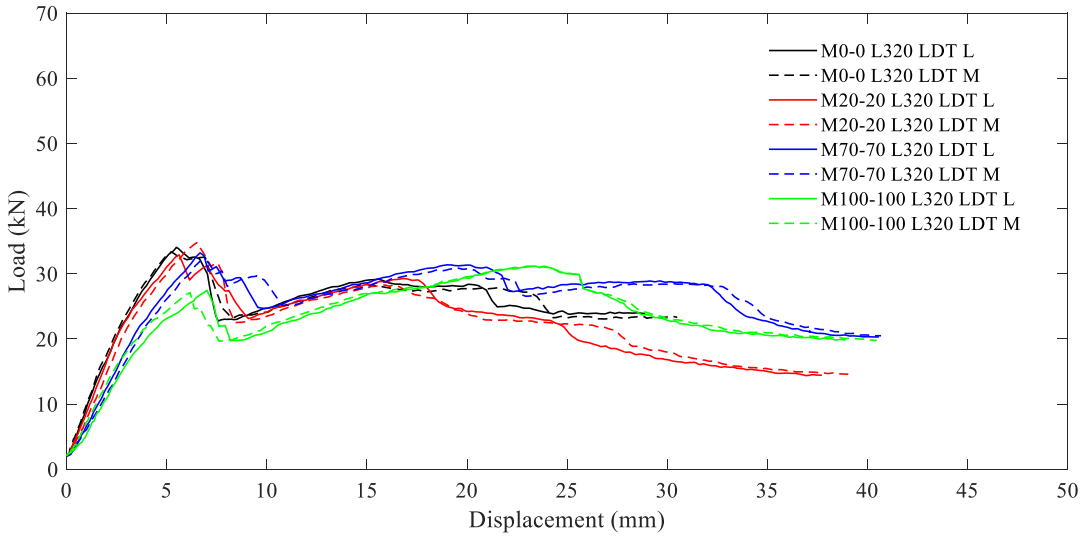

Figure 50. Average load-displacement curves for all mix designs with a span of 3.20 m, recorded using LDT L and LDT M.

6.2.3. Load versus horizontal displacements

Figure 51-Figure 53 illustrates the average load-horizontal displacement curves for each mix design, measured using LDT A&G and LDT E&H, corresponding respectively to span lengths of 2.40 m, 2.80 m, and 3.20 m. A general trend observed across all figures is that horizontal displacement remains negligible during the initial loading phase and increases significantly only once the debonding process initiates. The exact location at which initial slip occurs appears to be somewhat irregular, likely affected by local imperfections in the slab geometry, support positioning, or slight asymmetries in load application. Once the peak load is reached, a sharp drop in load is observed. Following this drop, a second phase emerges in which the curve exhibits a partial recovery of bearing capacity alongside a progressive increase in horizontal slip. Finally, in the third phase, the load stabilizes or slightly decreases while horizontal displacement continues to increase significantly.

As the span increases, the slip tends to occur at progressively lower loads. However, the development of slip generally occurs over a shorter load range as the span increases, except for M70-70 and M100-100, which exhibit both an earlier onset and a more sustained progression of slip. This suggests that higher RCA content accelerates the onset of interfacial damage while also reducing bond uniformity, resulting in a more extended debonding process.

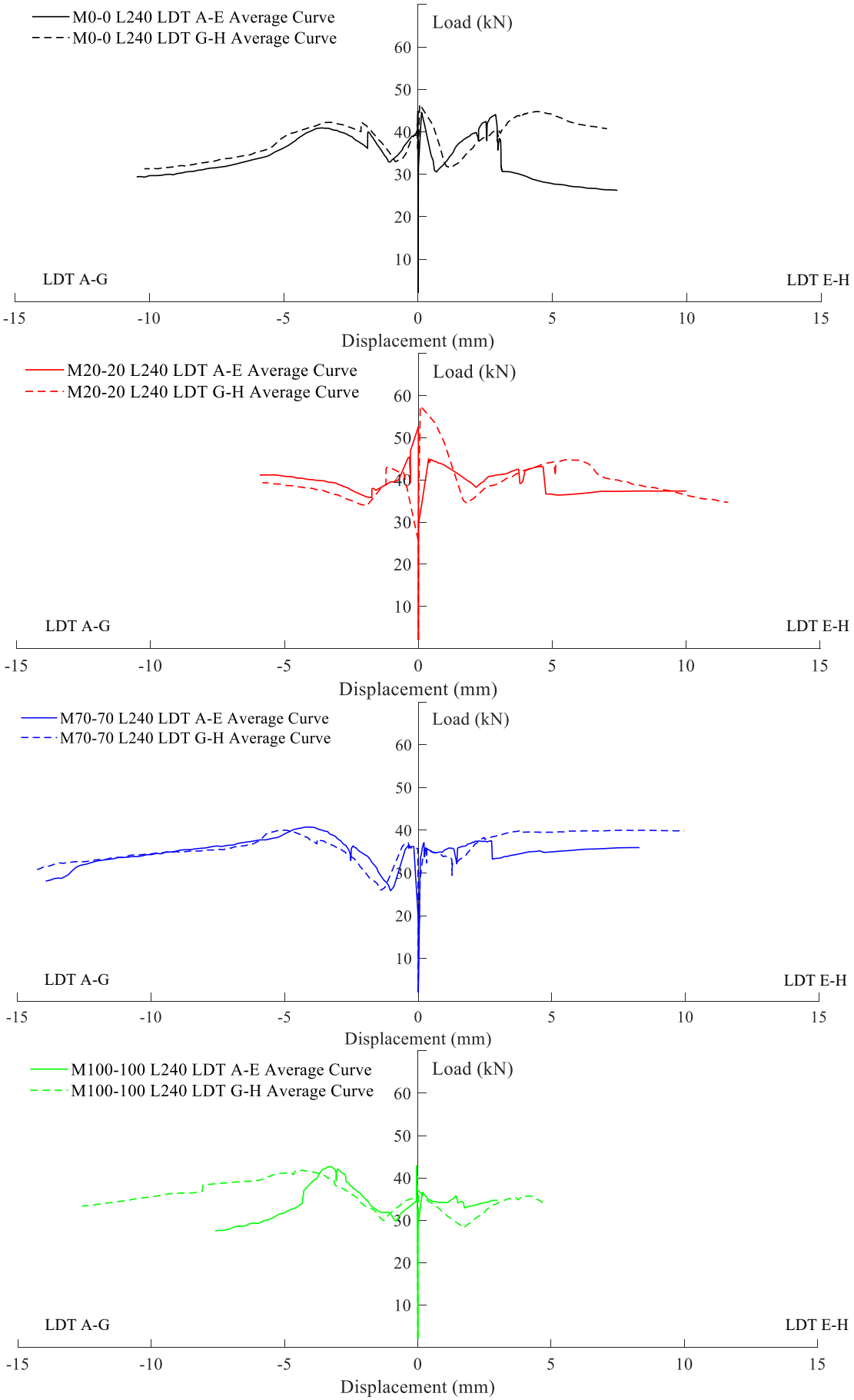

Figure 51. Average load-displacement curves for M0-0 (black), M20-20 (red), M70-70 (blue) and M100-100 (green) with a span of 2.40 m, recorded using LDT A-G (left) and LDT E-H (right).

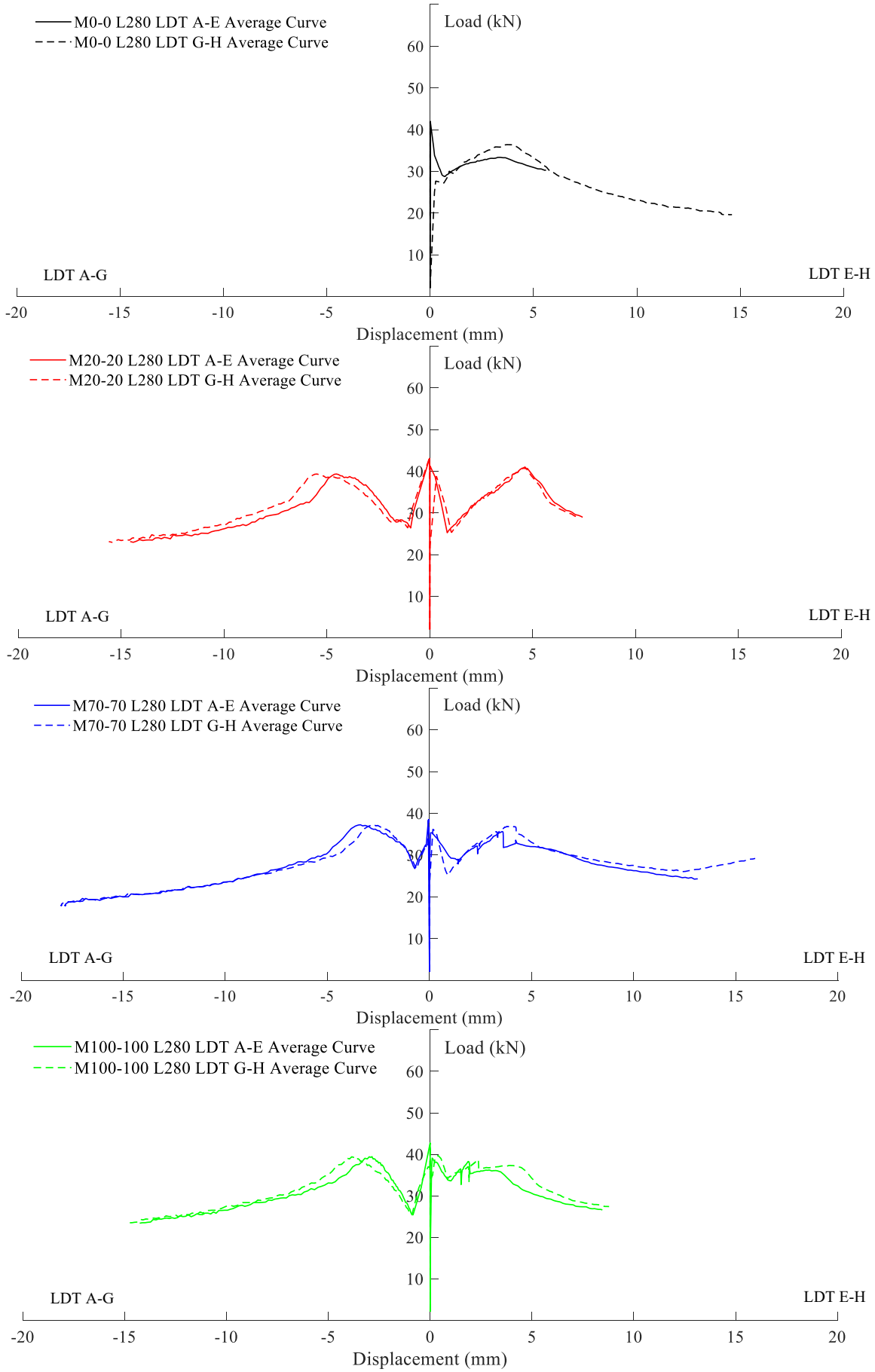

Figure 52. Average load-displacement curves for M0-0 (black), M20-20 (red), M70-70 (blue) and M100-100 (green) with a span of 2.80 m, recorded using LDT A-G (left) and LDT E-H (right).

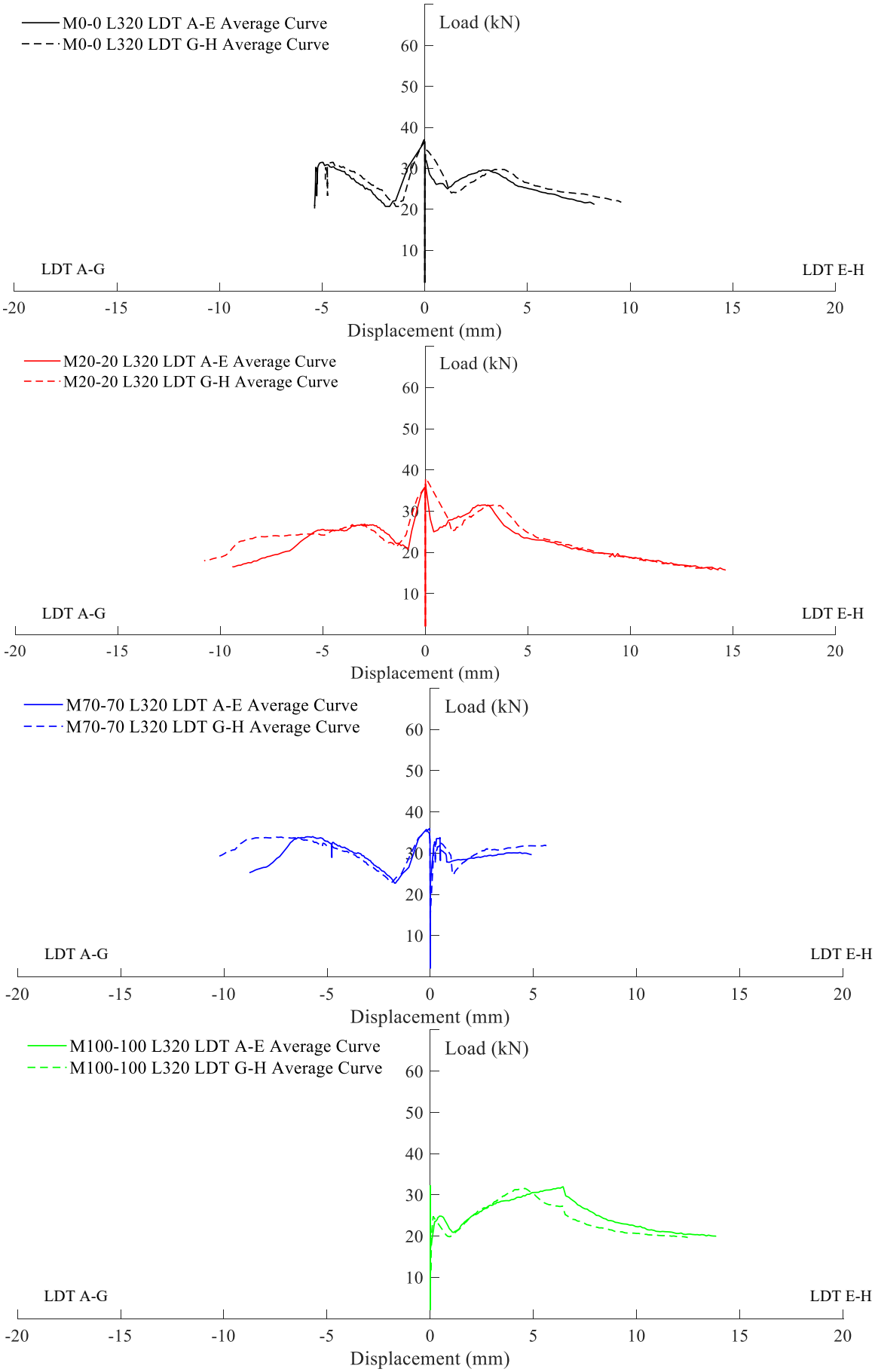

Figure 53. Average load-displacement curves for M0-0 (black), M20-20 (red), M70-70 (blue) and M100-100 (green) with a span of 3.20 m, recorded using LDT A-G (left) and LDT E-H (right).

6.2.4. Discussion

The experimental findings highlight the complex interaction between material composition, span length, and interfacial behaviour in composite slabs incorporating RCAs. The load–displacement curves consistently revealed the typical three-phase mechanical response observed in steel–concrete composite systems: an initial elastic stage, a debonding phase characterized by abrupt load drops, and a post-peak flexural regime associated with ductile deformation and gradual load redistribution. The presence of RCA substantially influenced both the amplitude and the progression of these phases, confirming that the bond mechanism at the steel–concrete interface is sensitive to the modified microstructural features of recycled aggregates.

At shorter spans (2.40 m), the enhanced peak load attained by the M20 mix suggests that moderate RCA replacement can contribute to a more efficient load transfer mechanism. This finding aligns with the hypothesis that limited quantities of recycled aggregates, due to their rough and irregular surface texture, may enhance frictional interlock at the steel–concrete interface, counterbalancing the moderate loss of intrinsic concrete strength. The behaviour corroborates previous observations by Zhang et al. [180] and Chen et al. [181], who identified that intermediate RCA ratios can yield competitive longitudinal shear resistance compared with natural aggregate concretes, provided that the interfacial transition zone (ITZ) remains sufficiently compact and continuous. For higher replacement ratios (M70 and M100), however, the interface becomes progressively more heterogeneous, leading to premature debonding and larger oscillations in the load signal, indicative of unstable shear transfer. This transition reflects a reduction in the stiffness of the bond–slip relationship, as documented in pull-out and push-off tests on RAC composite slabs, where τ–s curves show an earlier onset of slip and a lower ultimate bond stress compared with conventional concretes [180], [182].

The effect of increasing span length is equally significant. Longer spans (2.80 m and 3.20 m) reduced the peak load and accentuated the ductile post-peak branch, revealing that flexural deformation increasingly governs the global behaviour. The evolution of load recovery after initial slip—particularly pronounced in M20 at 2.80 m—suggests that partial interfacial degradation does not necessarily lead to total loss of composite action but can activate secondary load paths through frictional mechanisms. Such recovery phases are consistent with the multi-stage debonding mechanisms identified by Saccone et al. [53], where recycled concretes exhibited a more progressive redistribution of shear stresses after initial bond failure. In contrast, the full replacement mix (M100) demonstrated a more stable yet lower-strength response: its reduced initial stiffness was compensated by a smoother decay and sustained deformation capacity, confirming the potential of RCA concretes to maintain global ductility even when interfacial integrity is compromised.

The average collapse loads summarized in Table 4 confirm these trends quantitatively. The limited variation between M0 and M100 for short spans indicates that global load-bearing capacity is not solely governed by the compressive strength of the concrete but also by the interfacial efficiency and geometric stiffness of the composite section. Nevertheless, as the span increases, the influence of RCA content becomes more pronounced, with M100 showing a 12–15 % reduction in collapse load relative to the control mix. This reduction reflects the cumulative effect of lower modulus of elasticity and weaker aggregate–matrix bonding, which together accelerate slip initiation and decrease effective stiffness. Similar findings were reported by Lu et al. [182], who noted that higher RCA contents promote earlier interfacial

cracking but can still sustain stable load–deformation evolution under controlled flexural regimes.

From a design perspective, these results underscore the need to refine analytical formulations for longitudinal shear resistance in RAC-based composite slabs.

In summary, the experimental evidence confirms that moderate RCA replacement (≈20 %) can enhance interfacial efficiency and delay slip initiation, while excessive substitution (>70 %) compromises the stiffness and ultimate capacity of the slab. The distinct post-peak behaviour observed for fully recycled mixes, however, points to a beneficial ductile mechanism that ensures stable deformation under increasing displacement, an aspect of great interest for safety design under service and extreme conditions. Overall, the results support the conclusions drawn by Saccone et al. [53] that sustainable composite slabs with recycled concrete can achieve satisfactory longitudinal shear performance provided that mix design, span-to-depth ratio, and steel deck geometry are jointly optimized to balance stiffness, ductility, and bond integrity.

6.2.5. Theoretical Collapse Load by the Partial Shear Connection (PSC) Method

To predict the collapse load due to longitudinal shear of the 2024 RACCS slabs, the Partial Shear Connection (PSC) procedure—consistent with the provisions of *EN 1994-1-1* and the guidelines provided in the accompanying lecture notes—was applied. Within this framework, the theoretical moment resistance (M_{Rd}) of the composite section was first determined based on the degree of interaction between the concrete and the profiled steel sheeting. This calculated moment resistance was then converted into the corresponding collapse load (F_{EC4}) for the four-point bending configuration adopted in the experimental campaign. For a simply supported slab subjected to two symmetrically placed loads, located at a distance ($L_s = L/4$) from each support, the relationship between the applied load and bending moment is defined as equation (7):

$$M = \frac{F, L_s}{2} \quad \Rightarrow \quad F_{EC4} = \frac{2M_{Rd}}{L_s} \tag{7}$$

This expression allows the theoretical load-carrying capacity predicted by the PSC method to be directly compared with the experimentally observed collapse loads, providing a consistent basis for evaluating the longitudinal shear behaviour of the composite slabs.

The Partial Shear Connection (PSC) method was applied assuming that the ultimate limit state (ULS) is governed by longitudinal shear failure at the concrete–steel interface, where the steel deck behaves plastically and the concrete within the ribs provides no contribution to the overall resistance. The interface shear strength (τ_u) was assumed in the range 0.16–0.20 MPa. These values were adopted from the technical information provided by *Spinelli company* and refer to measurements performed by the manufacturer for conventional (natural-aggregate) concrete; therefore, they represent the characteristic shear capacity of the metal decking when used with standard concrete mixes. The key geometric and material parameters considered in the calculation include the effective slab width (b), concrete thickness above the steel deck (h_c), total slab depth (h_t), steel sheet area (A_p), plastic centroid eccentricities

(e) and (e_p), and the design strength of steel (f_{pd}) obtained from manufacturer data. The mean compressive strength of concrete (f_{cm}) was taken from the experimental results of the 2024 campaign.

The governing equations used in the PSC calculation are summarized as equations (8-(14:

Interface force and degree of interaction:

$$N_c = \tau_u \, b \, (L_0 + L_s), \quad \eta = \frac{N_c}{N_{cf}}$$

(8)

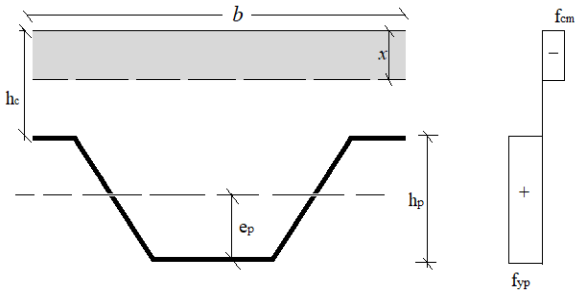

Figure 54. Stresses distribution on the composite section.

Concrete compression capacity (full interaction):

$$N_{cf} = b \, h_c \, 0.85 \, f_{cm}$$

(9)

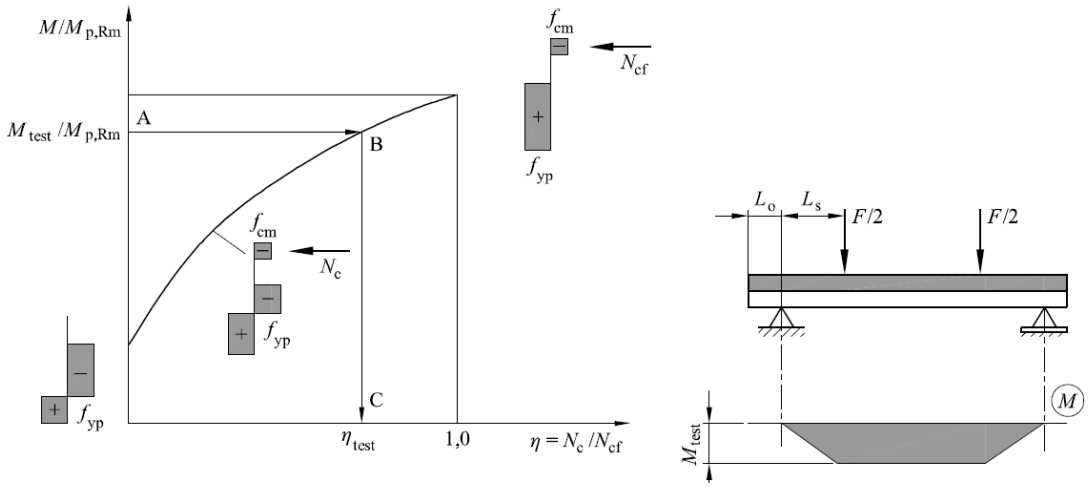

Figure 55. Approach for the determination of the degree of interaction (EC4).

Steel plastic tension capacity:

$$N_{pa} = A_p\, f_{pd}$$

(10)

Plastic moment component of the steel sheet (PSC reduction):

$$M_{pr} = 1.25\, M_{pa}\left(1 - \frac{N_{cf}}{A_p, f_{pd}}\right) \leq M_{pa}$$

(11)

Lever arm of the internal force couple:

$$z = h_t - 0.5h_c - e_p + \left(e_p - e\right)\frac{N_{cf}}{A_p\, f_{pd}}$$

(12)

Design moment resistance at longitudinal shear collapse:

$$M_{Rd} = M_{pr} + \eta\, N_{cf}\, z$$

(13)

Finally, the predicted collapse load corresponding to longitudinal shear failure in the four-point bending configuration is obtained as:

$$F_{EC4} = \frac{2M_{Rd}}{L_s}$$

(14)

This analytical framework allows for a consistent estimation of the theoretical collapse load for each RACCS slab configuration, enabling a direct comparison between experimental results and the predictions from the PSC method.

Table 9 presents the comparison between the experimental collapse loads ($P_{u,\exp}$) and the theoretical loads (F_{EC4}) calculated using the Partial Shear Connection (PSC) method. The results provide an evaluation of the predictive capability of the PSC approach for the 2024 composite slabs (RACCS) tested with varying RCA replacement ratios (0%, 20%, 70%, and 100%) and span lengths (2.40 m, 2.80 m, and 3.20 m).

Table 9. Comparison between experimental and theoretical collapse loads of RACCS slabs predicted by the Partial Shear Connection (PSC) method for different RCA contents and span lengths.

RCA (%)	Span (cm)	$P_{u,exp}$ (kN)	F_{EC4} (τ = 0.16)	*Error (%)*	F_{EC4} (τ = 0.20)	*Error (%)*
M 0-0	240	48	56	17	58	21
M 0-0	280	42	49	17	51	22
M 0-0	320	36	44	22	46	29
M 20-20	240	55	56	2	58	5
M 20-20	280	42	49	17	51	22
M 20-20	320	36	44	22	46	29
M 70-70	240	42	56	33	58	38
M 70-70	280	40	49	23	51	28
M 70-70	320	36	44	22	46	29
M100-100	240	47	56	19	58	23
M100-100	280	43	49	14	51	19
M100-100	320	32	44	37	46	45

In general, the predicted collapse loads obtained from the PSC method exhibit satisfactory agreement with the experimental results, with average discrepancies ranging between approximately 2% and 38%, depending on the assumed interface shear strength and RCA content. For ($\tau_u = 0.16$) MPa, the calculated loads tend to slightly overestimate the experimental results, with an average error around 20%, whereas adopting ($\tau_u = 0.20$) MPa provides a closer correlation in most cases, particularly for mixes M20-20 and M100-100. This range of variation is consistent with expected experimental uncertainties and modeling assumptions in longitudinal shear analyses of composite slabs.

The influence of RCA content on the analytical predictions appears to be moderate. For lower RCA percentages (M20-20), the theoretical and experimental loads show very close agreement, with differences as low as 2–5%, confirming that partial RCA replacement does not significantly alter the overall shear transfer mechanism. Conversely, for higher RCA contents (M70-70 and M100-100), the PSC model tends to slightly overpredict the collapse load, indicating that the real interface shear strength might be marginally lower than the nominal value assumed in the calculations. This observation aligns with the experimentally observed earlier onset of slip at the steel–concrete interface for high RCA mixes, which is likely due to the increased porosity and weaker ITZ associated with recycled aggregates.

The span length also plays a noticeable role in the prediction accuracy. Longer spans (3.20 m) show higher deviations, reaching up to 29–45%, which can be attributed to the amplified influence of shear lag and the redistribution of longitudinal stresses along the interface. Despite these differences, the overall trend of the theoretical predictions remains consistent with the experimental data, successfully reproducing the hierarchy of strengths among different mixes and span configurations.

The theoretical resistances calculated using the EC4 PSC method (Table 9) are generally higher than the experimental collapse loads observed in the RACCS tests. This overestimation can be explained by both material-related and methodological factors. First, the EC4 model was developed for conventional concrete with dense aggregate structure and does not explicitly

account for the higher porosity and weaker interfacial transition zone typical of recycled aggregate concretes. As a consequence, the model assumes higher stiffness and bond efficiency at the steel–concrete interface than those actually achieved in the RACCS specimens. Second, the simplified assumptions of the PSC method—such as the full plastic response of the steel deck at ultimate limit state and the neglect of local slip and partial debonding effects—lead to an idealized interaction that enhances the predicted load capacity. In contrast, the experimental slabs exhibited progressive slip and localized cracking that reduced the effective longitudinal shear transfer. Finally, the EC4 analytical framework does not include the reduction in interfacial cohesion caused by the rougher and more porous surface of RCA concrete. As a result, the predicted shear interaction and ultimate bending capacity appear higher than those measured experimentally. Overall, the higher theoretical values underline the need to introduce correction factors or modified interaction parameters for composite slabs incorporating recycled aggregates, to ensure that analytical predictions remain conservative and consistent with the experimental evidence.

To address the selection of the input parameters used in the EC4 Partial Shear Connection calculations, it is confirmed that the compressive strength of the concrete was taken individually for each mix based on the experimental 28-day test results reported in the mechanical characterization sections. This ensured that the PSC evaluation was representative of the actual material performance of each concrete type. The design yield stress of the steel sheeting (f_{pd}) was adopted from the manufacturer datasheet and remained constant for all specimens. The degree of interaction (η) was not assumed but was evaluated separately for every mix and span configuration based on the experimentally measured collapse moment and the PSC interaction domain. Therefore, the PSC calculations incorporate mix-specific concrete strengths and span-dependent interaction behavior, while the steel contribution remains constant due to the uniformity of the steel deck material across the tested slabs.

7. Conclusion

The use of recycled concrete aggregates (RCA) derived from construction and demolition waste (CDW) represents a significant advancement toward sustainable concrete production and the transition to a circular construction economy. This research has demonstrated that RCA offers substantial environmental benefits, including the reduction of landfill waste, conservation of natural resources, and lower energy demand associated with aggregate production. However, the mechanical and durability performance of recycled aggregate concrete (RAC) is strongly influenced by the characteristics of the recycled aggregates, such as the presence of adhered mortar, variable porosity, and contamination levels. These features often lead to reduced compressive and tensile strengths, higher permeability, and lower resistance to aggressive environmental exposure compared to concrete made with natural aggregates. Nevertheless, through suitable pretreatment methods—mechanical, chemical, or thermal—the quality of RCA can be significantly improved, reducing residual mortar content and enhancing bonding within the cement matrix. Similarly, optimized mix design strategies, the use of supplementary cementitious materials (SCMs), and extended curing times have proven effective in improving both strength and durability, enabling RAC to meet structural performance requirements while contributing to sustainability goals.

To comprehensively assess these aspects, this PhD research conducted two major experimental campaigns (2023 and 2024) encompassing both material-level and structural-scale investigations. The mechanical and durability properties of RAC were systematically evaluated through tests on compressive strength, tensile and flexural strength, elastic modulus, creep, oxygen and water permeability, carbonation depth, chloride penetration, and freeze–thaw resistance. The results consistently confirmed that the replacement level and quality of RCA are the dominant factors governing performance. In the 2023 campaign, which employed conventional RCA, the compressive strength at 28 days decreased from approximately 41.6 MPa for the control mix to 24 MPa for full replacement, while in the 2024 campaign—using higher-quality RCA with better gradation and lower porosity—the corresponding range was 40–35 MPa, with 90-day strength reaching up to 45.3 MPa. These findings highlight the crucial influence of RCA quality in mitigating strength loss and confirm that extended curing enhances performance by improving the interfacial transition zone (ITZ) between RCA and the cement paste.

Durability tests revealed parallel trends. Oxygen and water permeability coefficients increased with RCA content, particularly in the 2023 series, while the 2024 campaign exhibited significantly improved resistance due to the superior aggregate properties. Similarly, carbonation and chloride ingress depths were lower for the 2024 mixes, confirming the beneficial effect of well-graded, low-porosity RCA on limiting fluid and gas transport. Freeze–thaw tests further underscored the importance of RCA quality: although mass loss and surface damage intensified with RCA content in the 2023 campaign, the 2024 specimens displayed stable performance even at high replacement levels. Correlations between mechanical and durability indicators—such as between compressive strength and permeability, or carbonation depth and oxygen diffusion—validated the interdependence of these properties and emphasized the need for integrated durability evaluation frameworks.

Overall, the experimental evidence demonstrates that partial replacement of natural aggregates (up to 50–70%) can be safely adopted in structural concrete, provided that high-quality RCA, optimized mix design, and proper curing conditions are ensured. Extended curing periods were shown to substantially recover strength and improve durability at 90 days,

offsetting the inherent weaknesses of recycled aggregates. The results thus support the practical feasibility of RAC in structural applications, offering reliable data for future design and standardization efforts.

Beyond the material-scale investigations, this research extended to the structural performance of recycled aggregate concrete composite slabs (RACCS). A total of 48 full-scale slabs were produced encompassing six concrete mixes (M0-0, M20-20, M30-30, M50-50, M70-70, M100-100) and three span lengths (2.40 m, 2.80 m, and 3.20 m). The results confirmed that increasing RCA content led to a gradual reduction in compressive strength, tensile strength, and elastic modulus; however, all mixes met the minimum mechanical requirements for composite applications. Importantly, all specimens exhibited a consistent three-phase behavior: an initial elastic regime, a debonding phase, and a post-peak ductile response characterized by residual load-bearing capacity. Even at full RCA replacement, the slabs maintained ductile post-peak performance, confirming effective steel–concrete interaction.

Moderate RCA replacement levels (20–70%) yielded the most balanced results, combining high load-bearing capacity, controlled deformation, and ductile failure modes. The mix M20-20 achieved the highest collapse load (54.7 kN) for the 2.40 m span, while mixes with up to 70% RCA maintained comparable resistance at intermediate spans. The fully recycled mix (M100-100) showed reduced peak load but a more stable post-peak response, indicating improved energy dissipation and deformation capacity—an advantageous feature for seismic design. These results highlight the strong potential of RCA to enhance mechanical interlock and bonding with steel sheets, compensating for its lower intrinsic stiffness.

Collectively, the findings confirm that RCA-based composite slabs can achieve satisfactory structural performance and ductility when appropriate mix design and span configurations are adopted. The experimental outcomes contribute valuable data for the refinement of analytical models.

From a broader perspective, this research demonstrates that the integration of RCA in both conventional and composite concretes is not only feasible but also desirable from an environmental standpoint. Although a quantitative environmental assessment was not performed in this thesis, the use of recycled concrete aggregates is widely recognized in the literature as a strategy with potential environmental benefits, mainly related to the reduction of natural aggregate extraction and the diversion of construction and demolition waste from landfills. Therefore, the possible reduction in carbon footprint associated with RCA concrete should be interpreted as a qualitative implication derived from existing studies, rather than a result directly assessed within the present experimental work. A comprehensive Life Cycle Assessment (LCA) is recommended as a future research development to quantitatively evaluate the environmental impact of RCA incorporation in concrete.

Despite the encouraging outcomes, several challenges remain before RCA can be fully mainstreamed in construction practice. Future research should focus on developing standardized RCA treatment and quality control protocols, as well as establishing unified design guidelines for structural applications. Moreover, long-term investigations under cyclic, fatigue, and environmental loading conditions are necessary to assess time-dependent behavior and ensure reliability in service. Particular attention should be devoted to studying the performance of RCA-based composite slabs under repeated and seismic loading, where their ductile post-debonding response could provide significant advantages in terms of energy dissipation and structural resilience.

By addressing these remaining research gaps, recycled aggregates can evolve from a sustainable alternative into a primary construction resource. This transformation will not only reduce the environmental impact of the construction industry but also reinforce the foundation of circular economy principles in civil engineering. The results of this doctoral research thus provide both scientific evidence and practical guidance for integrating recycled materials into high-performance, sustainable concrete structures, paving the way for a new generation of environmentally responsible construction technologies.

8. Appendix

Figure 56-Figure 67 presents the complete set of load–displacement curves recorded during the 2024 experimental testing of all composite slab specimens from LDT F and LDT B, placed under the loading points to monitor local vertical displacements. These figures provide a comprehensive overview of the structural response for all mix configurations (M0-0, M20-20, M70-70, and M100-100) and span lengths (2.40 m, 2.80 m, and 3.20 m). The load–displacement curves depict the full loading process—from the initial elastic phase to the onset of debonding and the subsequent post-peak flexural behavior—demonstrating both the consistency of the experimental results and the influence of RCA content on overall ductility and residual load-bearing capacity.

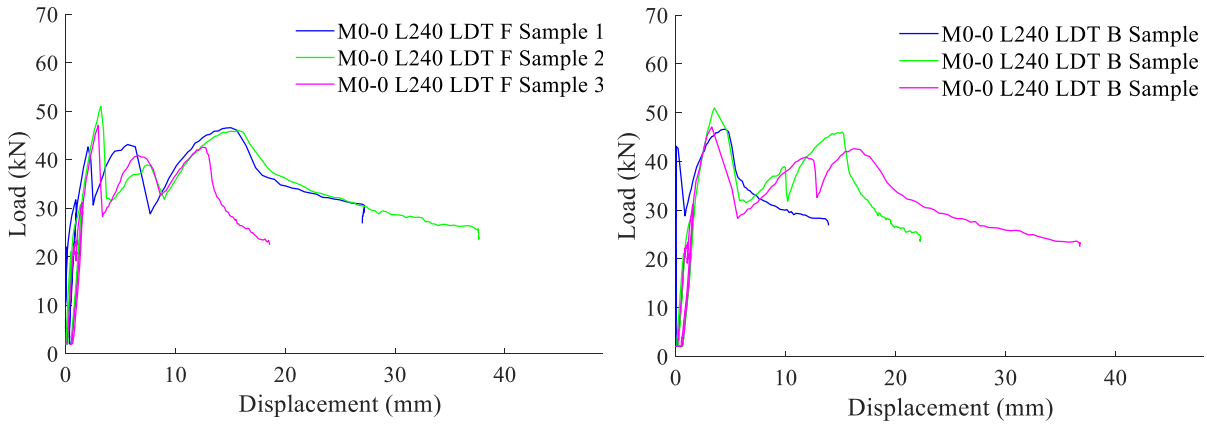

Figure 56. Load-displacement curves for sample M0-0 with a span of 2.40 m, recorded using LDT F (left) and LDT B (right).

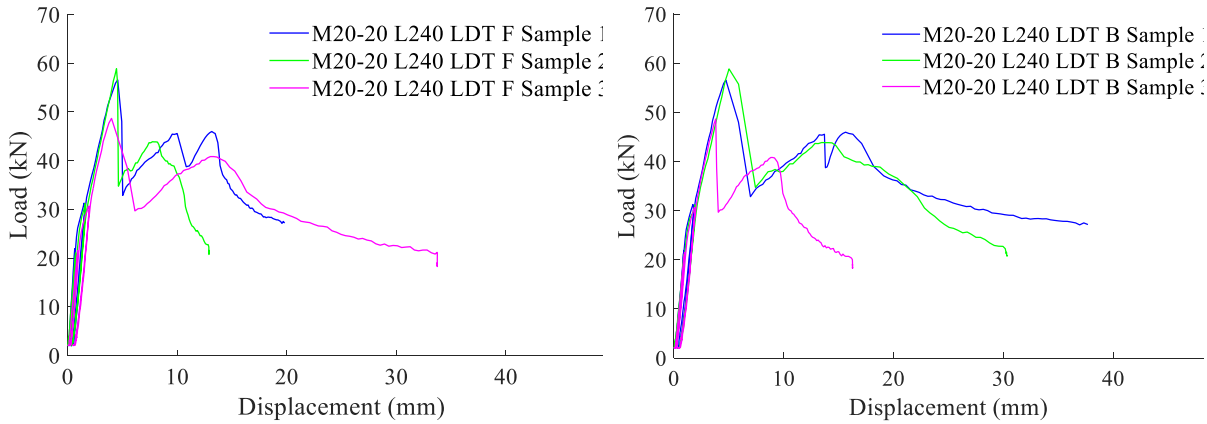

Figure 57. Load-displacement curves M20-20 with a span of 2.40 m, recorded using LDT F (left) and LDT B (right).

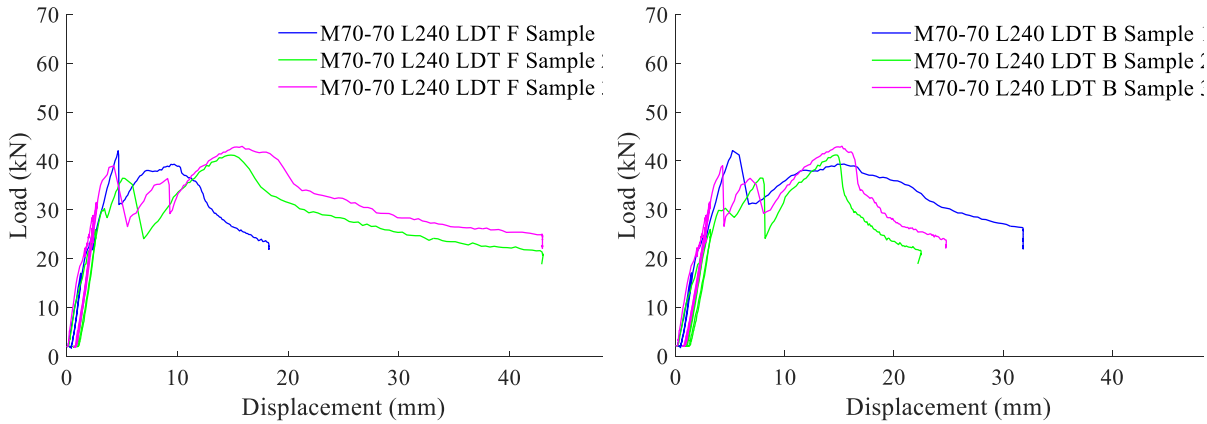

Figure 58. Load-displacement curves M70-70 with a span of 2.40 m, recorded using LDT F (left) and LDT B (right).

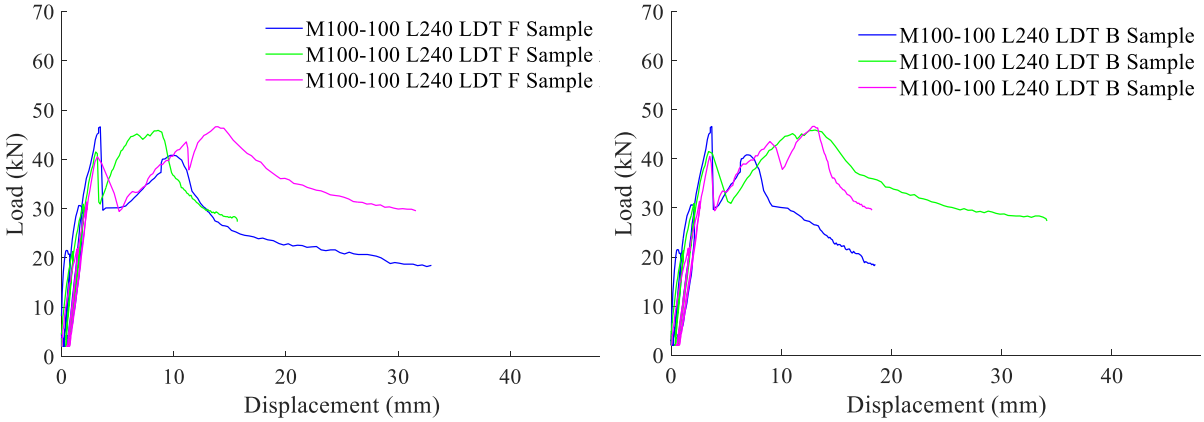

Figure 59. Load-displacement curves M100-100 with a span of 2.40 m, recorded using LDT F (left) and LDT B (right).

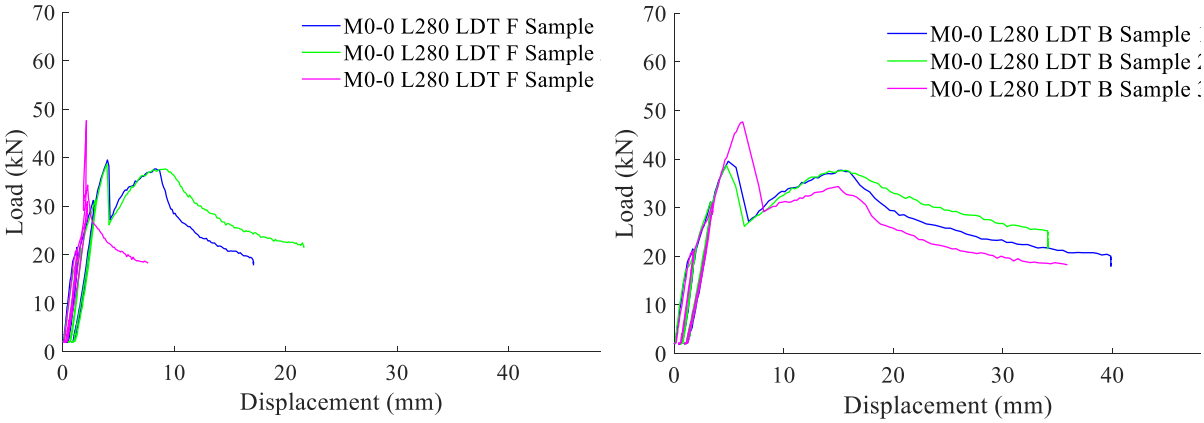

Figure 60. Load-displacement curves for sample M0-0 with a span of 2.80 m, recorded using LDT F (left) and LDT B (right).

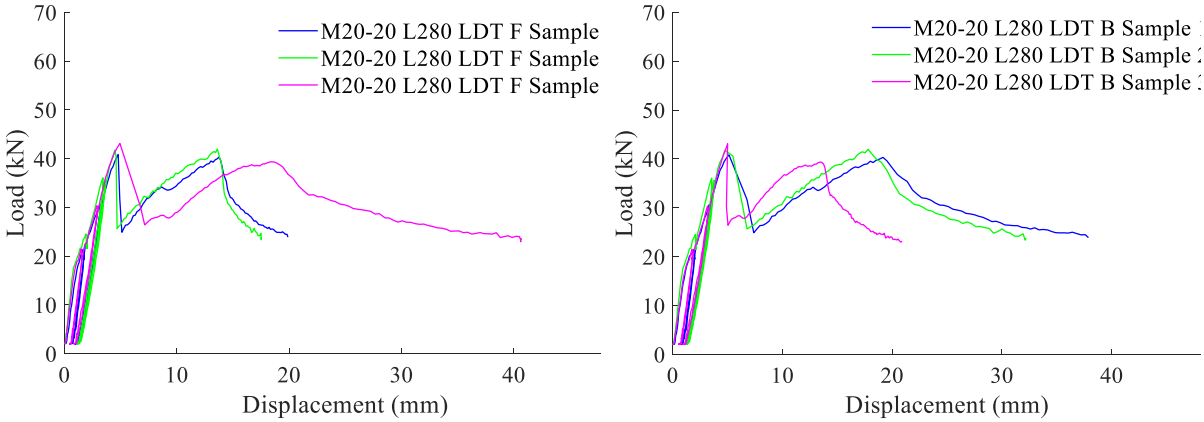

Figure 61. Load-displacement curves M20-20 with a span of 2.80 m, recorded using LDT F (left) and LDT B (right).

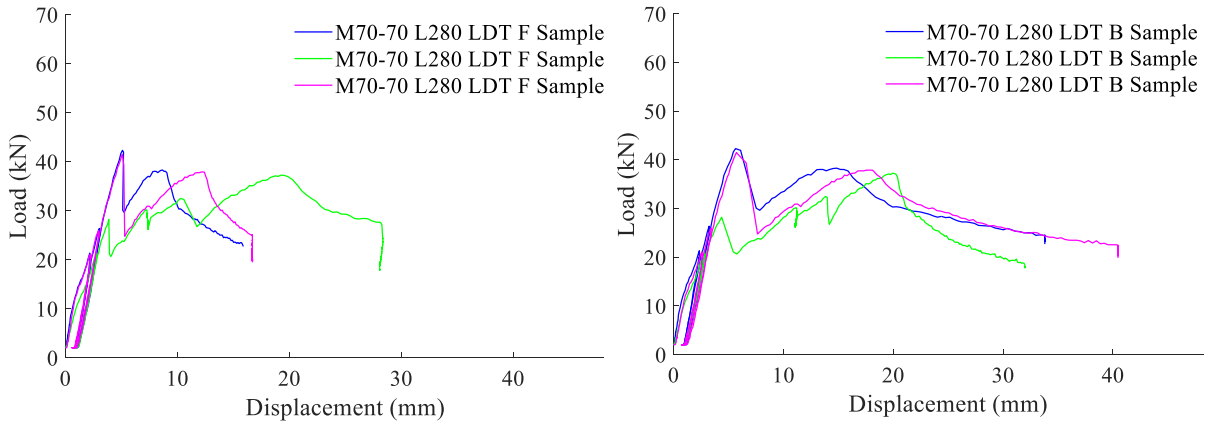

Figure 62. Load-displacement curves M70-70 with a span of 2.80 m, recorded using LDT F (left) and LDT B (right).

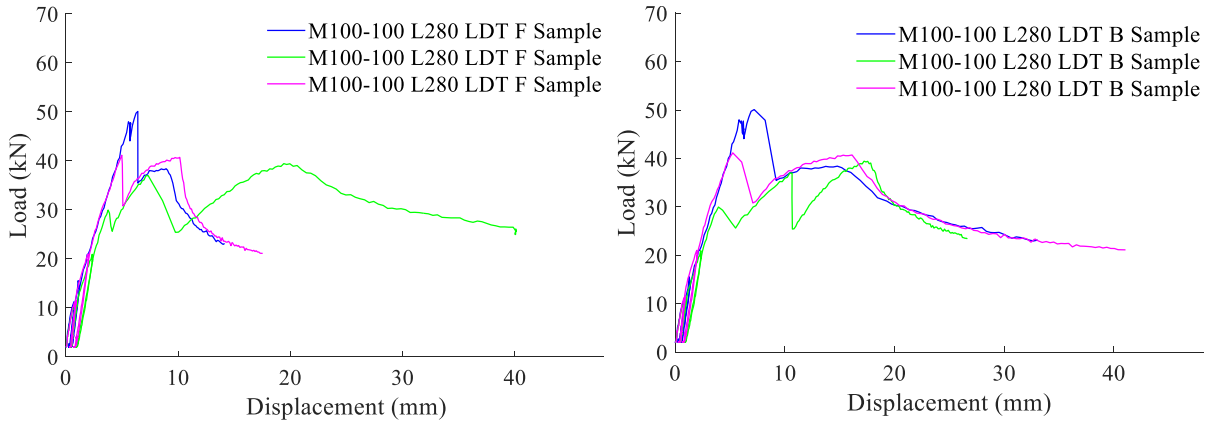

Figure 63. Load-displacement curves M100-100 with a span of 2.80 m, recorded using LDT F (left) and LDT B (right).

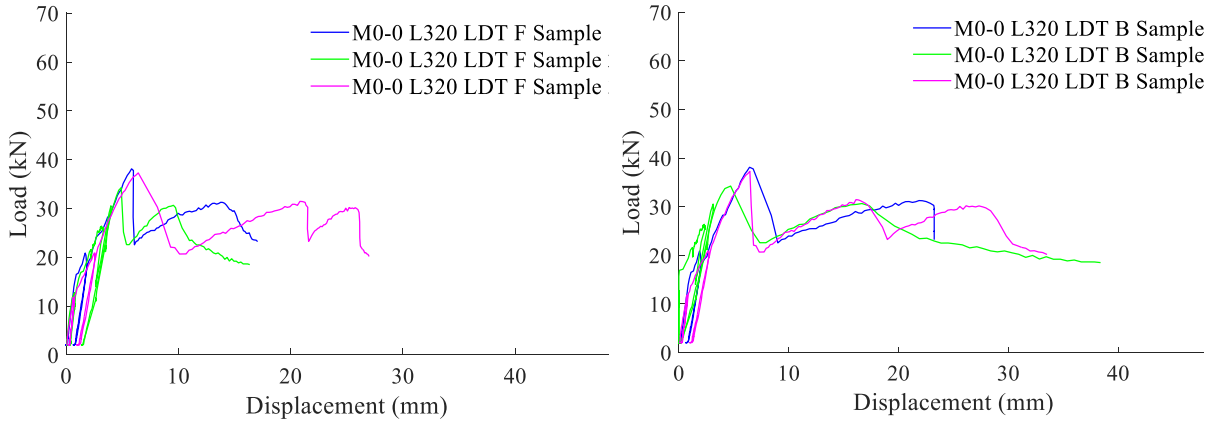

Figure 64. Load-displacement curves for sample M0-0 with a span of 3.20 m, recorded using LDT F (left) and LDT B (right).

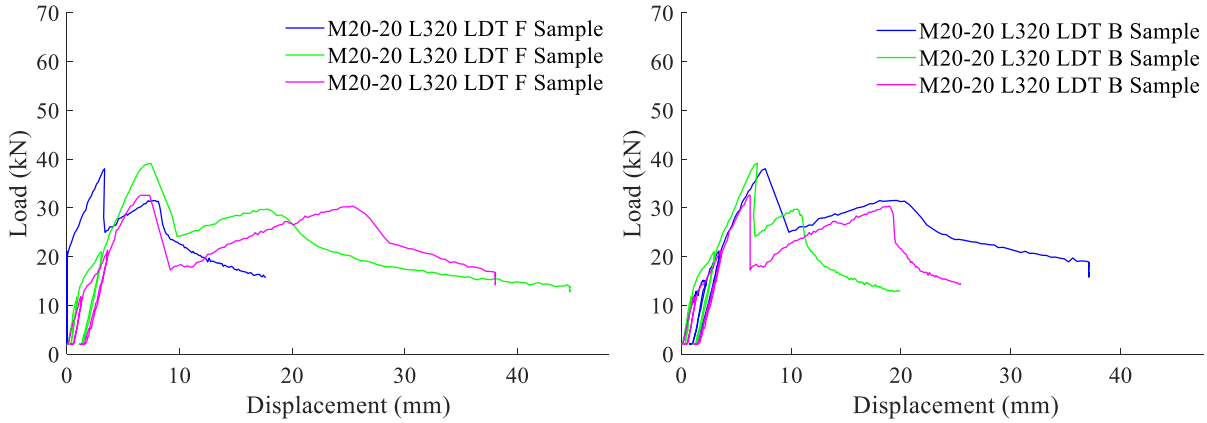

Figure 65. Load-displacement curves M20-20 with a span of 3.20 m, recorded using LDT F (left) and LDT B (right).

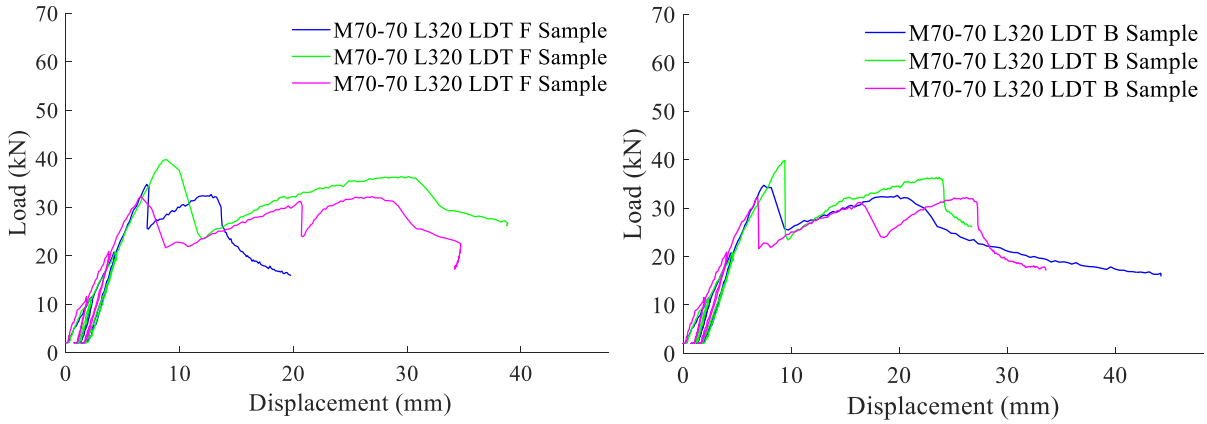

Figure 66. Load-displacement curves M70-70 with a span of 3.20 m, recorded using LDT F (left) and LDT B (right).

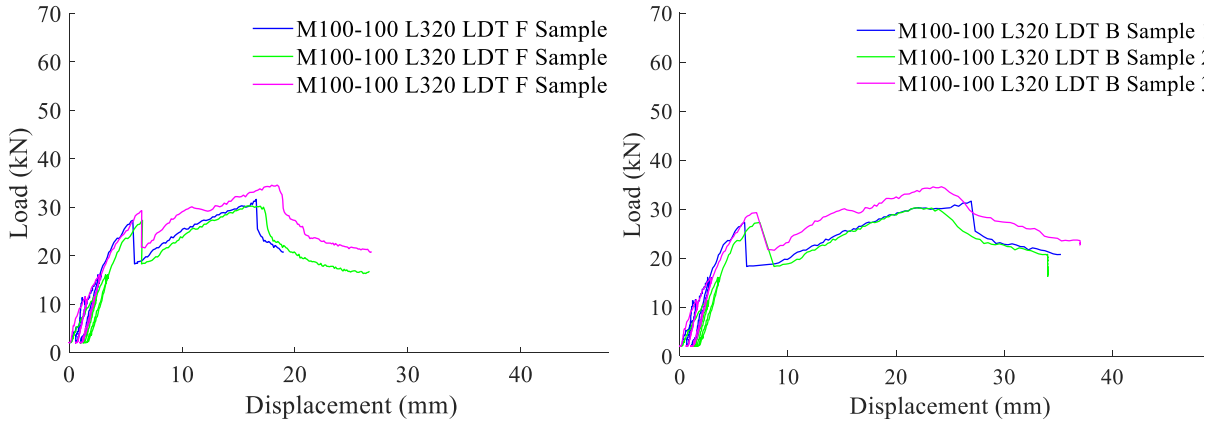

Figure 67. Load-displacement curves M100-100 with a span of 3.20 m, recorded using LDT F (left) and LDT B (right).

References

[1] S. Barbhuiya, B. Bhusan Das, F. Kanavaris, Biochar-concrete: A comprehensive review of properties, production and sustainability, Case Studies in Construction Materials 20 (2024) e02859. https://doi.org/10.1016/j.cscm.2024.e02859.

[2] W. M.Shaban, J. Yang, H. Su, K.H. Mo, L. Li, J. h Xie, Quality Improvement Techniques for Recycled Concrete Aggregate: A review, Journal of Advanced Concrete Technology 17 (2019) 151–167. https://doi.org/10.3151/jact.17.151.

[3] Global aggregates growth examined by GAIN convenor Jim O'Brien, Aggregates Business (2024). https://www.aggbusiness.com/feature/global-aggregates-growth-examined-gain-convenor-jim-obrien (accessed November 12, 2024).

[4] V.W.Y. Tam, M. Soomro, A.C.J. Evangelista, A review of recycled aggregate in concrete applications (2000–2017), Construction and Building Materials 172 (2018) 272–292. https://doi.org/10.1016/j.conbuildmat.2018.03.240.

[5] V.W.Y. Tam, M. Soomro, A.C.J. Evangelista, Quality improvement of recycled concrete aggregate by removal of residual mortar: A comprehensive review of approaches adopted, Construction and Building Materials 288 (2021) 123066. https://doi.org/10.1016/j.conbuildmat.2021.123066.

[6] I. Marie, H. Quiasrawi, Closed-loop recycling of recycled concrete aggregates, Journal of Cleaner Production 37 (2012) 243–248. https://doi.org/10.1016/j.jclepro.2012.07.020.

[7] S. Barbhuiya, F. Kanavaris, B.B. Das, M. Idrees, Decarbonising cement and concrete production: Strategies, challenges and pathways for sustainable development, Journal of Building Engineering 86 (2024) 108861. https://doi.org/10.1016/j.jobe.2024.108861.

[8] J. Yang, Y. Wu, G. Zhou, G. Xin, The dismantling method of wheel-spoke cable-strut tension structures based on experimental and numerical study, Structures 48 (2023) 1949–1963. https://doi.org/10.1016/j.istruc.2023.01.082.

[9] H. Zhang, Y. Geng, Y.-Y. Wang, X.-Z. Li, Experimental study and prediction model for bond behaviour of steel-recycled aggregate concrete composite slabs, Journal of Building Engineering 53 (2022) 104585. https://doi.org/10.1016/j.jobe.2022.104585.

[10] H. Zhang, Y. Geng, Y.-Y. Wang, Q. Wang, Long-term behavior of continuous composite slabs made with 100% fine and coarse recycled aggregate, Engineering Structures 212 (2020) 110464. https://doi.org/10.1016/j.engstruct.2020.110464.

[11] H.G. Gebremariam, S. Taye, A.G. Tarekegn, Parent Concrete Strength Effects on the Quality of Recycled Aggregate Concrete: A Review, Heliyon 10 (2024) e26212. https://doi.org/10.1016/j.heliyon.2024.e26212.

[12] F. Muhammad, M. Harun, A. Ahmed, N. Kabir, H.R. Khalid, A. Hanif, Influence of bonded mortar on recycled aggregate concrete properties: A review, Construction and Building Materials 432 (2024) 136564. https://doi.org/10.1016/j.conbuildmat.2024.136564.

[13] F. Stochino, M. Zucca, M. Simoncelli, A. Alibeigibeni, G. Concu, M. Valdes, M.A. Pisani, C. Bernuzzi, M. Saccone, L. Pani, Experimental Investigation on the Structural Performance of Steel-Concrete Composite Slabs Incorporating Recycled Aggregates from Construction and Demolition Waste, in: F.M. Mazzolani, V. Piluso, E. Nastri, A. Formisano (Eds.), Proceedings of the 11th International Conference on Behaviour of Steel Structures in Seismic Areas, Springer Nature Switzerland, Cham, 2024: pp. 108–117. https://doi.org/10.1007/978-3-031-62888-7_10.

[14] B. Mazhoud, T. Sedran, B. Cazacliu, A. Cothenet, J.-M. Torrenti, Influence of residual mortar volume on the properties of recycled concrete aggregates, Journal of Building Engineering 57 (2022) 104945. https://doi.org/10.1016/j.jobe.2022.104945.

[15] E.O. Fanijo, J.T. Kolawole, A.J. Babafemi, J. Liu, A comprehensive review on the use of recycled concrete aggregate for pavement construction: Properties, performance, and sustainability, Cleaner Materials 9 (2023) 100199. https://doi.org/10.1016/j.clema.2023.100199.

[16] Scopus - Document search results | Signed in, (n.d.). https://www.scopus.com/results/results.uri?st1=RCA&st2=&s=KEY%28Recycled+concrete+aggregate%29&limit=10&origin=resultslist&sort=plf-f&src=s&sot=b&sdt=cl&sessionSearchId=10c358f60a34f5b73ddeaa2f9e8947e5&yearFrom=2000&yearTo=2025 (accessed February 5, 2025).

[17] B.L. Chauhan, G.J. Singh, A. Kumar, R. Kumar, Strength and durability performance of acid-mechanically treated recycled aggregate concrete with metakaolin, lime powder, and A-fine, Construction and Building Materials 433 (2024) 136615. https://doi.org/10.1016/j.conbuildmat.2024.136615.

[18] Md.J. Islam, T. Ahmed, Md. Shahjalal, A.M. Jihad, Z. Based, Md.M. Hasan, Strength, durability, and impact behavior of recycled aggregate concrete with polypropylene aggregate, Construction and Building Materials 408 (2023) 133646. https://doi.org/10.1016/j.conbuildmat.2023.133646.

[19] R.V. Silva, J. de Brito, R.K. Dhir, Establishing a relationship between modulus of elasticity and compressive strength of recycled aggregate concrete, Journal of Cleaner Production 112 (2016) 2171–2186. https://doi.org/10.1016/j.jclepro.2015.10.064.
[20] R. Purushothaman, R.R. Amirthavalli, L. Karan, Influence of Treatment Methods on the Strength and Performance Characteristics of Recycled Aggregate Concrete, Journal of Materials in Civil Engineering 27 (2015) 04014168. https://doi.org/10.1061/(ASCE)MT.1943-5533.0001128.
[21] J. Wang, B. Vandevyvere, S. Vanhessche, J. Schoon, N. Boon, N. De Belie, Microbial carbonate precipitation for the improvement of quality of recycled aggregates, Journal of Cleaner Production 156 (2017) 355–366. https://doi.org/10.1016/j.jclepro.2017.04.051.
[22] S.M.S. Kazmi, M.J. Munir, Y.-F. Wu, I. Patnaikuni, Y. Zhou, F. Xing, Influence of different treatment methods on the mechanical behavior of recycled aggregate concrete: A comparative study, Cement and Concrete Composites 104 (2019) 103398. https://doi.org/10.1016/j.cemconcomp.2019.103398.
[23] A. Zia, I. Holly, Mechanical and durability properties of recycled aggregate concrete with end-of-life tire steel fibers: Short-term, prolonged, and rigid pavement implications, Construction and Building Materials 491 (2025) 142797. https://doi.org/10.1016/j.conbuildmat.2025.142797.
[24] C. Liu, J. Sun, X. Tang, Y. Ma, The durability of spray steel fiber-reinforced recycled coarse aggregate concrete, Construction and Building Materials 412 (2024) 134731. https://doi.org/10.1016/j.conbuildmat.2023.134731.
[25] N.J. John, S. Wanjari, A. Patel, Effects of particle shape and size on strength and durability of recycled concrete aggregates: An experimental and statistical approach, Construction and Building Materials 483 (2025) 141718. https://doi.org/10.1016/j.conbuildmat.2025.141718.
[26] X. Shang, Y. Qi, X. Zhang, B. Gong, J. Yang, Effects of wet carbonation with ethanol solution on the mechanical, durability properties, and microstructure of recycled concrete aggregates and derived block products, Construction and Building Materials 446 (2024) 138066. https://doi.org/10.1016/j.conbuildmat.2024.138066.
[27] R.P. Singh, B. Mohanty, Effect of waste glass powder on the durability and microstructural properties of fly ash-GGBS based alkali activated concrete containing 100 % recycled concrete aggregate, Construction and Building Materials 447 (2024) 138024. https://doi.org/10.1016/j.conbuildmat.2024.138024.
[28] A. Alibeigibeni, F. Stochino, M. Zucca, F.L. Gayarre, Enhancing Concrete Sustainability: A Critical Review of the Performance of Recycled Concrete Aggregates (RCAs) in Structural Concrete, Buildings 15 (2025) 1361. https://doi.org/10.3390/buildings15081361.
[29] H. Guo, C. Shi, X. Guan, J. Zhu, Y. Ding, T.-C. Ling, H. Zhang, Y. Wang, Durability of recycled aggregate concrete – A review, Cement and Concrete Composites 89 (2018) 251–259. https://doi.org/10.1016/j.cemconcomp.2018.03.008.
[30] A. Abdo, A. El-Zohairy, Y. Alashker, M.A.E.-A. Badran, S. Ahmed, Effect of Treated/Untreated Recycled Aggregate Concrete: Structural Behavior of RC Beams, Sustainability 16 (2024) 4039. https://doi.org/10.3390/su16104039.
[31] B.G. Salvoldi, H. Beushausen, M.G. Alexander, Oxygen permeability of concrete and its relation to carbonation, Construction and Building Materials 85 (2015) 30–37. https://doi.org/10.1016/j.conbuildmat.2015.02.019.
[32] C. Bu, L. Liu, X. Lu, D. Zhu, Y. Sun, L. Yu, Y. OuYang, X. Cao, Q. Wei, The Durability of Recycled Fine Aggregate Concrete: A Review, Materials 15 (2022) 1110. https://doi.org/10.3390/ma15031110.
[33] Z. Ma, M. Liu, Q. Tang, C. Liang, Z. Duan, Chloride permeability of recycled aggregate concrete under the coupling effect of freezing-thawing, elevated temperature or mechanical damage, Construction and Building Materials 237 (2020) 117648. https://doi.org/10.1016/j.conbuildmat.2019.117648.
[34] J. Wang, J. Zhang, D. Cao, Pore characteristics of recycled aggregate concrete and its relationship with durability under complex environmental factors, Construction and Building Materials 272 (2021) 121642. https://doi.org/10.1016/j.conbuildmat.2020.121642.
[35] M. Šefflová, T. Pavlů, The Durability of Fine Recycled Aggregate Concrete, Advanced Materials Research 1144 (2017) 59–64. https://doi.org/10.4028/www.scientific.net/AMR.1144.59.
[36] G.F. Peng, J. Yang, J.Y. Wang, Influence of Recycled Aggregate Defects on the Durability of Recycled Aggregate Concrete, Key Engineering Materials 629–630 (2015) 173–182. https://doi.org/10.4028/www.scientific.net/KEM.629-630.173.
[37] Y. Huo, J. Xiong, X. Guan, Experimental Study on Durability of Recycled Coarse Aggregate Concrete, in: Proceedings of the 2012 Second International Conference on Electric Technology and Civil Engineering, IEEE Computer Society, USA, 2012: pp. 1282–1285.
[38] D. Wang, C. Lu, Z. Zhu, Z. Zhang, S. Liu, Y. Ji, Z. Xing, Mechanical performance of recycled aggregate concrete in green civil engineering: Review, Case Studies in Construction Materials 19 (2023) e02384. https://doi.org/10.1016/j.cscm.2023.e02384.
[39] Bond Behavior of Recycled-Fiber Recycled Concrete and Reinforcement | Journal of Materials in Civil Engineering | Vol 35, No 5, (n.d.). https://ascelibrary.org/doi/10.1061/JMCEE7.MTENG-15027 (accessed September 24, 2025).

[40] J. Xu, F. Chang, J. Bai, C. Liu, Statistical analysis on the fracture behavior of rubberized steel fiber reinforced recycled aggregate concrete based on acoustic emission, Journal of Materials Research and Technology 24 (2023) 8997–9014. https://doi.org/10.1016/j.jmrt.2023.05.124.
[41] K. John, M. Ashraf, M. Weiss, R. Al-Ameri, Experimental study and numerical modelling of a novel two-way steel-concrete composite slab, Structures 57 (2023) 105096. https://doi.org/10.1016/j.istruc.2023.105096.
[42] M. Cordeiro Loureiro, É. Cassimiro Alves, A. Fernanda Grobério Calenzani, Geometry optimization of steel formwork for steel–concrete composite slabs, Structures 58 (2023) 105395. https://doi.org/10.1016/j.istruc.2023.105395.
[43] G. Ranzi, G. Leoni, R. Zandonini, State of the art on the time-dependent behaviour of composite steel–concrete structures, Journal of Constructional Steel Research 80 (2013) 252–263. https://doi.org/10.1016/j.jcsr.2012.08.005.
[44] H. Zhang, H.-Y. Zhang, Y. Geng, P.-Q. Fang, Y.-Y. Wang, Design formulae for Long-Term responses of continuous Steel-Recycled aggregate concrete composite slabs, Structures 45 (2022) 1477–1490. https://doi.org/10.1016/j.istruc.2022.09.092.
[45] EN 1994-1-1:2004 - UNI Ente Italiano di Normazione, (n.d.). https://store.uni.com/en-1994-1-1-2004 (accessed October 9, 2025).
[46] C. Bernuzzi, M.A. Pisani, M. Simoncelli, Debonding strain for steel-concrete composite slabs with trapezoidal metal deck, 1 49 (2023) 19–30.
[47] N.A. Hedaoo, L.M. Gupta, G.N. Ronghe, Design of composite slabs with profiled steel decking: a comparison between experimental and analytical studies, Int J Adv Struct Eng 4 (2012) 1. https://doi.org/10.1186/2008-6695-3-1.
[48] M. Cordeiro Loureiro, É. Cassimiro Alves, A. Fernanda Grobério Calenzani, Geometry optimization of steel formwork for steel–concrete composite slabs, Structures 58 (2023) 105395. https://doi.org/10.1016/j.istruc.2023.105395.
[49] K. John, M. Ashraf, M. Weiss, R. Al-Ameri, Experimental study and numerical modelling of a novel two-way steel-concrete composite slab, Structures 57 (2023) 105096. https://doi.org/10.1016/j.istruc.2023.105096.
[50] F. Stochino, A. Alibeigibeni, M. Zucca, M. Valdes, G. Concu, M. Simoncelli, M.A. Pisani, C. Bernuzzi, Mechanical behavior of composite slabs with recycled concrete aggregates: A preliminary study, Structures 70 (2024) 107838. https://doi.org/10.1016/j.istruc.2024.107838.
[51] B. Chen, T. Zhang, Y. Geng, Q. Wang, G. Zhao, J. Yang, Longitudinal shear tests and design methods for corrugated steel–concrete composite slabs with recycled coarse aggregate, Construction and Building Materials 400 (2023) 132870. https://doi.org/10.1016/j.conbuildmat.2023.132870.
[52] M.P. Ferreira, I.I.R. Damasceno, M.J.M. Pereira Filho, A.F. Lima Neto, M.H. Oliveira, J.A. Ribeiro Júnior, Effect of recycled concrete aggregates on the punching strength of slab-column connections without shear reinforcement, Journal of Building Engineering 95 (2024) 110174. https://doi.org/10.1016/j.jobe.2024.110174.
[53] M. Saccone, F. Stochino, M. Zucca, M. Simoncelli, Longitudinal shear behaviour in Recycled Aggregate Concrete Composite Slabs: A state-of-the-art review, Journal of Building Engineering 113 (2025) 114002. https://doi.org/10.1016/j.jobe.2025.114002.
[54] F. Kefyalew, T. Imjai, R. Garcia, N. Khanh Son, S. Chaudhary, Performance of recycled aggregate concrete composite metal decks under elevated temperatures: a comprehensive review, Journal of Asian Architecture and Building Engineering (n.d.) 1–23. https://doi.org/10.1080/13467581.2024.2309347.
[55] R.P. Neupane, T. Imjai, N. Makul, R. Garcia, B. Kim, S. Chaudhary, Use of recycled aggregate concrete in structural members: a review focused on Southeast Asia, Journal of Asian Architecture and Building Engineering 0 (n.d.) 1–24. https://doi.org/10.1080/13467581.2023.2270029.
[56] C. Wattanapanich, T. Imjai, R. Sridhar, R. Garcia, B.S. Thomas, Optimizing Recycled Aggregate Concrete for Severe Conditions Through Machine Learning Techniques: A Review, Engineered Science Volume 31 (October 2024) (2024) 1191.
[57] F. Aslani, Y. Zhang, 14 - Sustainable 3D printed concrete structures using high-quality secondary raw materials, in: A. Ashour, X. Wang, B. Han (Eds.), Sustainable Concrete Materials and Structures, Woodhead Publishing, 2024: pp. 399–443. https://doi.org/10.1016/B978-0-443-15672-4.00014-0.
[58] Home | ProjectSarcos, (n.d.). https://projectsarcos.it/ (accessed October 9, 2025).
[59] A. Ossa, J.L. García, E. Botero, Use of recycled construction and demolition waste (CDW) aggregates: A sustainable alternative for the pavement construction industry, Journal of Cleaner Production 135 (2016) 379–386. https://doi.org/10.1016/j.jclepro.2016.06.088.
[60] I. Papamichael, I. Voukkali, P. Loizia, A.A. Zorpas, Construction and demolition waste framework of circular economy: A mini review, Waste Manag Res 41 (2023) 1728–1740. https://doi.org/10.1177/0734242X231190804.
[61] J. Kim, Influence of quality of recycled aggregates on the mechanical properties of recycled aggregate concretes: An overview, Construction and Building Materials 328 (2022) 127071. https://doi.org/10.1016/j.conbuildmat.2022.127071.

[62] R.S. Paranhos, B.G. Cazacliu, C.H. Sampaio, C.O. Petter, R.O. Neto, F. Huchet, A sorting method to value recycled concrete, Journal of Cleaner Production 112 (2016) 2249–2258. https://doi.org/10.1016/j.jclepro.2015.10.021.
[63] S.-C. Kou, C.-S. Poon, Long-term mechanical and durability properties of recycled aggregate concrete prepared with the incorporation of fly ash, Cement and Concrete Composites 37 (2013) 12–19. https://doi.org/10.1016/j.cemconcomp.2012.12.011.
[64] D. Ferrández, P. Saiz, A. Zaragoza-Benzal, J.A. Zúñiga-Vicente, Towards a more sustainable environmentally production system for the treatment of recycled aggregates in the construction industry: An experimental study, Heliyon 9 (2023) e16641. https://doi.org/10.1016/j.heliyon.2023.e16641.
[65] A.M. Wagih, H.Z. El-Karmoty, M. Ebid, S.H. Okba, Recycled construction and demolition concrete waste as aggregate for structural concrete, HBRC Journal 9 (2013) 193–200. https://doi.org/10.1016/j.hbrcj.2013.08.007.
[66] Z. Wang, W. Xie, J. Liu, Regional differences and driving factors of construction and demolition waste generation in China, Engineering, Construction and Architectural Management 29 (2021) 2300–2327. https://doi.org/10.1108/ECAM-10-2020-0887.
[67] S. Ismail, M. Ramli, Engineering properties of treated recycled concrete aggregate (RCA) for structural applications, Construction and Building Materials 44 (2013) 464–476. https://doi.org/10.1016/j.conbuildmat.2013.03.014.
[68] C. Feng, B. Cui, J. Wang, H. Guo, W. Zhang, J. Zhu, Changing the soaking method of microbially induced calcium carbonate precipitation technology to improve the reinforcement effect of recycled concrete aggregates, Journal of Building Engineering 68 (2023) 106128. https://doi.org/10.1016/j.jobe.2023.106128.
[69] L. Pani, L. Francesconi, J. Rombi, F. Mistretta, M. Sassu, F. Stochino, Effect of Parent Concrete on the Performance of Recycled Aggregate Concrete, Sustainability 12 (2020) 9399. https://doi.org/10.3390/su12229399.
[70] L.W. Zhang, A.O. Sojobi, V.K.R. Kodur, K.M. Liew, Effective utilization and recycling of mixed recycled aggregates for a greener environment, Journal of Cleaner Production 236 (2019) 117600. https://doi.org/10.1016/j.jclepro.2019.07.075.
[71] N. Makul, R. Fediuk, M. Amran, A.M. Zeyad, A.R.G. de Azevedo, S. Klyuev, N. Vatin, M. Karelina, Capacity to Develop Recycled Aggregate Concrete in South East Asia, Buildings 11 (2021) 234. https://doi.org/10.3390/buildings11060234.
[72] X. Xu, Y. Luo, A. Sreeram, Q. Wu, G. Chen, S. Cheng, Z. Chen, X. Chen, Potential use of recycled concrete aggregate (RCA) for sustainable asphalt pavements of the future: A state-of-the-art review, Journal of Cleaner Production 344 (2022) 130893. https://doi.org/10.1016/j.jclepro.2022.130893.
[73] Y. Zheng, Y. Zhang, P. Zhang, Methods for improving the durability of recycled aggregate concrete: A review, Journal of Materials Research and Technology 15 (2021) 6367–6386. https://doi.org/10.1016/j.jmrt.2021.11.085.
[74] K. Ouyang, C. Shi, H. Chu, H. Guo, B. Song, Y. Ding, X. Guan, J. Zhu, H. Zhang, Y. Wang, J. Zheng, An overview on the efficiency of different pretreatment techniques for recycled concrete aggregate, Journal of Cleaner Production 263 (2020) 121264. https://doi.org/10.1016/j.jclepro.2020.121264.
[75] J.A. Forero, J. de Brito, L. Evangelista, C. Pereira, Improvement of the Quality of Recycled Concrete Aggregate Subjected to Chemical Treatments: A Review, Materials 15 (2022) 2740. https://doi.org/10.3390/ma15082740.
[76] A. Mistri, S.K. Bhattacharyya, N. Dhami, A. Mukherjee, S.V. Barai, A review on different treatment methods for enhancing the properties of recycled aggregates for sustainable construction materials, Construction and Building Materials 233 (2020) 117894. https://doi.org/10.1016/j.conbuildmat.2019.117894.
[77] H. Sasanipour, F. Aslani, Durability assessment of concrete containing surface pretreated coarse recycled concrete aggregates, Construction and Building Materials 264 (2020) 120203. https://doi.org/10.1016/j.conbuildmat.2020.120203.
[78] R.V. Silva, J. de Brito, R.K. Dhir, The influence of the use of recycled aggregates on the compressive strength of concrete: a review, European Journal of Environmental and Civil Engineering 19 (2015) 825–849. https://doi.org/10.1080/19648189.2014.974831.
[79] L. Evangelista, J. de Brito, Mechanical behaviour of concrete made with fine recycled concrete aggregates, Cement and Concrete Composites 29 (2007) 397–401. https://doi.org/10.1016/j.cemconcomp.2006.12.004.
[80] C.-C. Fan, R. Huang, H. Hwang, S.-J. Chao, Properties of concrete incorporating fine recycled aggregates from crushed concrete wastes, Construction and Building Materials 112 (2016) 708–715. https://doi.org/10.1016/j.conbuildmat.2016.02.154.
[81] L. Evangelista, J. de Brito, Durability performance of concrete made with fine recycled concrete aggregates, Cement and Concrete Composites 32 (2010) 9–14. https://doi.org/10.1016/j.cemconcomp.2009.09.005.
[82] H. Yaprak, H. Aruntaş, I. Demir, O. Şimşek, G. Durmuş, Effects of the fine recycled concrete aggregates on the concrete properties, International Journal of Physical Sciences 6 (2011) pp.2455-2461.
[83] J. Geng, J. Sun, Characteristics of the carbonation resistance of recycled fine aggregate concrete, Construction and Building Materials 49 (2013) 814–820. https://doi.org/10.1016/j.conbuildmat.2013.08.090.

[84] F. Cartuxo, J. de Brito, L. Evangelista, J.R. Jiménez, E.F. Ledesma, Rheological behaviour of concrete made with fine recycled concrete aggregates – Influence of the superplasticizer, Construction and Building Materials 89 (2015) 36–47. https://doi.org/10.1016/j.conbuildmat.2015.03.119.
[85] F. Cartuxo, J. De Brito, L. Evangelista, J.R. Jiménez, E.F. Ledesma, Increased Durability of Concrete Made with Fine Recycled Concrete Aggregates Using Superplasticizers, Materials 9 (2016) 98. https://doi.org/10.3390/ma9020098.
[86] R. Kumar, S.C.B. Gurram, A.K. Minocha, Influence of recycled fine aggregate on microstructure and hardened properties of concrete, Magazine of Concrete Research 69 (2017) 1288–1295. https://doi.org/10.1680/jmacr.17.00030.
[87] J.M. Khatib, Properties of concrete incorporating fine recycled aggregate, Cement and Concrete Research 35 (2005) 763–769. https://doi.org/10.1016/j.cemconres.2004.06.017.
[88] D. Pedro, J. de Brito, L. Evangelista, Structural concrete with simultaneous incorporation of fine and coarse recycled concrete aggregates: Mechanical, durability and long-term properties, Construction and Building Materials 154 (2017) 294–309. https://doi.org/10.1016/j.conbuildmat.2017.07.215.
[89] Z. Guo, Chen ,Chen, Lehman ,Dawn E., Xiao ,Wenguang, Zheng ,Songlin, B. and Fan, Mechanical and durability behaviours of concrete made with recycled coarse and fine aggregates, European Journal of Environmental and Civil Engineering 24 (2020) 171–189. https://doi.org/10.1080/19648189.2017.1371083.
[90] A.E.B. Cabral, V. Schalch, D.C.C.D. Molin, J.L.D. Ribeiro, Mechanical properties modeling of recycled aggregate concrete, Construction and Building Materials 24 (2010) 421–430. https://doi.org/10.1016/j.conbuildmat.2009.10.011.
[91] R. Kurad, J.D. Silvestre, J. De Brito, H. Ahmed, Effect of incorporation of high volume of recycled concrete aggregates and fly ash on the strength and global warming potential of concrete, Journal of Cleaner Production 166 (2017) 485–502. https://doi.org/10.1016/j.jclepro.2017.07.236.
[92] C. Wang, J. Xiao, Evaluation of the stress-strain behavior of confined recycled aggregate concrete under monotonic dynamic loadings, Cement and Concrete Composites 87 (2018) 149–163. https://doi.org/10.1016/j.cemconcomp.2017.12.012.
[93] R.V. Silva, J. de Brito, R.K. Dhir, Tensile strength behaviour of recycled aggregate concrete, Construction and Building Materials 83 (2015) 108–118. https://doi.org/10.1016/j.conbuildmat.2015.03.034.
[94] X. Yang, Y. Liu, J. Liang, Y. Meng, H. Rong, D. Li, Y. Chen, J. Lv, Y. Jiang, Y. Liu, Straightening methods for RCA and RAC—a review, Cement and Concrete Composites 141 (2023) 105145. https://doi.org/10.1016/j.cemconcomp.2023.105145.
[95] R. Wang, N. Yu, Y. Li, Methods for improving the microstructure of recycled concrete aggregate: A review, Construction and Building Materials 242 (2020) 118164. https://doi.org/10.1016/j.conbuildmat.2020.118164.
[96] J. Wang, Z. Che, K. Zhang, Y. Fan, D. Niu, X. Guan, Performance of recycled aggregate concrete with supplementary cementitious materials (fly ash, GBFS, silica fume, and metakaolin): Mechanical properties, pore structure, and water absorption, Construction and Building Materials 368 (2023) 130455. https://doi.org/10.1016/j.conbuildmat.2023.130455.
[97] G. Dimitriou, P. Savva, M.F. Petrou, Enhancing mechanical and durability properties of recycled aggregate concrete, Construction and Building Materials 158 (2018) 228–235. https://doi.org/10.1016/j.conbuildmat.2017.09.137.
[98] C.S. Poon, Z.H. Shui, L. Lam, Effect of microstructure of ITZ on compressive strength of concrete prepared with recycled aggregates, Construction and Building Materials 18 (2004) 461–468. https://doi.org/10.1016/j.conbuildmat.2004.03.005.
[99] R.V. Silva, J. de Brito, R.K. Dhir, Properties and composition of recycled aggregates from construction and demolition waste suitable for concrete production, Construction and Building Materials 65 (2014) 201–217. https://doi.org/10.1016/j.conbuildmat.2014.04.117.
[100] M. Etxeberria, E. Vázquez, A. Marí, M. Barra, Influence of amount of recycled coarse aggregates and production process on properties of recycled aggregate concrete, Cement and Concrete Research 37 (2007) 735–742. https://doi.org/10.1016/j.cemconres.2007.02.002.
[101] V.W.Y. Tam, X.F. Gao, C.M. Tam, Microstructural analysis of recycled aggregate concrete produced from two-stage mixing approach, Cement and Concrete Research 35 (2005) 1195–1203. https://doi.org/10.1016/j.cemconres.2004.10.025.
[102] J.M.V. Gómez-Soberón, Porosity of recycled concrete with substitution of recycled concrete aggregate: An experimental study, Cement and Concrete Research 32 (2002) 1301–1311. https://doi.org/10.1016/S0008-8846(02)00795-0.
[103] R. Zaharieva, F. Buyle-Bodin, F. Skoczylas, E. Wirquin, Assessment of the surface permeation properties of recycled aggregate concrete, Cement and Concrete Composites 25 (2003) 223–232. https://doi.org/10.1016/S0958-9465(02)00010-0.
[104] A.M. Ashteyat, R. Al-Tarawneh, N. Shatarat, Bond Strength between Steel and Recycled Asphalt Pavement Aggregate and Recycled Concrete Aggregate, Civil Engineering and Architecture 12 (2024) 1190–1203. https://doi.org/10.13189/cea.2024.120237.

[105] A. Abushanab, W. Alnahhal, Bond strength of corroded reinforced recycled aggregate concrete with treated wastewater and fly ash, Journal of Building Engineering 79 (2023) 107778. https://doi.org/10.1016/j.jobe.2023.107778.
[106] M. Yusuf, S. Sarhat, H. Hajiloo, M.F. Green, Bond strength between steel reinforcement and RCA concrete during and after exposure to elevated temperatures, Construction and Building Materials 345 (2022) 128362. https://doi.org/10.1016/j.conbuildmat.2022.128362.
[107] W. Zou, J. Liang, D. Liu, G. Zhang, Bond Behavior between Steel Rebar and RCA Concrete after Exposure to Elevated Temperatures, Advances in Materials Science and Engineering 2020 (2020) 5230295. https://doi.org/10.1155/2020/5230295.
[108] M. Alhawat, A. Ashour, Bond strength between corroded steel reinforcement and recycled aggregate concrete, Structures 19 (2019) 369–385. https://doi.org/10.1016/j.istruc.2019.02.001.
[109] C. Namarak, W. Tangchirapat, C. Jaturapitakkul, Bar-concrete bond in mixes containing calcium carbide residue, fly ash and recycled concrete aggregate, Cement and Concrete Composites 89 (2018) 31–40. https://doi.org/10.1016/j.cemconcomp.2018.02.017.
[110] M.J.R. Prince, B. Singh, Bond strength of deformed steel bars in high-strength recycled aggregate concrete, Mater Struct 48 (2015) 3913–3928. https://doi.org/10.1617/s11527-014-0452-y.
[111] J. Xiao, H. Falkner, Bond behaviour between recycled aggregate concrete and steel rebars, Construction and Building Materials 21 (2007) 395–401. https://doi.org/10.1016/j.conbuildmat.2005.08.008.
[112] S.-W. Kim, H.-D. Yun, Influence of recycled coarse aggregates on the bond behavior of deformed bars in concrete, Engineering Structures 48 (2013) 133–143. https://doi.org/10.1016/j.engstruct.2012.10.009.
[113] J. de Brito, R.V. Silva, Sustainability in Structural Concrete Design, International Association for Bridge and Structural Engineering, 2024.
[114] C.-Q. Lye, R.K. Dhir, G.S. Ghataora, H. Li, Creep strain of recycled aggregate concrete, Construction and Building Materials 102 (2016) 244–259. https://doi.org/10.1016/j.conbuildmat.2015.10.181.
[115] G. Soberón, J.M. Vicente, Creep of concrete with substitution of normal aggregate by recycled concrete aggregate, Malhotra, V.M., 2002. https://upcommons.upc.edu/handle/2117/2562 (accessed September 11, 2024).
[116] Y. Fan, J. Xiao, V.W.Y. Tam, Effect of old attached mortar on the creep of recycled aggregate concrete, Structural Concrete 15 (2014) 169–178. https://doi.org/10.1002/suco.201300055.
[117] D. Gómez-Cano, Y.P. Arias-Jaramillo, R. Bernal-Correa, J.I. Tobón, Effect of enhancement treatments applied to recycled concrete aggregates on concrete durability: A review, Materiales de Construcción 73 (2023) e308–e308. https://doi.org/10.3989/mc.2023.296522.
[118] C. Chen, R. Liu, P. Zhu, H. Liu, X. Wang, Carbonization Durability of Two Generations of Recycled Coarse Aggregate Concrete with Effect of Chloride Ion Corrosion, Sustainability 12 (2020) 10544. https://doi.org/10.3390/su122410544.
[119] M. Etxeberria, S. Castillo, How the Carbonation Treatment of Different Types of Recycled Aggregates Affects the Properties of Concrete, Sustainability 15 (2023) 3169. https://doi.org/10.3390/su15043169.
[120] Y. Pu, L. Li, Q. Wang, X. Shi, C. Luan, G. Zhang, L. Fu, A. El-Fatah Abomohra, Accelerated carbonation technology for enhanced treatment of recycled concrete aggregates: A state-of-the-art review, Construction and Building Materials 282 (2021) 122671. https://doi.org/10.1016/j.conbuildmat.2021.122671.
[121] G.N. Malysz, V.G. Cappellesso, L. Silvestro, D.C.C. Dal Molin, A.B. Masuero, Natural and Accelerated Carbonation in Concrete Associated with Recycled Coarse Aggregate Treated by Air Jigging Technology, Journal of Materials in Civil Engineering 34 (2022) 04022133. https://doi.org/10.1061/(ASCE)MT.1943-5533.0004276.
[122] N. Russo, F. Lollini, Effect of carbonated recycled coarse aggregates on the mechanical and durability properties of concrete, Journal of Building Engineering 51 (2022) 104290. https://doi.org/10.1016/j.jobe.2022.104290.
[123] H. Liu, M. Hua, P. Zhu, C. Chen, X. Wang, Z. Qian, Y. Dong, Effect of Freeze–Thaw Cycles on Carbonation Behavior of Three Generations of Repeatedly Recycled Aggregate Concrete, Applied Sciences 11 (2021) 2643. https://doi.org/10.3390/app11062643.
[124] J.M. Torrenti, O. Amiri, L. Barnes-Davin, F. Bougrain, S. Braymand, B. Cazacliu, J. Colin, A. Cudeville, P. Dangla, A. Djerbi, M. Doutreleau, A. Feraille, M. Gueguen, X. Guillot, Y. Hou, L. Izoret, Y.-P. Jacob, J. Jeong, J.D.L. Hiu Hoong, P.-Y. Mahieux, J. Mai-Nhu, H. Martinez, V. Meyer, V. Morin, T. Pernin, J.-M. Potier, L. Poulizac, P. Rougeau, M. Saadé, L. Schmitt, T. Sedran, M. Sereng, A. Soive, G.S. Dos Reys, P. Turcry, The FastCarb project: Taking advantage of the accelerated carbonation of recycled concrete aggregates, Case Studies in Construction Materials 17 (2022) e01349. https://doi.org/10.1016/j.cscm.2022.e01349.
[125] A. Gholizadeh-Vayghan, A. Bellinkx, R. Snellings, B. Vandoren, M. Quaghebeur, The effects of carbonation conditions on the physical and microstructural properties of recycled concrete coarse aggregates, Construction and Building Materials 257 (2020) 119486. https://doi.org/10.1016/j.conbuildmat.2020.119486.
[126] Y. Wang, J. Liao, B. Zhang, A Review of Chloride Penetration of Recycled Concrete with Enhancement Treatment and Service Life Prediction, Materials 17 (2024) 1349. https://doi.org/10.3390/ma17061349.
[127] S. Pandey, P. Rajhans, Durability assessment of quaternary blended recycled aggregate concrete under chloride environment, Materials Today: Proceedings (2023). https://doi.org/10.1016/j.matpr.2023.03.686.

[128] H. Jiang, L. Wu, L. Guan, M. Liu, X. Ju, Z. Xiang, X. Jiang, Y. Li, J. Long, Durability life evaluation of marine infrastructures built by using carbonated recycled coarse aggregate concrete due to the chloride corrosive environment, Front. Mar. Sci. 11 (2024). https://doi.org/10.3389/fmars.2024.1357186.
[129] D. Lu, H. Cao, Q. Shen, Y. Gong, C. Zhao, X. Yan, Dynamic Characteristics and Chloride Resistance of Basalt and Polypropylene Fibers Reinforced Recycled Aggregate Concrete, Advances in Polymer Technology 2020 (2020) 6029047. https://doi.org/10.1155/2020/6029047.
[130] S. Gao, Y. Ji, A. Liu, H. Zhang, Z. Qin, W. Long, The adsorption and diffusion behavior of chloride in recycled aggregate concrete incorporated with calcined LDHs, Cement and Concrete Composites 148 (2024) 105452. https://doi.org/10.1016/j.cemconcomp.2024.105452.
[131] Stephen O.Ekolu, Permeation properties of recycled concretes containing various types of recovered aggregates, (n.d.). https://ujcontent.uj.ac.za/esploro/outputs/conferencePaper/Permeation-properties-of-recycled-concretes-containing/9911129407691 (accessed September 19, 2024).
[132] C. Suvash, G. Paul, G. van Zijl, Van, Durability Index Test Performance of Recycled Concrete Aggregate Mixed with Natural Aggregate, (2013). https://www.researchgate.net/publication/256692659_Durability_Index_Test_Performance_of_Recycled_Concrete_Aggregate_Mixed_with_Natural_Aggregate (accessed September 19, 2024).
[133] S. Ismail, W.H. Kwan, M. Ramli, Mechanical strength and durability properties of concrete containing treated recycled concrete aggregates under different curing conditions, Construction and Building Materials 155 (2017) 296–306. https://doi.org/10.1016/j.conbuildmat.2017.08.076.
[134] B. Cantero, M. Bravo, J. de Brito, I.F. Sáez del Bosque, C. Medina, Assessment of the Permeability to Aggressive Agents of Concrete with Recycled Cement and Mixed Recycled Aggregate, Applied Sciences 11 (2021) 3856. https://doi.org/10.3390/app11093856.
[135] K. Kapoor, S.P. Singh, B. Singh, Water Permeation Properties of Self Compacting Concrete Made with Coarse and Fine Recycled Concrete Aggregates, Int J Civ Eng 16 (2018) 47–56. https://doi.org/10.1007/s40999-016-0062-x.
[136] W. Mahmood, A.-R. Khan, T. Ayub, Mechanical and Durability Properties of Concrete Containing Recycled Concrete Aggregates, Iran J Sci Technol Trans Civ Eng 46 (2022) 2111–2130. https://doi.org/10.1007/s40996-021-00692-x.
[137] C. Thomas, J. Setién, J.A. Polanco, P. Alaejos, M. Sánchez de Juan, Durability of recycled aggregate concrete, Construction and Building Materials 40 (2013) 1054–1065. https://doi.org/10.1016/j.conbuildmat.2012.11.106.
[138] Md. Safiuddin, U.J. Alengaram, Md.M. Rahman, Md.A. Salam, Mohd.Z. Jumaat, Use of recycled concrete aggregate in concrete: a review, Journal of Civil Engineering and Management 19 (2013) 796–810. https://doi.org/10.3846/13923730.2013.799093.
[139] B.J. Zhan, D.X. Xuan, W. Zeng, C.S. Poon, Carbonation treatment of recycled concrete aggregate: Effect on transport properties and steel corrosion of recycled aggregate concrete, Cement and Concrete Composites 104 (2019) 103360. https://doi.org/10.1016/j.cemconcomp.2019.103360.
[140] H. Sasanipour, F. Aslani, J. Taherinezhad, Chloride ion permeability improvement of recycled aggregate concrete using pretreated recycled aggregates by silica fume slurry, Construction and Building Materials 270 (2021) 121498. https://doi.org/10.1016/j.conbuildmat.2020.121498.
[141] D. Xuan, B. Zhan, C.S. Poon, Durability of recycled aggregate concrete prepared with carbonated recycled concrete aggregates, Cement and Concrete Composites 84 (2017) 214–221. https://doi.org/10.1016/j.cemconcomp.2017.09.015.
[142] P. Velardo, I.F. Sáez del Bosque, M.I. Sánchez de Rojas, N. De Belie, C. Medina, Durability of concrete bearing polymer-treated mixed recycled aggregate, Construction and Building Materials 315 (2022) 125781. https://doi.org/10.1016/j.conbuildmat.2021.125781.
[143] W. Kubissa, R. Jaskulski, M. Brodnan, Influence of SCM on the Permeability of Concrete with Recycled Aggregate, Periodica Polytechnica Civil Engineering 60 (2016) 583. https://doi.org/10.3311/PPci.8614.
[144] Y. Gao, Y. Jiang, Y. Tao, P. Shen, C.S. Poon, Accelerated carbonation of recycled concrete aggregate in semi-wet environments: A promising technique for CO2 utilization, Cement and Concrete Research 180 (2024) 107486. https://doi.org/10.1016/j.cemconres.2024.107486.
[145] T. Pernin, J.-M. Torrenti, J.-M. Potier, L. Izoret, J. Mai-Nhu, Accelerated Carbonation of Recycled Concrete Aggregates: Impact on Durability of Concrete, in: J.A.O. Barros, V.M.C.F. Cunha, H.S. Sousa, J.C. Matos, J.M. Sena-Cruz (Eds.), 4th Fib International Conference on Concrete Sustainability (ICCS2024), Springer Nature Switzerland, Cham, 2024: pp. 36–43. https://doi.org/10.1007/978-3-031-80724-4_5.
[146] S. Braymand, S. Roux, V. Vial, J. Bertola, B. Cazacliu, Collaborative laboratory experiments to measure the rate of CO2 captured after accelerated carbonation by a calcimetric method, in: 1st RILEM International Conference on Mineral Carbonation for Cement and Concrete, 16-17th April 2024, Aachen, Germany, Aix-la-Chapelle, Germany, 2024. https://hal.science/hal-04650692 (accessed February 19, 2025).
[147] T. Jiang, X. Cao, H. Duan, K. Shu, Recycling efficiency mechanism of recycled concrete aggregate to improve the CO2 uptake and anti-leakage properties of CO2 sequestration functional backfills, Construction and Building Materials 458 (2025) 139663. https://doi.org/10.1016/j.conbuildmat.2024.139663.

[148] P. Ang, W. Goh, J. Bu, S. Cheng, Assessing Carbon Capture and Carbonation in Recycled Concrete Aggregates: A Holistic Life Cycle Assessment Perspective with Simulation at Industrial Scale, Journal of Cleaner Production 474 (2024) 143553. https://doi.org/10.1016/j.jclepro.2024.143553.
[149] W. Goh, S. Ye, R. Ou Yong, K.H. Tham, C. Wang, L. Tao, S. Cheng, Techno-Economic Analysis of Mineralization and Utilization of CO2 in Recycled Concrete Aggregates, Processes 13 (2025) 410. https://doi.org/10.3390/pr13020410.
[150] X. Zhu, T. Wang, Z. Yi, Z. Zhu, Kinetics and structure analysis of CO2 mineralization for recycled concrete aggregate (RCA), Journal of Cleaner Production 448 (2024) 141571. https://doi.org/10.1016/j.jclepro.2024.141571.
[151] K.H. Tham, T. Seah, Q.Y. Kouk, W. Goh, S. Cheng, C. Wang, J. Bu, L. Tao, Developing an integrated CO2 capture and mineralization process with lower energy consumption, Int J Energ Water Res (2024). https://doi.org/10.1007/s42108-024-00308-w.
[152] Y. Chong, G.F. Chua, M. Zhao, C. Yip, S.B. Daneti, F. Jin, Aqueous CO2 Sequestration for Low-Carbon Ready-Mix Concrete, Vysoké učení technické v Brně,Fakulta stavební, 2024. https://hdl.handle.net/11012/245414 (accessed February 19, 2025).
[153] J. Bergmans, H. Kazemi Kamyab, D. Ghosh, P. Van Mierloo, H. Carens, P. Nielsen, Carbonation of Recycled Concrete Aggregates for New Concrete and Concrete Fines to Make Cement-Free Hollow Blocks, Sustainability 16 (2024) 3494. https://doi.org/10.3390/su16083494.
[154] W. Huang, H. Wang, Comprehensive assessment of engineering and environmental attributes of geopolymer pervious concrete with natural and recycled aggregate, Journal of Cleaner Production 468 (2024) 143138. https://doi.org/10.1016/j.jclepro.2024.143138.
[155] X. Huang, Z. Huang, Y. Zhou, R. Hu, B. Hu, Life cycle assessment and cost analysis of LC3 concrete considering sustainability and uncertainty, Journal of Building Engineering 102 (2025) 111960. https://doi.org/10.1016/j.jobe.2025.111960.
[156] A. Manan, P. Zhang, A. Majdi, W. Alattyih, J. Ahmad, Utilizing waste materials in concrete: a review on mechanical and sustainable performance, Green Materials (2025) 1–18. https://doi.org/10.1680/jgrma.24.00122.
[157] X. Ma, H. Hu, Y. Luo, W. Yao, Y. Wei, A. She, A carbon footprint assessment for usage of recycled aggregate and supplementary cementitious materials for sustainable concrete: A life-cycle perspective in China, Journal of Cleaner Production 490 (2025) 144772. https://doi.org/10.1016/j.jclepro.2025.144772.
[158] S. Pradhan, S. Kumar, S.V. Barai, Particle Packing Method for Recycled Aggregate Concrete, Springer Nature, Singapore, 2024. https://doi.org/10.1007/978-981-99-7516-7.
[159] ASTM C1602/C1602M-18 - Standard Specification for Mixing Water Used in the Production of Hydraulic Cement Concrete, iTeh Standards (n.d.). https://standards.iteh.ai/catalog/standards/astm/33765c0f-cdda-44ec-8b02-127ef922a86a/astm-c1602-c1602m-18 (accessed September 23, 2025).
[160] EN 12390-3:2019 - Testing hardened concrete - Part 3: Compressive strength of test specimens, iTeh Standards (n.d.). https://standards.iteh.ai/catalog/standards/cen/7eb738ef-44af-436c-ab8e-e6561571302c/en-12390-3-2019 (accessed September 23, 2025).
[161] EN 12390-6:2023 - Testing hardened concrete - Part 6: Tensile splitting strength of test specimens, iTeh Standards (n.d.). https://standards.iteh.ai/catalog/standards/cen/fb090705-62c2-4751-8bab-b945b6450a1c/en-12390-6-2023 (accessed September 24, 2025).
[162] EN 206:2013 - Concrete - Specification, performance, production and conformity, iTeh Standards (n.d.). https://standards.iteh.ai/catalog/standards/cen/0e839092-9d2c-4b1c-ada2-b4d7f585e33b/en-206-2013 (accessed September 24, 2025).
[163] EN 12390-13:2021 - Testing hardened concrete - Part 13: Determination of secant modulus of elasticity in compression, iTeh Standards (n.d.). https://standards.iteh.ai/catalog/standards/cen/d1ea21c6-6068-47d5-92f5-60f759bf2aab/en-12390-13-2021 (accessed September 23, 2025).
[164] UNI 11164:2005 - UNI Ente Italiano di Normazione, (n.d.). https://store.uni.com/en/p/UNI1116400/uni-111642005-77421/UNI1116400_EIT (accessed September 23, 2025).
[165] C. Thomas, J. Setién, J.A. Polanco, P. Alaejos, M. Sánchez de Juan, Durability of recycled aggregate concrete, Construction and Building Materials 40 (2013) 1054–1065. https://doi.org/10.1016/j.conbuildmat.2012.11.106.
[166] EN 12390-8:2019 - Testing hardened concrete - Part 8: Depth of penetration of water under pressure, iTeh Standards (n.d.). https://standards.iteh.ai/catalog/standards/cen/d87d755e-09e0-4eb9-bfbd-916f0983e69e/en-12390-8-2019 (accessed September 23, 2025).
[167] S.C. Kou, C.S. Poon, Enhancing the durability properties of concrete prepared with coarse recycled aggregate, Construction and Building Materials 35 (2012) 69–76. https://doi.org/10.1016/j.conbuildmat.2012.02.032.
[168] EN 12390-12:2020 - Testing hardened concrete - Part 12: Determination of the carbonation resistance of concrete - Accelerated carbonation method, iTeh Standards (n.d.). https://standards.iteh.ai/catalog/standards/cen/df5d0825-632e-48c9-be99-96af08b4739a/en-12390-12-2020 (accessed September 23, 2025).

[169] CEN/TS 12390-9:2016 - Testing hardened concrete - Part 9: Freeze-thaw resistance with de-icing salts - Scaling, iTeh Standards (n.d.). https://standards.iteh.ai/catalog/standards/cen/ba399d8b-cdd7-419d-87f0-c00b3033fcd9/cen-ts-12390-9-2016 (accessed September 23, 2025).
[170] C1202 Standard Test Method for Electrical Indication of Concrete's Ability to Resist Chloride Ion Penetration, (n.d.). https://store.astm.org/c1202-22.html (accessed September 23, 2025).
[171] R.V. Silva, J. de Brito, R.K. Dhir, Properties and composition of recycled aggregates from construction and demolition waste suitable for concrete production, Construction and Building Materials 65 (2014) 201–217. https://doi.org/10.1016/j.conbuildmat.2014.04.117.
[172] nordtqxv, Concrete, mortar and cement-based repair materials: Chloride migration coefficient from non-steady-state migration experiments (NT BUILD 492), NORDTEST (1999). https://www.nordtest.info/wp/1999/11/21/concrete-mortar-and-cement-based-repair-materials-chloride-migration-coefficient-from-non-steady-state-migration-experiments-nt-build-492/ (accessed September 23, 2025).
[173] J.P. Hwang, H.B. Shim, S. Lim, K.Y. Ann, Enhancing the durability properties of concrete containing recycled aggregate by the use of pozzolanic materials, KSCE Journal of Civil Engineering 17 (2013) 155–163. https://doi.org/10.1007/s12205-013-1245-5.
[174] Z. Lu, Q. Tan, J. Lin, D. Wang, Properties investigation of recycled aggregates and concrete modified by accelerated carbonation through increased temperature, Construction and Building Materials 341 (2022) 127813. https://doi.org/10.1016/j.conbuildmat.2022.127813.
[175] B. Mohamed El Ghazali, CORRELATION PERMEABILITY/CARBONATION AND ITS INFLUENCE ON THE SERVICE LIFE OF REINFORCED CONCRETE STRUCTURES, 2021.
[176] L.J. Butler, J.S. West, S.L. Tighe, Bond of Reinforcement in Concrete Incorporating Recycled Concrete Aggregates, Journal of Structural Engineering 141 (2015) B4014001. https://doi.org/10.1061/(ASCE)ST.1943-541X.0000928.
[177] A. Modz, Eurocode 4: Design of composite steel and concrete structures — Part 1-1: General rules and rules for buildings, (n.d.). https://www.academia.edu/10073042/Eurocode_4_Design_of_composite_steel_and_concrete_structures_Part_1_1_General_rules_and_rules_for_buildings (accessed May 7, 2025).
[178] EN 1993-1-3: Eurocode 3: Design of steel structures - Part 1-3: General rules - Supplementary rules for cold-formed members and sheeting, (n.d.). https://www.phd.eng.br/wp-content/uploads/2015/12/en.1993.1.3.2006.pdf (accessed September 24, 2025).
[179] F. Stochino, A. Alibeigibeni, M. Zucca, M. Valdes, G. Concu, M. Simoncelli, M.A. Pisani, C. Bernuzzi, Mechanical behavior of composite slabs with recycled concrete aggregates: A preliminary study, Structures 70 (2024) 107838. https://doi.org/10.1016/j.istruc.2024.107838.
[180] H. Zhang, Y. Geng, Y.-Y. Wang, X.-Z. Li, Experimental study and prediction model for bond behaviour of steel-recycled aggregate concrete composite slabs, Journal of Building Engineering 53 (2022) 104585. https://doi.org/10.1016/j.jobe.2022.104585.
[181] B. Chen, T. Zhang, Y. Geng, Q. Wang, G. Zhao, J. Yang, Longitudinal shear tests and design methods for corrugated steel–concrete composite slabs with recycled coarse aggregate, Construction and Building Materials 400 (2023) 132870. https://doi.org/10.1016/j.conbuildmat.2023.132870.
[182] L. Lu, W. Wang, L. Zhang, Y. Shao, Longitudinal shear strength of recycled aggregate concrete prefabricated superimposed slabs, Engineering Structures 281 (2023) 115745. https://doi.org/10.1016/j.engstruct.2023.115745.

This thesis was produced while attending the PhD programme in Civil and Architectural Engineering at the University of Cagliari, Cycle XXXVIII, with the support of a scholarship co-financed by the Ministerial Decree no. 352 of 9th April 2022, based on the National Recovery and Resilience Plan (NRRP) – funded by the European Union – NextGenerationEU – Mission 4 “Education and Research”, Component 2 “From Research to Business”, Investment 3.3, and by the company Heidelberg Materials.